ALMOST LOCALIZED FERMI LIQUID AND ITS INSTABILITIES AGAINST MOTT-LOCALIZED AND SPIN-LIQUID STATES

Paweł Korbel

Praca doktorska
wykonana w Zakładzie Teorii Materii Skondensowanej
Instytutu Fizyki Uniwersytetu Jagiellońskiego

Promotor pracy: Prof. dr hab. Józef Spałek

Kraków, 1997

Dedykuję Rodzicom

PODZIĘKOWANIE

Panie Profesorze, pragnę tą drogą w sposób szczególny wyrazić Panu moją wdzięczność za Pana olbrzymi wkład w przygotowanie niniejszej pracy doktorskiej, jak również za to, że przyczynił się Pan do lepszego zrozumienia przeze mnie przynajmniej niektórych zagadnień fizyki.

Paweł Kowbel

Kraków, 1.07.1997

Contents

Chapter 1

Correlated electrons in a narrow band and their metal-insulator transition

1.1 Introduction

The description of electronic states in solids involves two different calculation schemes, which concern two physically distinct models, namely the Bloch-Wilson band theory and the localized-particle model or Heitler-London approach. The band picture represents the electrons as almost free, described by the Bloch wave-function and moving in an effective periodic potential . The interaction between electrons are expressed through a self-consistent potential. Such scheme is successful in describing the electronic states of normal metals and semiconductors. On the other hand, the localized

approach provides a purely atomic description of solids. Contrary to the band picture, the intra-atomic interaction plays then the crucial role. It is assumed that these interactions are strong enough so that the electrons remain almost localized on atoms. This model successfully describes the properties of magnetic insulators, for which the Heisenberg picture of localized magnetic moments is appropriate. One needs to realize that the both above mentioned theories were based on the construction the appropriate wave functions. So, it might seem almost impossible to construct such a general theoretical description that would combine in one the nature of localized and delocalized states. The more so, as it was originally presumed that the Heitler-London and Bloch-Wilson schemes were just representing different approximations to the same exact wave function. Mott [1] was first to suggested that the source of such a description dichotomy may come not from mathematical difficulties, but rather from deeper physical reasons. The essential points of Mott's arguments were illustrated on the example with periodic lattice of hydrogen atoms, each with one electron per atom [2]. According to the Bloch-Wilson theory the systems with a partially filled band lead to metals. As the lattice constant is steadily increased, the band theory would still predict a metallic behavior while, in fact, it is intuitively expected that for large values of the lattice constant one is left with an insulating system of almost independent hydrogen atoms or molecules. In this manner, one encounters the breakdown of a conventional, one-electron band theory. In other words, within the band theory a paramagnetic system with an odd number of electrons per atom should be always metallic. The other fundamental achievement of Mott analysis is the analysis based on Thomas-Fermi approach to the screening of electron-electron interaction.

Namely, one can infer from it that electron correlation effects may lead to a first-order transition between conducting and insulating states. Since the correlation effects depend on the electron density, Mott determined the critical value of the density, above which the metallic state is stable, and below which the proper ground state is that of a magnetic insulator. Indeed, in practice the metal-insulator transition may be induced by change of pressure, temperature or a material composition. It occurs in a wide variety of materials such as transition metal and rare-earth compounds, organic salts, heavily doped semiconductors, amorphus solids and metal-ammonia solutions - to name a few [1,2,3,4].

As an example of a compound whose properties cannot be explained by conventional Bloch-Wilson band theory is MnO. It contains five 3d electrons formula unit. The band theory predicts then that MnO should be metallic. However, the room temperature conductivity of pure MnO is 10^{-15} $(\Omega * cm)^{-1}$, placing it among the best insulators occurring in nature. MnO is thus an example of a Mott insulator. It orders antiferromagnetically without any change in the nature of electronic states at the magnetic transition. A large class of transition metal oxides such as $V0_2$, V_2O_3, V_4O_7, V_5O_9, Ti_2O_3, Ti_4O_7, undergo metal-insulator transitions as a function of temperature pressure or doping. In general, the mechanisms that govern those individual metal-insulator transitions may be quite different. An alternative to the correlation effects as a driving force of the transition may be lattice distortion, order-disorder transformation, excitonic insulator formation [3] , etc. The theoretical interpretation of these driving mechanisms behind some of these transitions still remains a challenging problem. This thesis is mainly concerned with the theoretical approach to

transitions driven by electron correlation effects in narrow band systems. The starting point for this analysis is the Hubbard model formulated first in 1963 [5] , which will be described briefly next.

1.2 The Hubbard model

The behavior of a system of N interacting particles is determined by N-particle wave function obeying the Schrödinger equation

$$i\hbar\frac{\partial}{\partial t}\Psi(x_1,...,x_N) = H\Psi(x_1,...,x_N). \tag{1.1}$$

The Hamiltonian H is given by

$$H = \sum_{k=1}^{N} T(x_k) + \frac{1}{2}\sum_{i\neq j=1}^{N} V(x_i,x_j), \tag{1.2}$$

where $T(x_k)$ is a kinetic energy operator for a single particle, V is the two-body interaction potential, here taken as the Coulomb repulsive force. Of course, the solution of the equation (1.1) is in general impossible to find. The reformulation of the whole problem within the second-quantization formalism make it possible to tackle. There are at least two main reasons for implementation of this method. The first is that the statistical aspect of a problem is included authomaticaly through the anticommutation relations for anihilation and creation operators. Thus one avoids a procedure of antisymetrization of the wave function. Of course, in order to extract the one-particle properties of a system one has to determine the proper Green function. The second reason of expressing Hamiltonian (1.2) in the second quantization is that, one can separate it into terms whose physical meaning is clear. Therefore, for a given

physical situation one can simplify the original problem (1.1) by retaining only the terms that are of main importance and neglect all others. This is just what Hubbard did when trying to investigate the effects of electron correlations in a narrow energy band in the simplest situation. The terms that are retained express two dominant processes, that is those responsible for delocalized nature of the states and those containing the short-range Coulomb repulsion between the particles. Usually the model is written in the following form:

$$H = t \sum_{<i,j>\sigma} c^{\dagger}_{i\sigma} c_{j\sigma} + U \sum_{i} n_{i_\uparrow} n_{i_\downarrow} - \mu N_e, \tag{1.3}$$

where $c_{i\sigma}$ and $c^{\dagger}_{i\sigma}$ are respectively annihilation and creation operators of an electron on site i with spin $\sigma = \pm 1$, and $n_{i\sigma} = c^{\dagger}_{i\sigma} c_{i\sigma}$ is the particle number operator. The summation over the $< ij >$ in formula (1.3) indicates that the hopping is considered only between the nearest neighboring atoms. The last term in is the product of chemical potential μ and total number of electrons N_e and serves as a reference energy for the system.

The first term in (1.3) is the so-called hopping term, since it describes the electron transport through a crystal by hops of an electron from given atom to the neighboring one. This one-particle interaction favors itinerant state of electrons as $t < 0$. This term describes also the chemical bonding in small systems. The second term describes Coulomb repulsion between two electrons when both are on the same atom. In the situation with the doubly occupied configuration this term yields an additional energy U. There is a third factor, namely, the Pauli exclusion principle. The competition between those three factors determines the overall system behavior and, in particular,

the stability of various magnetic phases.

There are two fundamental parameters in the model: the dimensionless ratio, t/U (or equivalently, the ratio W/U, where W is the width of the bare band), and the average electron density per site

$$n = \frac{1}{N}\sum_{i\sigma} < n_{i\sigma} > = \frac{1}{N}\sum_{i} < n_i > . \tag{1.4}$$

The total electron number, $N_e = \sum_{i\sigma} c^{\dagger}_{i\sigma} c_{i\sigma}$, commutes with the Hamiltonian, the electron density is then a good quantum number and hence, the calculations at different densities are independent. Another quantity that is conserved is the total spin of the particles in the system

$$\mathrm{S} = \sum_{i} \mathrm{S}_i = \frac{1}{2}\sum_{i\sigma\sigma'} c^{\dagger}_{i\sigma} \boldsymbol{\sigma}^{\sigma\sigma'} c_{i\sigma'}, \tag{1.5}$$

where $\boldsymbol{\sigma} = (\boldsymbol{\sigma}_x, \boldsymbol{\sigma}_y, \boldsymbol{\sigma}_z)$ denotes the Pauli matrices. Thus the consideration of the states with different total magnetic moments decouple. In the case when the system is placed in the external magnetic field H_a, the Hubbard Hamiltonian contains the Zeeman term and then the ratio $\mu_B H_a/t$ becomes another relevant parameter (obviously in such treatment we neglect the Landau structure).

Depending on the value U/W the two characteristic limits are reached. In the case of $U \rightarrow 0$ (the so-called metallic limit), one obtains a pure band behavior just due to the overlap of the atomic wave functions. The Hubbard Hamiltonian reduces then to a tight-binding Hamiltonian with the hopping integral t_{ij}. The complementary limit $U \rightarrow \infty$ represents the so-called limit of strong correlations. There are no double occupied sites for $n = 1$ and each atom contains electron localized on it. The system is called the Mott-Hubbard insulator. The intermediate range of U is

of particular interest, since then $U \sim W$, i.e. the competition between the band effects and localization due to correlations is most acute. Moreover, the theoretical description in this is not trivial, since the both terms in the Hamiltonian (1.3) are of comparable magnitude. In the next paragraph we provide a brief summary of some basic results obtained in earlier papers concerning the approximate solution of the Hubbard model in the paramagnetic phase.

1.3 Hubbard III solution

The first quantitative treatment of the problem developed by Hubbard [5] was based on one-particle Green function treated within the equation of motion method followed by a decoupling scheme. Three fundamental features of the model were obtained that way. First, the theory yields the exact solutions in the two opposite limiting cases: $U = 0$ and $U \to \infty$. Second, and most spectacular feature, is the appearance of the metal-insulator transition. Namely, Hubbard in his third paper in 1964, [5] showed that with increasing U/W ratio one encounters a critical value $(U/W)_c$ above which a single-band splits into two subbands separated by an energy gap, called later the Mott-Hubbard or the correlation gap. Thus in a case of a half filled band (i.e. for $n = 1$) and in a region of $U/W > (U/W)_c \sim 1$, the lower band is completely filled while the upper is empty. The system is in the insulating state. Since the gap decreases slowly to zero with decreasing U/W ratio, the insulator-metal transition expressed in the Hubbard's scheme (contrary to the Mott prediction [6]) is continuous. This gradual character of the transition at temperature $T = 0$ could be due to the complete neglect

of interatomic Coulomb terms, i.e. disregard of the screening effects invoked by Mott that made the sharp transition possible.

The original Hubbard solutions was analyzed (and criticized) by other authors. It was pointed out by Edwards and Hewson [7], that even in the metallic phase (i.e. for $U << W$) the Fermi surface is not properly defined. Next, since the Hubbard restricted his discussion to spatially uniform solutions, the magnetic effects were not taken into account. The simple decoupling scheme also fails to reduce to the Hartree-Fock approximation in the limit of week interaction [8]. This is because, strictly speaking the Hubbard solution is exact only in the limits: $U = 0$ or $t_{ij} = 0$. Also, the Hubbard results are in contradiction with the exact results of Lieb and Wu in one dimensional case [9]. In general, one needs to use a self-consistent method that allows for a determination of the system ground-state energy in the mean-field approximation and then calculate the fluctuation corrections around that state. The next section is devoted to discussion of the Gutzwiller solution, i.e. to the variational method proposed first by Gutzwiller [10]. This allows to determine the ground state properties of correlated electrons and define the order parameter characterizing the metallic phase. Also, it will be shown later that this approximate solution corresponds to the mean-field approximation within the slave-boson approach in the paramagnetic case.

1.4 Gutzwiller solution and the quasiparticles

The simplest non-perturbative, mean-field solution is provided by the Hartree-Fock approximation. This approach is based on the assumption that for a given operators

$\widehat{a}_1$ and $\widehat{a}_2$ we neglect their correlation fluctuations, i.e. put

$$[\widehat{a}_1 - < \widehat{a}_1 >][\widehat{a}_2 - < \widehat{a}_2 >] \simeq 0, \tag{1.6}$$

where $< \widehat{a}_1 >, < \widehat{a}_2 >$ are the mean field value of the relevant operator in the non-interacting ground state. So, the two-particle interaction is replaced by effective single-particle term, namely

$$\widehat{a}_1 \cdot \widehat{a}_2 \simeq < \widehat{a}_1 > \widehat{a}_2 + < \widehat{a}_2 > \widehat{a}_1 - < \widehat{a}_1 >< \widehat{a}_2 > . \tag{1.7}$$

It is well known that with the increasing Hubbard U, the Hartree-Fock solution favors a magnetic state [11]. To understand the reason for this, it is convenient to express the repulsive Hubbard term in terms of the particle number operator $n_{i\sigma}$ and the magnetization $m_i = 2S_i^z$, where S_i^z is the z-component of the spin operator and expressed in the second quantization representation takes the form $S_i^z = \frac{1}{2}(n_{i_\uparrow} - n_{i_\downarrow})$. Thus $n_{i\sigma} = n_i - \sigma S_i^z$, where $n_i = \sum_\sigma n_{i\sigma}$. We choose the energy scale in such a way that $\mu = 0$. The Hubbard Hamiltonian (1.3) takes the form

$$H = t \sum_{<i,j>\sigma} c_{i\sigma}^\dagger c_{j\sigma} + \frac{U}{4} \sum_i (n_i^2 - m_i^2). \tag{1.8}$$

The form (1.8) shows that fluctuations in the local density number $n_{i\sigma}$ causes an increase in repulsive energy, whereas the onset of magnetic moment leads to the lowering in potential energy and hence might be stabilized. In the Hartree-Fock approximation the term in the electron density is in fact irrelevant, since it leads only to a constant shift of the total energy. The important contribution, however, is the magnetization, which provides a proper order parameter for the problem. Indeed, the appearance of a molecular field, $H_m \sim U\langle m_i \rangle$, favors moments orientation in

a spontaneously chosen direction. The system is ferromagnetic if such a magnetic moment is spatially homogenous. For band filling n, the Hartree-Fock approximation gives the probability of finding two electrons on the same lattice site, $\langle \widehat{n}_{i_\uparrow} \widehat{n}_{i_\downarrow} \rangle = \frac{1}{4} n^2$. In the limit $U >> t$, this causes the strong enhancement in total energy of the system through the contribution of $\frac{1}{4} U n^2$. Thus the system is forced to order magnetically, since the magnetic moment formation ($\langle m_i \rangle \neq 0$) correlations reduces the Hubbard repulsion. Gutzwiller showed [10] that there are already correlations in the paramagnetic phase, which reduce energetically expensive Hubbard repulsion. To realize that he considered a trial wave function for the ground state by starting with the Bloch function Ψ_0, for non-interacting electrons and then reduced the number of doubly occupied sites by means of a projection operator. The wave function for the correlated state, Ψ_G, is assumed as

$$\mid \Psi_G \rangle = \prod_i [1 - (1 - g) n_{i_\uparrow} n_{i_\downarrow} \mid \Psi_0 \rangle, \tag{1.9}$$

where g, $(0 \leq g \leq 1)$, is the parameter that needs to be determined variationally. State $\mid \Psi_0 \rangle$, is the uncorrelated state that corresponds to wave function Ψ_0, namely, the Slater determinant of Bloch wave functions (transformed to the Wannier representation). The operator $n_{i_\uparrow} n_{i_\downarrow}$, has a value of unity when site i is occupied by the electrons with spin up and down, or has a value of zero otherwise. Thus, in the sense of the system average configuration, the state with double occupied site has assigned a weight of g. For $g = 1$, according to (1.9), $\mid \Psi_G \rangle$ reduces to the ground state of uncorrelated system $\mid \Psi_0 \rangle$. In the opposite limit $g = 0$, ground state is the state where no doubly occupied sites are included. The variational parameter g, furnishes as a

measure of correlation effects and my be determined by minimization of the ground state energy. Using the fact that $\widehat{\mathrm{D}}_i \equiv n_{i_\uparrow} n_{i_\downarrow}$ has eigenvalues one and zero only, relation (1.9) may be written as

$$\mid \Psi_G\rangle = g^{\widehat{\mathrm{D}}} \mid \Psi_0\rangle, \tag{1.10}$$

where $\widehat{\mathrm{D}} = \sum_i \widehat{\mathrm{D}}_i$, is the total number of doubly occupied sites. To find the ground state energy one needs to evaluate the following expression

$$\begin{aligned} E_G &= \frac{\langle \Psi_G \mid H \mid \Psi_G\rangle}{\langle \Psi_G \mid \Psi_G\rangle} \\ &= \frac{t \sum\limits_{<i,j>\sigma} \langle \Psi_G \mid c^\dagger_{i\sigma} c_{j\sigma} \mid \Psi_G\rangle}{\langle \Psi_G \mid \Psi_G\rangle} + \frac{U \sum\limits_i \langle \Psi_G \mid n_{i_\uparrow} n_{i_\downarrow} \mid \Psi_G\rangle}{\langle \Psi_G \mid \Psi_G\rangle}. \end{aligned} \tag{1.11}$$

Due to the fact that $\mid \Psi_G\rangle$ is an eigenstate of the number operator, the interaction term in (1.11) simply gives the value of UD, $(D \equiv \langle \Psi_G \mid \widehat{\mathrm{D}} \mid \Psi_G\rangle)$. The whole problem reduces to the evaluation of the matrix elements of the kinetic energy and the norm of the wave function. Finally, one finds that both searched quantities namely, the matrix elements of the kinetic energy and the norm of the wave function are written in terms of determinants. After some assumption concerning the n-th order density functions and phase relations between different spin configurations the problem were reduced to pure combinatorics. The strength of this method, however, relies on an extremely simple expression for the ground state energy (per site) that comes out, namely

$$\frac{E_G}{N} = \sum_\sigma q_\sigma(\eta) \cdot \bar{\varepsilon} + U\eta. \tag{1.12}$$

were $\eta \equiv \frac{D}{N}$ is the fraction of doubly occupied sites and appears as an another

variational parameter. Also, the average energy per spin in the uncorrelated state

$$\overline{\varepsilon} = \frac{1}{N} \cdot t \sum_{<i,j>\sigma} \langle \Psi_0 | c^{\dagger}_{i\sigma} c_{j\sigma} | \Psi_0 \rangle = \sum_{|\mathbf{k}|<k_F,\sigma} \varepsilon(\mathbf{k}) < 0, \tag{1.13}$$

where k_F is a Fermi momentum in that state. The quantities q_σ in (1.12) are the discontinuities in the momentum distributions function at the Fermi surface of correlated system and are given by

$$q_\sigma = \frac{\left(\sqrt{(n_\sigma - \eta)(1 - n + \eta)} + \sqrt{\eta(n_{\overline{\sigma}} - \eta)}\right)^2}{n_\sigma(1 - n_{\overline{\sigma}})}. \tag{1.14}$$

So, the expression (1.12) still needs to be minimized with respect to η . Note, that since $0 \leqslant \eta \leqslant n_\sigma, n_{\overline{\sigma}}$, for $\sigma = \pm 1$, $q_\sigma \leqslant 1$ ($q_\sigma = 1$ only if $U = 0$). Thus, along with decrease of doubly occupied sites the kinetic term is reduced through the factor q_σ, which means that the effective electron hopping turns out to be energetically unfavorable. One of the most spectacular feature of the Gutzwiller solution was discussed by Brinkman and Rice [12]. They note that for a half-filled band ($n = 1$), $n_\uparrow = n_\downarrow$ and $q_\uparrow = q_\downarrow = q$, (i.e. in the paramagnetic state) we have that

$$q = 8\eta(1 - 2\eta). \tag{1.15}$$

Next, minimizing the ground state energy (1.12) with respect to η they obtained the set of predictions:

$$\eta = \frac{1}{4}\left(1 - \frac{U}{U_c}\right), \tag{1.16}$$

$$q = 1 - \left(\frac{U}{U_c}\right)^2, \tag{1.17}$$

$$\frac{E_G}{N} = \overline{\varepsilon}\left(1 - \frac{U}{U_c}\right)^2, \tag{1.18}$$

where $U_c = 8 \mid \bar{\varepsilon} \mid$. This clearly means that at critical value $U = U_c$, the probability η of double occupancy vanishes. At that point there is no contribution to the energy coming from the kinetic energy as well as from the interaction term. This indicates that the localization of the particles and consequently the metal-insulator transition takes place. The above authors also showed that both the effective mass ratio m^*/m, and spin susceptibility χ_s, are enhanced as $U \rightarrow U_c$, namely

$$\frac{m^*}{m} = \frac{1}{q} = \frac{1}{1 - (\frac{U}{U_c})^2}, \tag{1.19}$$

and

$$\chi_s = \rho(\varepsilon_F) \cdot \frac{1}{1 - (\frac{U}{U_c})^2} \cdot \frac{(1 + \frac{U}{U_C})^2}{(1 - U\rho(\varepsilon_F))(1 + \frac{U}{2U_C})}. \tag{1.20}$$

Here $\rho(\varepsilon_F)$ is the band structure density of states at the Fermi energy level. Thus as U approaches U_c both, the susceptibility and effective mass have a divergent factor $1/(1 - (\frac{U}{U_c})^2)$. The divergence of χ_s as $U \rightarrow U_c$ indicates that we approach a true phase transition.

Much effort has been undertaken to generalize and simplify the Gutzwiller scheme. Ogawa et. al. [13] showed that the approximation made by Gutzwiller concerns the dependence of the energy expectation values on spins configuration of the wave function. In other words, it was shown that Gutzwiller results for the kinetic energy may be reproduced if the nearest neighbor configuration are specified but all other spatial correlations are neglected. Razafimandimby [14] showed that a simple factorization procedure equivalent to one-site cluster expansion reproduce the Gutzwiller's result for the ground state energy in the case of paramagnetic, half-filled case. It was also shown [14] that in the case of two-site cluster expansion Gutzwiller's results becomes

exact in the asymptotic limit of infinite lattice dimensionality, while in three dimensions gives only very small corrections. In one-dimension case Kaplan, Horsh and Fulde [15] showed that the ground state energy when calculated exactly due to the Gutzwiller ansatz, Eq.(1.9), in the limit $U >> t$ yields $E = -at^2/U$, which is coherent with the result obtained by Lieb an Wu [9]. However, due to the earlier paper of Bonner and Fisher [16] the value of the coefficient a is too small compared with the exact result. Thus, Kaplan et al. [15] removed this discrepancy by introducing second variational parameter. Vulović and Abrahams [17] introduced a very transparent combinatorical technique that allow to obtain easily well known results for the Hubbard model, as well as it can be extended to approach the ground state energy for the Anderson lattice model. Finally, Vollhardt [18] has provided a very lucid discussion devoted to the Gutzwiller approach and redefined it in the Fermi-liquid context.

The most elementary way of recovering the Gutzwiller's results for the case of half-filled band is shown by Spałek et al. [19]. They assumed that the expectation value of the ground state energy per lattice site in the paramagnetic case is

$$\frac{E_G}{N} = \Phi(\eta)\bar{\varepsilon} + U\eta, \tag{1.21}$$

where $\eta =< n_{i_\uparrow} n_{i_\downarrow} >$ is a fundamental parameter that must be determined variationally by calculating the balance between the kinetic and potential energy term. $\Phi(\eta)$ is a function that describes a motion of electrons exposed to 'on-site' Coulomb repulsion force. In order to determine $\Phi(\eta)$ it was assumed that it may be approximated by the Taylor expansion terminated at the second order term, namely

$$\Phi(\eta) = f_0 + f_1\eta + f_2\eta. \tag{1.22}$$

The coefficients f_0, f_1, f_2 can be determined due to the boundary conditions for the limit cases $U = 0$ and $\eta = 0$. Then, by minimizing the energy (1.21) with respect to η one obtains already well known results (1.16),(1.17),(1.18). Although the assumption (1.22), concerning very simplified structure of the $\Phi(\eta)$ function in general may lead to quantitatively incorrect results, at least in the region of very small η one may expect the validity of assumption made, as one may really observe so. On the other hand, such a simple scheme demonstrating the metal-insulator transition realizes that η plays the role of relevant order parameter.

Apart from the discussion of Brinkman and Rice, one can make an additional observations based on the Gutzwiller's solution. Namely, Spałek et al. [20] assumed that one can introduce individual quasiparticle states, which have energy

$$E_k = \Phi(\eta)\varepsilon_k. \tag{1.23}$$

So far $\Phi(\eta)$ played the role of so called 'band narrowing factor'. This terminology is quite clear due to formulas (1.21) and (1.18). In the limit $\Phi \rightarrow 0$ an effective contribution from the hopping (kinetic) term vanishes, so the metallic phase disappears also. Obviously, the band energy (1.18) can be obtained by using the relation (1.23) as a definition of renormalized band spectrum. However, one needs to realize that now one can reinterpret the overall system behavior starting from the concept of quasiparticles as particles with renormalized energy. Such a reinterpretation determines automatically the value of band energy for non-zero temperature ($T > 0$) regime, namely

$$\frac{E_B}{N} = \sum_{\mathrm{k}\sigma} E_{\mathrm{k}} f_{\mathrm{k}\sigma}, \tag{1.24}$$

where

$$f_{k\sigma} = \frac{1}{e^{(E_k-\mu)/kT}+1}, \tag{1.25}$$

as these quasiparticles are assumed to obey the Fermi-Dirac statistics with the distribution function $f_{k\sigma}$. Furthermore, such a description of the interaction shows the principal difference with respect to the Landau Fermi-liquid theory. Here the effective mass is determined by self-consistent, variational calculations. For paramagnetic half-filled case Φ coincides with q_σ, Eq. (1.14). In general, the discontinuities in the single-particle occupation number at the Fermi surface can be easily related to the quasiparticle, $spin-dependent$, effective mass m^*_σ, namely through the relation

$$\frac{m^*_\sigma}{m} = \frac{1}{q_\sigma}. \tag{1.26}$$

The idea of the renormalized quasiparticle mass due to the electron correlations appears in a natural manner in the more recent, functional integral approach, proposed by Kotliar and Ruckenstein [21]. This theoretical formulation will be discussed in details in the next chapter and is one of the main features of this thesis.

1.5 The aim and the scope of the thesis

The Hubbard model describes electronic states of a simple narrow band system of interacting fermions. As outlined above, the model provides the two opposite limit cases: first, the so-called metallic limit and second, the limit of strong correlations, which in the case the half filled band, as well as for $U \geqslant U_c$ leads to the Mott localization transition. The metallic state is the termed the almost localized Fermi

liquid, by we understand the fermion system which is in the metallic phase but close to the border of the localization. In the case close but away from the half filling, i.e. for $n \neq 1$, the localization does not occur, and we say that we deal then with the almost localized fermions. The call 'almost localized' can be better understood in the light of the quasiparticle interpretation of the Hubbard model. Eqs.(1.19) or (1.26) shows that the effective mass of the quasiparticles provides a natural measure of the effective fermion interaction. The more heavy are the quasiparticle's masses the lower is the free energy contribution coming from the kinetic part and the system gets closer to the localization threshold. At the localization boundary the effective mass is divergent.

The thesis concerns mainly the mean field solution of the Hubbard model in the paramagnetic and antiferromagnetic phases, as of magnitude of interaction and for an arbitrary band filling. Additionally, we describe metamagnetism for an arbitrary band filling and a transition to a non-Fermi liquid in an applied magnetic field. We start from the brief theoretical introduction (Chapter 2) in which we summarize the saddle point approximation as well as the representation of the fermionic degrees of freedom by the Grassmann variables.

The mean field solutions discussed in the thesis is formulated starting from the auxiliary-field method, the so called slave-boson method, which applied to the Hubbard model allows to eliminate exactly the fermionic degrees of freedom via functional integration over the Grassmann variables with the relations between the Fock-space representation for fermions and bosons.

In Chapter 4, we show how the mathematical tools described in Chapters 2 and

3 allow to derive the system of the self-consistent mean-field equations in an applied magnetic field H_a describing the average number of doubly occupied sites in the form of the algebraic equation with the parameters $u = U/2W$, n, and $h = \mu_B H_a/W$. This in turn allows to illustrate easily the dependence of various physical quantities on the mentioned parameters. Namely, in Chapter 5, we discuss the concept of the spin-dependent effective mass and related to it de Haas-van Alphen oscillations with quantum beats, as well to determine the nonlinear molecular field induced by electronic correlations.

The metal-insulator transition (discussed earlier) may occur, of course, only for the half-filled band case $n = 1$. However, in the applied field and, for $n \neq 1$,one may encounter another type of the fermionic quantum liquid, which appears at the metamagnetic point, when the Fermi liquid of almost localized fermions becomes unstable. This Fermi liquid instability against, the so-called statistical spin liquid is discussed in Chapter 6.

Finally, in the Chapter 7, we discuss in detail the mean field solution of the Hubbard model in the antiferromagnetic phase. In particular, we determine a crossover from the Slater to Mott-Hubbard picture of an antiferromagnetic insulator. We also discuss the principal characteristics of that phase such as the Slater gap, the magnetic moment and the ground state energy.

As said above, the present thesis is based on the mean-field slave-boson picture of correlated narrow-band electrons. The main emphasis is put on the quasiparticle picture of the resultant Fermi liquid and its instabilities against the Mott localized state (for $n = 1$) or against the correlated spin liquid (for $n \neq 1$). We offer a coherent

picture of almost localized fermions not elaborated in detail in the literature. The results of the thesis have been published or submitted for publication as a series of papers [22-27].

REFERENCES

[1] N. F. Mott, *Proc. R. Soc.* **A62**, 416 (1949).

[2] N. F. Mott, *Metal Insulator Transitions*, (Taylor and Francis, London) (1974).

[3] H.I. Halperin and T.M. Rice, in *Solid State Physics*, vol 21, edited by I. Seitz et al, Academix Press, New York, (1968).

[4] P. W. Anderson, *in* "Frontiers and Borderlines in Many-Particle Physics" (R. A. Broglia and J.R. Schrieffer, Eds.), North Holland, Amsterdam (1988).

[5] J. Hubbard, *Proc. R. Soc.* **A276**, 238 (1963); **A281**, 401 (1964).

[6] N.F. Mott, *Phil. Mag.* **6**, 287 (1961).

[7] D.M. Edwards and A.C. Hewson, *Rev. Mod. Phys.* **40**, 810 (1968).

[8] R.A. Bari and J.A. Kaplan *Phys. Lett.* **33**, 400 (1970); M.Acquarone, D.K. Ray and J. Spałek, J. Phys. C: Solid State Phys., **15**, 959 (1982).

[9] E.H. Lieb and F.Y. Wu, *Phys. Rev. Lett.* **20**, 1445 (1968).

[10] M.C. Gutzwiller, *Phys. Rev. Lett.* **10**, 159 (1963); *Phys. Rev.* **134**, A932; *Phys Rev.* **137**, A1726 (1965).

[11] D.R. Penn, *Phys. Rev.* **142**, 350 (1966).

[12] W.F. Brinkman and T.M. Rice, *Phys. Rev.* **B2**, 4302 (1970).

[13] T. Ogawa, K. Kanda and T. Matsubara, *Prog. Theor. Phys.* **53**, 614 (1975)

[14] H.A. Razafimandimby, *Z. Phys.* **B 49**, 33 (1982).

[15] A.T. Kaplan, P. Horsh and P.Fulde, *Phys. Rev. Lett.* **49**, 889 (1982).

[16] J. Bonner and M.E. Fisher, *Phys. Rev.* **135**, A640 (1964).

[17] Z. Vulović and E. Abrahams, *Phys. Rev.* **B36**, 2614 (1987).

[18] D. Vollhardt, *Rev. Mod. Phys.* **56**, 99 (1984).

[19] J. Spałek, A.M. Oleś and J.M. Honig, *Phys. Rev.* **B28**, 6802 (1983); J. Spałek *J. Solid. State. Chem.* **88**, 70 (1990).

[20] J. Spałek, A. Datta and J.M. Honig, *Phys. Rev. Lett.* **59**, 728 (1987); J. Spałek, M. Kokowski and J.M. Honig, *Phys. Rev.* **B39**, 4175 (1989).

[21] G. Kotliar and A.R. Ruckenstein, *Phys. Rev. Lett.* **57**, 1362 (1986).

[22] P. Korbel, J Spałek, W. Wójcik and M. Acquarone, *Phys. Rev.* **B52**, (RC) R2213-16 (1995).

[23] J. Spałek P. Korbel and W. Wójcik, *Phys. Rev.* **B56**, 1 (1997).

[24] P. Korbel, J Spałek and W. Wójcik, *Proc. of the Euroconference Physisc of Magnetism,* Poznań 1996, *Acta Phys. Polon* **A**, in press.

[25] J Spałek, W. Wójcik and P. Korbel, *Proc. of the Euroconference Physisc of Magnetism,* Poznań 1996, *Acta Phys. Polon* **A**, in press.

[26] J Spałek, W. Wójcik and P. Korbel, *Proc. of the Conf. on Strongly Correlated Electron Systems (SCES'*96), *Physica* **B**, 620 (1997).

[27] J Spałek, W. Wójcik and P. Korbel, in *Proc. Int. School of Theoretical Phys.* Ustroń 1997, *Molecular Phys. Rep.* **17**, (1997).

[28] P. Korbel and J.Spałek," Antiferromagnetism of almost localized fermions: From Slater to Mott-Hubbard picture" submitted for publication in *Phys. Rev.* **B.**

Chapter 2

Path integration method in quantum statistical mechanics

One of the most serious problem in the theoretical physics is the description of the interacting quantum many-body systems and their phase transitions. In order to describe many-body problems one needs to solve N-particle Schrödinger equation (1.1). As it was already mentioned in Chapter 1, the problem is usually impossible to tackle this way. A new formulation of that problem is provided by the second quantization method combined with the functional integration. This methods will be used through this thesis and follows the book by J.W. Negele and H. Orland [1]. Below we summarize briefly the necessary tools and afterwards.

2.1 Coherent state representation for bosons

The main purpose of introducing the coherent states is to obtain the analytical expressions for the transition amplitudes of many-particle system in the situation when operators are written in the second quantized form. The coherent state $|\Phi>$ is defined as a vector in the Fock space, which is an eigenvector of the annihilation operator. It is defined by the following expansion

$$|\Phi>=\sum_{n_{k_1}...n_{k_p}...}\phi_{n_{k_1}...n_{k_p}...}|n_{k_1}...n_{k_p}...>. \tag{2.1}$$

Here $|n_{k_1}...n_{k_p}...>$ denotes a normalized state with n_{k_1} particles in the state $|k_1>$, n_{k_2} particles in state $|k_2>$, etc.; $\{|k_i>\}$ is one-particle orthonormal basis. The summation in (2.1) runs overall possible values of $n_{k_1},...n_{k_p},...$

Since the state $|n_{k_1}...n_{k_p}...>$ expressed in the second quantized form is

$$|n_{k_1}...n_{k_p}...>=\frac{\left(a_{k_1}^{\dagger}\right)^{n_{k_1}}}{\sqrt{n_{k_1}!}}...\frac{\left(a_{k_p}^{\dagger}\right)^{n_{k_p}}}{\sqrt{n_{k_p}!}}...|0>, \tag{2.2}$$

the coefficients $\phi_{n_{k_1}...n_{k_p}...}$ in Eq.(2.1) are related to the single particle basis. By definition, the factorization of $\phi_{n_{k_1}...n_{k_p}...}$ yields

$$\phi_{n_{k_1}...n_{k_p}...}=\frac{\left(\phi_{k_1}\right)^{n_{k_1}}}{\sqrt{n_{k_1}!}}...\frac{\left(\phi_{k_p}\right)^{n_{k_p}}}{\sqrt{n_{k_p}!}}, \tag{2.3}$$

so the state (2.1) may be rewritten in the form

$$|\Phi>=\sum_{n_{k_1}...n_{k_p}...}\frac{\left(\phi_{k_1}a_{k_1}^{\dagger}\right)^{n_{k_1}}}{n_{k_1}!}...\frac{\left(\phi_{k_p}a_{k_p}^{\dagger}\right)^{n_{k_p}}}{n_{k_p}!}...|0>=e^{\sum_k \phi_k a_k^{\dagger}}|0>, \tag{2.4}$$

where ϕ_k is the eigenvalue belonging to a_k. In the case of bosons, when there is no limit for particle occupation number in a given state, i.e. $0 \leqslant n_{k_1}...n_{k_p}... \leqslant \infty$, the

relation

$$a_k|\Phi>=\phi_k|\Phi>, \tag{2.5}$$

is authomatically obeyed. The coefficient $\phi_{n_{k_1}...n_{k_p}...}$ are complex number, or equivalently, each of the ϕ_{n_k} commute with one another, i.e.

$$\left[\phi_{n_k},\phi_{n_l}\right]_- = 0. \tag{2.6}$$

In the case when expansion (2.1) is to represent a fermion state the situation is more complicated. Namely, let us assume that we have succeeded in constructing such a state $|\Phi>$, which fulfills the condition (2.5). Since the operator a_k is now the fermion annihilation operator $<\Phi|a_k a_k|\Phi>=0=\phi_k^2$. Thus if ϕ_k is different from zero, it cannot be any longer an ordinary number. The coefficients ϕ_{n_k} become now so-called, Grassmann variables, i.e. they obey the anticommutation rule

$$\left[\phi_{n_k},\phi_{n_l}\right]_+ = 0.$$

Their properties are going to be discussed next.

2.2 Grassmann variables

The anticommuting variables, called the Grassmann variables, are defined by a set of generators $\{\eta_k\}$, $k=1,2,...,n$, which anticommute with each other, i.e.

$$\eta_k\eta_l+\eta_l\eta_k=0. \tag{2.7}$$

For the particular case $l=k$ we have that

$$\eta_k^2=0, \tag{2.8}$$

which asserts that there is no two particles carrying the same quantum number k in the coherent state $|\Phi>$.

The important thing is that in order to use the Grassmann algebra there is no need to know the concrete analytic representation for generators $\{\eta_k\}$. It is sufficient to know general algebraic rules, by which these anticommuting entities are governed. The differentiation and integration with these numbers are pure mathematical constructions and along with above mentioned rules may be viewed as a set of definitions. The most important results concerning the Grassmann numbers are listed below.

A generator the η_k^* is called to be conjugated with a given generator η_k , if for any complex number c occurs

$$(c\eta_k)^* = c^*\eta_k^*, \tag{2.9}$$

and for any product of generators

$$(\eta_{k_1}\eta_{k_2}...\eta_{k_n})^* = \eta_{k_n}^*...\eta_{k_2}^*\eta_{k_1}^*. \tag{2.10}$$

The last rule means that the Grassmann conjugation is analogous to Hermitian conjugation.

Due to the Eq. (2.8) any function defined on this algebra must be a liner function, i.e.

$$F(\eta) = c_0 + c_1\eta. \tag{2.11}$$

Similarly, an operator expressed in the fermion coherent state representation will be a function of η^* and η which must have the form

$$A(\eta^*, \eta) = c_0 + c_1\eta + c_2\eta^* + c_{12}\eta^*\eta. \tag{2.12}$$

A derivative from a Grassmann variable function is identical with derivative of complex variable function. The exception is the derivative operator $\frac{\partial}{\partial\eta}$ must act on variable η directly, otherwise η has to be anticommuted through until it is adjacent to $\frac{\partial}{\partial\eta}$. For instance:

$$\frac{\partial}{\partial\eta}(\eta^*\eta) = \frac{\partial}{\partial\eta}(-\eta\eta^*) = -\eta^*. \tag{2.13}$$

In the case of integration there is no analog with the Riemann integral for ordinary variables. However there is a correspondence to the integration over an exact differential form of the function that vanishes at infinity. Such an integral is simple equal to zero. Thus one define the definite Grassmann integral

$$\int d\eta 1 = 0, \tag{2.14}$$

since 1 is derivative of η, and

$$\int d\eta\eta = 1, \tag{2.15}$$

since η is not a derivative of any Grassmann function. Eqs. (2.14) and (2.15) holds the same for conjugated variables and like in Eq.(2.13), in order to apply (2.15), one has to anticommute the variable η as required to bring it next to $d\eta$.

The integration rules performed above leads to the useful formula for the Gaussian integral. Namely, if m_{kl} is a positive Hermitian matrix, then

$$\int \prod_k d\eta_k^* d\eta_k e^{-\sum_{kl}\eta_k^* m_{kl}\eta_l} = \det(m). \tag{2.16}$$

This property is crucial for further analysis performed in Chapter 3.

2.3 Fermion coherent states

Due to Eq.(2.1), any fermion state $|\Phi_F>$ is a vector of a generalized Fock space since the expansion coefficients are now Grassmann numbers. It is defined

$$|\Phi_F>= e^{-\sum_k \eta_k a_k^\dagger}|0>=\prod_k (1-\eta_k a_k^\dagger)|0> . \tag{2.17}$$

In order to operate on expressions containing combinations of Grassmann variables and creation and anihilation operators, as well as to obtain the results analogous to those obtained for bosons one needs additionally to assume that the following relations are fulfilled

$$[\widetilde{\eta}, \widetilde{a}]_+ = 0, \tag{2.18}$$

and

$$(\widetilde{\eta a})^\dagger = \widetilde{a}^\dagger \eta^*, \tag{2.19}$$

where $\widetilde{\eta}$ is any Grassmann variable out of $\{\eta, \eta^*\}$ and $\widetilde{a}$ is any operator out of $\{a, a^\dagger\}$.

The properties of Grassmann algebra outlined above along with the definition of the fermion coherent state provides

$$a_k|\Phi_F>= \eta_k|\Phi_F>, \tag{2.20}$$

and similarly for the adjoint of the coherent state is

$$<\Phi_F|a_k^\dagger =<\Phi_F|\eta_k^*. \tag{2.21}$$

The scalar product of two coherent states, like in the boson case, has the form

$$<\Phi_F \mid \Phi'_F>= e^{\sum_k \eta_k^* \eta'_k}. \tag{2.22}$$

Relations (2.20)- (2.22) shows that a matrix element of an normal-ordered operator $A(a^\dagger, a)$ between coherent state is

$$< \Phi_F \mid A(a_k^\dagger, a_k) \mid \Phi'_F >= e^{\sum_k \eta_k^* \eta'_k} A(\eta^*, \eta). \tag{2.23}$$

It can be shown that the unity operator in the physical Fermion Fock space, written in the form of coherent states is

$$\mathbf{1} = \int \prod_k d\eta_k^* d\eta_k e^{-\sum_k \eta_k^* \eta'_k} \mid \Phi_F >< \Phi_F \mid, \tag{2.24}$$

which shows the overcompletness of coherent states in the Fock space, since due to the choice of the state $\mid \Phi_F >$ is not unique. Thus Eq.(2.24) allows to express any Fock space vector $|\Psi_F >$ in the form

$$|\Psi_F >= \int \prod_k d\eta_k^* d\eta_k e^{-\sum_k \eta_k^* \eta'_k} \psi(\phi^*) \mid \Phi_F >, \tag{2.25}$$

where

$$\psi(\phi^*) =< \Phi_F | \Psi_F >, \tag{2.26}$$

is the coherent state representation of the state $\mid \Psi_F >$.

Finally, if $\{|n >\}$ is a complete set of states in the Fock space, then the trace of an operator A takes the form

$$\begin{aligned} TrA &= \sum_n < n|A|n > \\ &= \int \prod_k d\eta_k^* d\eta_k e^{-\sum_k \eta_k^* \eta_k} \sum_n < n|\Phi_F >< \Phi_F|A|n > \\ &= \int \prod_k d\eta_k^* d\eta_k e^{-\sum_k \eta_k^* \eta_k} < -\Phi_F|A|\Phi_F > . \end{aligned} \tag{2.27}$$

The sign (-) that appears in the matrix element in the 2-nd equation comes from the fact that the states $|\Phi_F >$ contains Grassmann numbers, so replacing by positions

those two matrix elements leads to the change in sign of the whole expression.. Consequently, this will lead to antiperiodic boundary conditions, which fermion states have to obey when a partition function is calculated in the form of Feynman path integral.

The fermion coherent states are not contained in the fermion Fock space and, since they are not physically observed, there is no correspondence between them and any classical field. For instance, the expectation value for the number operator expressed in terms of Grassmann numbers is

$$\frac{<\Phi_F|\widehat{N}|\Phi_F>}{<\Phi_F|\Phi_F>} = \sum_k \eta_k^* \eta_k, \tag{2.28}$$

so, the concept of the average number of particles in a fermion coherent state is meaningless. However, fermion coherent states are very useful in formally unifying many-fermion and many-boson problems. Moreover, the path integral method discussed next, allows to get rid of the fermion degrees of freedom in cases when a Hamiltonian is a bilinear form in Grassmann variables. Thus, one is left only with the boson fields, which supply the final, physical results for condensed quantum states and their dynamic properties.

2.4 Functional integral representation of the partition function

Relation (2.27) allows to write the many-particle partition function in the form

$$Z = Tre^{-\beta(\widehat{H}-\mu\widehat{N})} = \int \prod_q \phi_q^* \phi_q e^{-\sum_q \phi_q^* \phi_q} < \zeta\Phi|e^{-\beta(\widehat{H}-\mu\widehat{N})}|\Phi >, \tag{2.29}$$

where $\zeta = 1(-1)$ for bosons (fermions). Of course, in the latter case the integration variables are the Grassmann numbers. The matrix element in Eq. (2.29) may be viewd as the imaginary-time transition amplitude, however, between the states with imposed periodic boundary conditions for bosons

$$\phi_{q,M} = \phi_{q,0}, \tag{2.30}$$

or antiperiodic boundary conditions in the case for fermions

$$\phi_{q,M} = -\phi_{q,0},$$

where $\phi_{q,0}$ $(\phi_{q,M})$ denotes the appropriate field variable taken at the initial (final), imaginary-time moment $\tau = 0$ $(\tau = M)$.

Expressing this transition amplitude as the Feynman path integral, one finds that the resulting partition function is

$$Z = \lim_{M\to\infty} \int \prod_{k=1}^{M-1} \prod_{q} \frac{1}{R} d\phi^*_{q,k} d\phi_{q,k} e^{-S(\phi^*\phi)}, \tag{2.31}$$

where

$$\begin{aligned} S(\phi^*\phi) \;=\; & \varepsilon \left(\sum_q \phi^*_{q,1} \left(\frac{\phi_{q,1} - \varsigma\phi_{q,M}}{\varepsilon} - \mu\varsigma\phi_{q,M} \right) + H(\phi^*_{q,1}, \varsigma\phi_{q,M}) \right) \\ & + \varepsilon \sum_{k=2}^{M} \left(\sum_q \phi^*_{q,k} \left(\frac{\phi_{q,k} - \phi_{q,k-1}}{\varepsilon} - \mu\phi_{q,k-1} \right) + H(\phi^*_{q,k}, \phi_{q,k-1}) \right). \end{aligned} \tag{2.32}$$

Thus in the functional-intergral notation the partition function takes the form

$$Z = \int\limits_{\phi_q(\beta)=\varsigma\phi_q(0)} D[\phi^*_q(t)\phi_q(t)] e^{-\frac{1}{\hbar}\int_0^{\beta\hbar} d\tau \left[\sum \phi^*_q(t)(\hbar\frac{\partial}{\partial\tau} - \mu)\phi_q(t) + H(\phi^*_q(t)\phi_q(t))\right]}. \tag{2.33}$$

The correct evaluation of expressions (2.31) or (2.33) is done by performing the path integral over the action S discretesised with respect to M imaginary-time steps

and then taking the limit $M \to \infty$. However, the Hubbard model discussed in the thesis is a purely fermionic model. The partition function (2.33) performed in this case will contain only the Grassmann variables, which due to the Hubbard interaction term can not be integrated out. Thus, the next chapter is devoted to another Fock-space representation, called the slave-bosons representation, in which by introducing new Bose and Fermi auxiliary fields, the Hubbard model becomes exactly integrable over the fermion degrees of freedom. The resultant expression in Bose fields is still to be evaluated by one of the many-body technique. In the simplest case of the saddle-point approximation the physical free energy is evaluated by minimization of the corresponding Bose functional with respect to the amplitudes of the condensed fields.

REFERENCES

[1] J.W. Negele and H. Orland, *Quantum Many-Particle Systems,* (Addison-Wesley, Redwood City, 1988); see also: C. Itzykson and J. B. Zuber, *Quantum Field Theory,* pp. 425-442 (McGraw-Hill, Inc., 1985).

Chapter 3

Slave-boson representation of the Hubbard model

3.1 Representation of Kotliar and Ruckenstein

The Hubbard Hamiltonian (1.3), is

$$H = \sum_{ij\sigma} t_{ij} c^{\dagger}_{i\sigma} c_{j\sigma} + U \sum_{i} c^{\dagger}_{i\uparrow} c_{i\uparrow} c^{\dagger}_{i\downarrow} c_{i\downarrow}, \tag{3.1}$$

where the Hilbert space $\mathcal{H}$, is a tensor product of Hilbert spaces $\mathcal{H}_i$, namely, $\mathcal{H} = \mathcal{H}_1 \otimes \mathcal{H}_2 \otimes ...$, where $\mathcal{H}_i$ can describe up to four electron; the corresponding Fock-states is assigned to every lattice site i contains the configuration: unoccupied, singly occupied with spin up or down, and doubly occupied. This can be written briefly as $\mathcal{H}_i \equiv \{|0_i\rangle_{ph}, |\uparrow_i\rangle_{ph}, |\downarrow_i\rangle_{ph}, |\uparrow\downarrow_i\rangle_{ph}\}$, where

$$|0_i\rangle_{ph} \equiv |0\rangle, \tag{3.2}$$

is the state with no electrons (empty site), and

$$|\uparrow_i\rangle_{ph} = c^\dagger_{i_\uparrow}|0\rangle\,, \tag{3.3}$$

$$|\downarrow_i\rangle_{ph} = c^\dagger_{i_\downarrow}|0\rangle\,, \tag{3.4}$$

$$|\uparrow\downarrow_i\rangle_{ph} = c^\dagger_{i_\uparrow}c^\dagger_{i_\downarrow}|0\rangle\,. \tag{3.5}$$

The four-fermion term appearing in (3.1) causes that the integration over Grassmann variables, when determining partition function, cannot be easily evaluated. Thus, the method of the functional integration can not be applied directly in this case. One needs to find another Fock-space representation, in which all the fermion degrees of freedom can be exactly integrated out .

In order to construct such a representation, let us assume that the physical processes due to the electron-electron interaction can be described in the Hilbert space rather then $\mathcal{H}$. Namely, the new Hilbert space $\mathcal{H}'$, with the vacuum state $|vac\rangle$, will contain fermionic as well bosonic degrees of freedom. Let us denote any state of the original Fock representation (3.2)-(3.5) as $|ph(n)_i\rangle$, where $n = 0, 1_\uparrow, 1_\downarrow, 2$, corresponds to the state with a different fermion occupation number . Similarly, let us denote by $|sb(n)_i\rangle$ an $n-$fermion state in the new representation. Since our main aim is to evaluate the partition function Z, it is sufficient to demand the equivalence of both representation in the sense of equality of corresponding matrix elements of the Hubbard Hamiltonian, evaluated between the corresponding states of both representations, namely

$$\langle ph(n)_i|H|ph(m)_j\rangle = \langle sb(n)_i|H_{sb}|sb(m)_j\rangle\,, \tag{3.6}$$

where H is simply the Hubbard Hamiltonian in the form (3.1), and H_{sb} denotes the

Hubbard Hamiltonian written in the new representation that belongs to $\mathcal{H}'$.

In the spirit of representations equivalence condition (3.6), Kotliar and Ruckenstein proposed the representation in which, to each of the four different fermion physical states we ascribe a different Bose field. In other words, we make the following mapping:

$$\mid 0_i\rangle_{ph} \longleftrightarrow \mid 0_i\rangle_{sb} = e_i^\dagger \mid vac\rangle\,, \tag{3.7}$$

$$\mid \uparrow_i\rangle_{ph} \longleftrightarrow \mid \uparrow_i\rangle_{sb} = f_{i\uparrow}^\dagger p_{i\uparrow}^\dagger \mid vac\rangle\,, \tag{3.8}$$

$$\mid \downarrow_i\rangle_{ph} \longleftrightarrow \mid \downarrow_i\rangle_{sb} = f_{i\downarrow}^\dagger p_{i\downarrow}^\dagger \mid vac\rangle\,, \tag{3.9}$$

$$\mid \uparrow\downarrow_i\rangle_{ph} \longleftrightarrow \mid \uparrow\downarrow_i\rangle_{sb} = f_{i\uparrow}^\dagger f_{i\downarrow}^\dagger d_i^\dagger \mid vac\rangle\,. \tag{3.10}$$

If one neglect Bose fields operators: $e^\dagger, p_\uparrow^\dagger, p_\downarrow^\dagger$ or $d^\dagger$, the resulting fermion representation is identical with the initial one (3.3)-(3.5). However, since the physical state is represented by a combination of fermions and boson operators, the quantities $f_{i\uparrow}$, $f_{i\downarrow}$ are pseudofermion fields and the fields e, p_σ, and d are auxiliary Bose fields. This is the Kotliar and Ruckenstein [1] representation. In order to express the Hubbard Hamiltonian in the new representation, one derives the following correspondence between the operators

$$c_{i\sigma}^\dagger c_{j\sigma} \rightarrow \begin{cases} \widetilde{z}_{i\sigma}^\dagger \widetilde{z}_{j\sigma} f_{i\sigma}^\dagger f_{j\sigma} & for \quad i \neq j, \\ f_{i\sigma}^\dagger f_{i\sigma} & for \quad i = j, \end{cases} \quad with \quad \widetilde{z}_{j\sigma} = e_j^\dagger p_{j\sigma} + p_{j\bar{\sigma}}^\dagger d_j, \tag{3.11}$$

and

$$n_{i\uparrow} n_{i\downarrow} \rightarrow d_i^\dagger d_i. \tag{3.12}$$

The above relations are easy to proof assuming that we consider only the physical states (3.7)-(3.10). The Hubbard Hamiltonian written in the Kotliar-Ruckenstein

representation takes then the form

$$H_{sb} = \sum_{ij\sigma} t_{ij} \widetilde{z}^{\dagger}_{i\sigma} \widetilde{z}_{j\sigma} f^{\dagger}_{i\sigma} f_{j\sigma} + U \sum_{i} d^{\dagger}_{i} d_{i} - \mu \sum_{i\sigma} f^{\dagger}_{i\sigma} f_{i\sigma}, \tag{3.13}$$

where $\sigma = \{\uparrow, \downarrow\}$. So, the new Hamiltonian H_{sb} does not contain four-fermion operator term any longer. Instead, it contains fermion-boson interaction in the hopping part. What is more important, (3.13) represents a properly defined field-theoretical model of interacting fields for an arbitrary value of U.

By replacing the Hilbert space $\mathcal{H}$ of fermions, by the Hilbert space $\mathcal{H}'$of pseudo fermions and auxiliary bosons, we have introduced additional states, which are not physical. In order to guarantee the physical meaning of $\mathcal{H}'$ one needs to impose constraints. To determine these constraints one needs to specify the characteristic features of the representation (3.7)-(3.10). First, each state on site i is occupied by one boson only, which may be expressed as a completeness condition

$$e^{\dagger}_{i} e_{i} + p^{\dagger}_{i_{\uparrow}} p_{i_{\uparrow}} + p^{\dagger}_{i_{\downarrow}} p_{i_{\downarrow}} + d^{\dagger}_{i} d_{i} - 1 = 0. \tag{3.14}$$

Next, with each single fermion field f_{σ} we associate one boson field p_{σ}. On the other hand, when site i is doubly occupied by spin up and down fermions, we associate with them one spinless d boson. These conditions are insured by the two more constraints, namely for $\sigma = \{\uparrow, \downarrow\}$ we have

$$f^{\dagger}_{i\bar{\sigma}} f_{i\sigma} - p^{\dagger}_{i\bar{\sigma}} p_{i\sigma} - d^{\dagger}_{i} d_{i} = 0. \tag{3.15}$$

The number of introduced additional bosonic fields is four. On the other hand, there are only three constraints, so one has an additional degree of freedom left. Thus,

the form of the Hamiltonian (3.13) is not unique. Any transformation defined as

$$\widetilde{z}_{i\sigma} \rightarrow z_{i\sigma} = U_{i\sigma}\widetilde{z}_{i\sigma}V_{i\sigma}, \tag{3.16}$$

which does not change the eigenvalues and eigenvectors of the $\widetilde{z}_{i\sigma}$ leads to the equivalent Hamiltonian and the same energy spectrum as long as the constraints are treated exactly. Effectively, one is left with one boson field which has to be determined variationally. We chose the field d for that purpose.

The mean-field approximation used in the following satisfies the constraints only on average and leads to different results, depending on the special choice of $z_{i\sigma}$. In other words, the transformation (3.16), which may be called the gauge transformation for the Hubbard model in the slave-boson representation, makes possible choosing the ground state properties and next to calculate quantum fluctuations around that state. The special choice of $z_{i\sigma}$ made by Kotliar and Ruckenstein [1] will be discussed in the next section. In fact, if one evaluate all quantum corrections it is assumed that the final result is independent on the choice of $z_{i\sigma}$.

In contrast to the original Fock representation, Eqs. (3.2)-(3.5), the slave-boson representation (3.7)-(3.10), does not express the spin-rotation invariance of the Hubbard Hamiltonian explicitly. In order to include this symmetry Li et al [2] introduced the generalized, spin-rotation invariant representation. In this representation the single electron state $|\sigma i>$ transforms as $SU(2)$ spinor and is defined as

$$|\sigma i> = \sum_{\sigma'} p^{\dagger}_{i\sigma\sigma'} f^{\dagger}_{i\sigma'} |vac>, \tag{3.17}$$

where $p^{\dagger}_{i\sigma\sigma'}$ is two-component Bose fields matrix defined as a linear combination of unity matrix (τ_0) multiplied by a scalar boson field p_{0i}, and the Pauli matrixes $\tau =$

(τ_1, τ_2, τ_3) multiplied respectively by three coordinates of the vector boson $\mathbf{p}_i = (p_{1i}, p_{2i}, p_{3i})$, namely

$$p_{i\bar{\sigma}\bar{\sigma}'} = p_{0i}\,(\tau_0)_{\sigma\sigma'} + \mathbf{p}_i \cdot (\boldsymbol{\tau})_{\sigma\sigma'}\,. \tag{3.18}$$

Spalek et al [3] showed that the fundamental commutation relations for the Bose fields (3.18) lead authomaticaly to the properly defined constraints. However, we choose the Kotliar-Ruckenstein representation as simpler. Both representations lead to the same results at the mean field level [4].

3.2 Free-energy functional in the saddle-point approximation

In order to calculate the partition function Z for the Hubbard Hamiltonian (3.13) one needs to express Z as a functional integral over coherent states of Fermi and Bose fields. The constraints (3.14)-(3.15) commute with the Hamiltonian (3.13) so, the physical Hilbert space is preserved under time evolution. The constraints are thus enforced at each lattice site by time-independent Lagrange multipliers denoted as $\lambda^{(1)}$, $\lambda^{(2)}_{\uparrow}$, and $\lambda^{(2)}_{\downarrow}$. The partition function can be thus written as

$$Z = \int D[f^{\dagger}_{\sigma} f_{\sigma}] D[e^{\dagger} e] D[p^{\dagger}_{\sigma} p_{\sigma}] D[d^{\dagger} d] \prod_{i\sigma} [d\lambda^{(1)}_i][d\lambda^{(2)}_{i\sigma}] e^{-\int_0^{\beta} d\tau L(\tau)} \tag{3.19}$$

where the Lagrangian is

$$\begin{aligned} L(\tau) \;=\; & \sum_i \left(e^{\dagger}_i(\tau) \frac{\partial}{\partial\tau} e_i(\tau) + \sum_{\sigma} \left(p^{\dagger}_{i\sigma}(\tau) \frac{\partial}{\partial\tau} p_{i\sigma}(\tau) \right) + d^{\dagger}_i(\tau) \left(\frac{\partial}{\partial\tau} + U \right) d_i(\tau) \right) \\ & + \sum_{ij\sigma} \left(t_{ij} f^{\dagger}_{i_\sigma} \tilde{z}^{\dagger}_{i_\sigma} \tilde{z}_{j_\sigma} f_{j_\sigma} \right) + \sum_{\sigma} \left(f^{\dagger}_{i\sigma}(\tau) \left(\frac{\partial}{\partial\tau} - \mu - \sigma H_a \right) f_{i\sigma}(\tau) \right) + \end{aligned}$$

$$+\sum_i \lambda_i^{(1)}\left(e_i^\dagger(\tau)e_i(\tau)+\sum_\sigma\left(p_{i\sigma}^\dagger(\tau)p_{i\sigma}(\tau)\right)+d_i^\dagger(\tau)d_i(\tau)-1\right)$$
$$+\sum_{i\sigma}\lambda_{i\sigma}^{(2)}\left(f_{i\sigma}^\dagger(\tau)f_{i\sigma}(\tau)-p_{i\sigma}^\dagger(\tau)p_{i\sigma}(\tau)-d_i^\dagger(\tau)d_i(\tau)\right). \qquad (3.20)$$

The chemical potential μ is adjusted to fix the average occupation number n (the band filling) at each site. Additionally, the electron energy in the external magnetic field $\mathbf{H}_a$ was included through the Zeeman term: $-\mu_B S_i^z H_a \equiv -\sigma H_a$, $(\sigma = \pm 1)$, where μ_B is Bohr magneton. This is because we can express the z-component of the spin operator as $S_i^z = \frac{1}{2}\left(f_{i_\uparrow}^\dagger f_{i_\uparrow} - f_{i_\downarrow}^\dagger f_{i_\downarrow}\right) = \frac{1}{2}\left(p_{i_\uparrow}^\dagger p_{i_\uparrow} - p_{i_\downarrow}^\dagger p_{i_\downarrow}\right)$, as can be seen explicitly fro the constraint (3.15).

By using the standard rules for integration over the Grassmann variables $f^\dagger, f$ (cf. Eq. (2.16)), one reexpresses Z in terms of the effective Lagrangian including exclusively Bose fields, namely

$$Z = \int D[e^\dagger e]D[p_\uparrow^\dagger p_\uparrow]D[p_\downarrow^\dagger p_\downarrow]D[d^\dagger d]\prod_{i\sigma}[d\lambda_i^{(1)}][d\lambda_{i\sigma}^{(2)}]e^{-\int_0^\beta d\tau L_{eff}(\tau)}, \qquad (3.21)$$

where

$$\begin{aligned} L_{eff}(\tau) &= \sum_i\left[e_i^\dagger(\tau)\left(\frac{\partial}{\partial\tau}+\lambda_i^{(1)}\right)e_i(\tau)+\sum_\sigma\left(p_{i\sigma}^\dagger(\tau)\left(\frac{\partial}{\partial\tau}+\lambda_i^{(1)}-\lambda_{i\sigma}^{(2)}\right)p_{i\sigma}(\tau)\right)\right] \\ &+\sum_i\left[d_i^\dagger(\tau)\left(\frac{\partial}{\partial\tau}+U+\lambda_i^{(1)}-\sum_\sigma\lambda_{i\sigma}^{(2)}\right)d_i(\tau)-\lambda_i^{(1)}\right] \\ &+Tr\ln\left[\left(t_{ij}\widetilde{z}_{i_\sigma}^\dagger\widetilde{z}_{j_\sigma}\right)+\delta_{ij}\left(\frac{\partial}{\partial\tau}-\mu-\sigma H_a+\lambda_{i\sigma}^{(2)}\right)\right]. \end{aligned} \qquad (3.22)$$

In the saddle point approximation all Bose fields and the Lagrange multipliers are taken to be independent of space and time. The special choice of $\widetilde{z}_{i_\sigma}$ (3.16) in this approximation unfortunately leads to the incorrect result in the metallic limit $(U \to 0)$. Namely, in this limit and for the half-filled case $(n = 1)$, the average value of

Bose fields are respectively $e^2 = p_\uparrow^2 = p_\downarrow^2 = d^2 = \frac{1}{4}$. Thus $< \widetilde{z}_{i_\sigma}^\dagger \widetilde{z}_{j_\sigma} >= \frac{1}{4}$ rather then unity, as should follow from the expression (3.1). Therefore, in the spirit of Gutzwiller solution, Kotliar and Ruckenstein [1] proposed the other choice of $\widetilde{z}_{i_\sigma}$, namely

$$\widetilde{z}_{i_\sigma} \rightarrow z_{i_\sigma} = \frac{1}{\sqrt{1 - p_{i_\sigma}^\dagger p_{i_\sigma} - d_i^\dagger d_i}} \widetilde{z}_{i_\sigma} \frac{1}{\sqrt{1 - p_{i_{\bar{\sigma}}}^\dagger p_{i_{\bar{\sigma}}} - d_i^\dagger d_i}}, \tag{3.23}$$

which already leads to the correct results in the case of metallic ($U = 0$) as well atomic ($W = 0$) limits.

Finally, the saddle-point free energy functional $F = N k_B T \ln Z + \mu N$ takes the form

$$\begin{aligned} \frac{F}{N} &= -k_B T \sum_\sigma \int d\varepsilon \rho(\varepsilon) \ln \left(1 + e^{-\beta(q_\sigma \varepsilon - \mu - \sigma h + \lambda_\sigma^{(2)})}\right) + U d^2 \\ &\quad -\lambda^{(1)} \left(1 - e^2 - p_\uparrow^2 - p_\downarrow^2 - d^2\right) - \sum_\sigma \lambda_\sigma^{(2)} (p_\sigma^2 + d^2) + \mu n, \end{aligned} \tag{3.24}$$

where $q_\sigma = \langle z_{i_\sigma}^\dagger z_{j_\sigma} \rangle$, and $\rho(\varepsilon)$ is the density of states for bare electrons.

The importance of the factor q_σ derives from the fact that at the mean field level it describes the quasiparticle properties due to the electron correlations.. Furthermore, q_σ strictly corresponds to the band narrowing factor $\Phi(\eta)$ (1.23), discussed by Spałek [5], now placed in the framework of quantum field theory. In the next chapter we show that the saddle-point approximation is equivalent to the Gutzwiller solution in the paramagnetic phase. However, this new solution contains also features going beyond the original Gutzwiller results.

REFERENCES

[1] G. Kotliar and A.R. Ruckenstein, *Phys. Rev. Lett.* **57**, 1362 (1986).

[2] T.Li, P. Wölfle and P.J. Hirschfeld, *Phys. Rev.* **B40**, 6817 (1989); R. Frésard and P. Wölfle, *Int. J. Mod. Phys.* **B6**, 237 (1992); **B6**, 3087(E) (1992).

[3] J. Spałek, unpublished.

[4] see e.g. J. Spałek and W. Wójcik in *Spectroscopy of Mott Insulators and Correlated metals*, ed. by A. Fujimori and Y. Tokura (Springer-Verlag, Berlin, 1995) pp. 41-65.

[5] J. Spałek, A. Datta and J.M. Honig, *Phys. Rev. Lett.* **59**, 728 (1987); J. Spałek, M. Kokowski and J.M. Honig, *Phys. Rev.* **B39**, 4175 (1989).

Chapter 4

Mean-field solution for the Hubbard model within the slave-boson approach

4.1 System of mean-field equations

The starting point is the functional (3.24). In the saddle-point approximation the quasiparticle-energy renormalization factor q_σ in the uniformly polarized state takes the form

$$q_\sigma = \frac{e^2 p_\sigma^2 + d^2 p_{\bar{\sigma}}^2 + 2edp_\sigma p_{\bar{\sigma}}}{(1 - d^2 - p_\sigma^2)(1 - e^2 - p_{\bar{\sigma}}^2)}, \tag{4.1}$$

where e, p_σ and d are now the real variables still to be determined. It is convenient to introduce new variables which we denote as p^2, m, λ_0 and β_m, defined as

$$\begin{aligned} 2p^2 &= p_\uparrow^2 + p_\downarrow^2 \quad , & m &= p_\uparrow^2 - p_\downarrow^2, \\ 2\lambda_0 &= \lambda_\uparrow^{(2)} + \lambda_\downarrow^{(2)}, & 2\beta_m &= \lambda_\uparrow^{(2)} - \lambda_\downarrow^{(2)}, \end{aligned} \tag{4.2}$$

which gives

$$\begin{aligned} p_\sigma^2 &= p^2 + \tfrac{1}{2}\sigma m, \\ \lambda_\sigma^{(2)} &= \lambda_0 - \sigma\beta_m. \end{aligned} \tag{4.3}$$

The functional (3.24) written again in the new variables takes the form

$$\begin{aligned} \frac{F}{N} &= Ud^2 + \mu n - \frac{k_B T}{N}\sum_{k\sigma} \ln\left(1 + e^{-\beta(q_\sigma \varepsilon_k - \mu + \lambda_0 - \sigma(H_a - \beta_m))}\right) \\ &\quad -\lambda^{(1)}\left(1 - e^2 - 2p^2 - d^2\right) \\ &\quad -(\lambda_0 - \beta_m)(p^2 + \frac{m}{2} + d^2) - (\lambda_0 + \beta_m)(p^2 - \frac{m}{2} + d^2), \end{aligned} \tag{4.4}$$

with q_σ defined now as

$$q_\sigma = \frac{e^2(p^2 + \sigma\frac{m}{2}) + d^2(p^2 - \sigma\frac{m}{2}) + 2ed\sqrt{p^4 - m^2}}{\left(1 - d^2 - (p^2 + \sigma\frac{m}{2})\right)\left(1 - e^2 - (p^2 - \sigma\frac{m}{2})\right)}. \tag{4.5}$$

So, the free energy functional depends on eight parameters: $\{\lambda^{(1)}, \lambda_0, p, m, \beta_m, e, d, \mu\}$ $\equiv \{x_i\}$,which are determined from the saddle point equations: $\partial F/\partial x_i = 0$, $i = 1, ..., 8$.

The minimization of the free-energy functional with respect to $\lambda^{(1)}$ and λ_0 yields

$$\frac{1}{N}\frac{\partial F}{\partial \lambda^{(1)}} = e^2 + 2p^2 + d^2 - 1 = 0, \tag{4.6}$$

and

$$\frac{1}{N}\frac{\partial F}{\partial \lambda_0} = n_\uparrow + n_\downarrow - 2(p^2 + d^2) = 0, \tag{4.7}$$

where

$$n_\sigma = \frac{1}{N}\sum_{\mathbf{k}} \frac{1}{e^{\beta(\widetilde{E}_{\mathbf{k}\sigma}-\mu)}+1} \equiv \frac{1}{N}\sum_{\mathbf{k}} f(\widetilde{E}_{\mathbf{k}\sigma}), \tag{4.8}$$

is the average number of particles with spin σ per lattice site, and the quasiparticle energy is

$$\widetilde{E}_{\mathbf{k}\sigma} = q_\sigma \varepsilon_{\mathbf{k}} + \lambda_0 - \sigma(H_a - \beta_m). \tag{4.9}$$

Note that the quantity $H_a - \beta_m$ is the effective magnetic field acting on the spin degrees of freedom. It is a molecular field. Similarly, the conditions for μ and the field β_m yields

$$\frac{1}{N}\frac{\partial F}{\partial \mu} = -n_\uparrow - n_\downarrow + n = 0, \tag{4.10}$$

and

$$\frac{1}{N}\frac{\partial F}{\partial \beta_m} = n_\uparrow - n_\downarrow - m = 0. \tag{4.11}$$

So, m is the magnetic moment per site.

Eqs. (4.6)-(4.11) can be written again in the simplified form using the obtained relations

$$p^2 = \frac{n}{2} - d^2, \tag{4.12}$$

$$e^2 = 1 - n + d^2, \tag{4.13}$$

$$n = n_\uparrow + n_\downarrow, \tag{4.14}$$

and

$$m = n_\uparrow - n_\downarrow. \tag{4.15}$$

The functional (4.4) takes then simplified form

$$\frac{F}{N} = -\frac{k_B T}{N}\sum_{\mathbf{k}\sigma} \ln\left(1 + e^{-\beta(\widetilde{E}_{\mathbf{k}\sigma}-\mu)}\right) + Ud^2 + (\mu - \lambda_0)n + m\beta_m, \tag{4.16}$$

where q_σ factor included in the quasiparticle energy (4.9) is now written as

$$q_\sigma = \frac{4\left(\frac{n}{2}-d^2\right)\left(1-n+2d^2\right)+8\sqrt{\left(d^2(1-n)+d^4\right)\left(\left(\frac{n}{2}-d^2\right)^2-\frac{m^2}{4}\right)}}{\left(n(2-n)-m^2\right)+\sigma\left(2m(1-n)\right)}. \tag{4.17}$$

In the low-temperature regime the functional (4.16) can be expressed in terms of effective band energy and entropy contributions. Explicitly

$$\frac{F}{N} = \frac{E_B}{N} - TS, \tag{4.18}$$

where the band energy per lattice site is

$$\frac{E_B}{N} = \frac{1}{N}\sum_{\mathrm{k}\sigma}\widetilde{E}_{\mathrm{k}\sigma}\left(\frac{1}{e^{\beta\left(\widetilde{E}_{\mathrm{k}\sigma}-\mu\right)}+1}\right) + Ud^2 + (\mu-\lambda_0)n + m\beta_m, \tag{4.19}$$

and the entropy

$$S = -\frac{1}{N}\sum_{\mathrm{k}\sigma}\left[f\left(\widetilde{E}_{\mathrm{k}\sigma}\right)\ln f\left(\widetilde{E}_{\mathrm{k}\sigma}\right) + \left(1-f\left(\widetilde{E}_{\mathrm{k}\sigma}\right)\right)\ln\left(1-f\left(\widetilde{E}_{\mathrm{k}\sigma}\right)\right)\right]. \tag{4.20}$$

The expression (4.16) can be simplified further. By introducing the spin-dependent chemical potential

$$\mu_\sigma \equiv \mu^{(1)} + \sigma\mu^{(2)} = (\mu-\lambda_0) + \sigma(H_a-\beta_m), \quad \sigma = \pm 1, \tag{4.21}$$

the band energy (4.19) can be written as

$$\begin{aligned}\frac{E_B}{N} &= \frac{1}{N}\sum_{\mathrm{k}\sigma}\left(q_\sigma\varepsilon_{\mathrm{k}}-\mu_\sigma\right)\left(\frac{1}{e^{\beta\left(q_\sigma\varepsilon_{\mathrm{k}}-\mu_\sigma\right)}+1}\right) + Ud^2 + \mu^{(1)}n - \left(H-\mu^{(2)}\right)m \\ &= \frac{1}{N}\sum_{\mathrm{k}\sigma}E_{\mathrm{k}\sigma}f_\sigma\left(E_{\mathrm{k}\sigma}\right) - Hm + Ud^2 + \mu^{(1)}n + \mu^{(2)}m - \mu_\uparrow n_\uparrow - \mu_\downarrow n_\downarrow. \end{aligned} \tag{4.22}$$

Here $E_{\mathrm{k}\sigma} \equiv q_\sigma\varepsilon_{\mathrm{k}}$, is now an effective quasiparticle energy and due to the dependence of the spin of μ_σ, the Fermi-Dirac distribution function f_σ is now also spin-dependent, namely

$$f_\sigma(\epsilon) = \frac{1}{e^{\beta(\epsilon-\mu_\sigma)}+1}. \tag{4.23}$$

One can easily check that due to the Eqs. (4.21) and (4.14) last four terms in (4.22) cancels out so the free energy functional finally takes the transparent form

$$\frac{F}{N} = \sum_{\mathrm{k}\sigma} E_{\mathrm{k}\sigma} f_\sigma(E_{\mathrm{k}\sigma}) + Ud^2 - H_a m - TS. \tag{4.24}$$

Note that $f(\widetilde{E}_{\mathrm{k}\sigma}) \equiv f_\sigma(E_{\mathrm{k}\sigma})$, so the entropy term is authomaticaly expressed through the spin-dependent Fermi-Dirac function (4.23).

Expression (4.24) essentially represents the free energy for noninteracting fermions, with quasiparticle energies $E_{\mathbf{k}\sigma}$ subjected to self-consistently adjusted fields (*i.e.*, they are obtained via the minimization with respect to d and m). Indeed, the parameters $\mu - \lambda = \mu^{(1)}$ and $H_a - \beta_m = \mu^{(2)}$, appearing in the chemical potential μ_σ can be expressed as a functions of the magnetization m and the average particle number n, by solving the system of equations (4.14) and (4.15), which can be written again in explicit form

$$n = \frac{1}{N}\sum_{\mathrm{k}} f_\uparrow(E_{\mathrm{k}_\uparrow}) + \frac{1}{N}\sum_{\mathrm{k}} f_\downarrow(E_{\mathrm{k}_\downarrow}), \tag{4.25}$$

$$m = \frac{1}{N}\sum_{\mathrm{k}} f_\uparrow(E_{\mathrm{k}_\uparrow}) - \frac{1}{N}\sum_{\mathrm{k}} f_\downarrow(E_{\mathrm{k}_\downarrow}). \tag{4.26}$$

The Eqs. (4.24), (4.25),(4.26) along with the conditions

$$\frac{1}{N}\frac{\partial F}{\partial d} = 0, \tag{4.27}$$

and

$$\frac{1}{N}\frac{\partial F}{\partial m} = 0, \tag{4.28}$$

create a closed system of algebraic equations. The solution of that system allows to express the magnetization m, the probability of double occupancy d^2, the molecular

field β_m, as well as q_σ, as the functions of three parameters U, H_a and n. However, there are still two parameters left, namely p^2 and e, for which the free-energy minimum conditions were not used so far. These two additional equations, along with the previously obtained results, allow to determine the proper chemical potential μ of the system.

By minimizing the free energy functional (4.4) with respect to p^2 and e fields, one obtains respectively

$$\frac{1}{N}\frac{\partial F}{\partial p^2} = \sum_{k\sigma} \varepsilon_k f_\sigma(q_\sigma \varepsilon_k)\frac{\partial q_\sigma}{\partial p^2} - 2\lambda^{(1)} - 2\lambda_0 = 0, \tag{4.29}$$

and

$$\frac{1}{N}\frac{\partial F}{\partial e} = \sum_{k\sigma} \varepsilon_k f_\sigma(q_\sigma \varepsilon_k)\frac{\partial q_\sigma}{\partial e} - 2\lambda^{(1)} e = 0. \tag{4.30}$$

By evaluating of $\lambda^{(1)}$ from the Eq. (4.29) and substituting it to Eq. (4.30) one obtains the expression for λ_0, namely

$$\lambda_0 = \sum_{k\sigma} \varepsilon_k f_\sigma(q_\sigma \varepsilon_k)\frac{1}{2}\left(\frac{\partial q_\sigma}{\partial p^2} - \frac{1}{e}\frac{\partial q_\sigma}{\partial e}\right). \tag{4.31}$$

Since $\mu^{(1)}$ defined in Eq. (4.21) is assumed to be already a function of known parameters, the final formula for the chemical potential is

$$\mu = \mu^{(1)} + \sum_{k\sigma} \varepsilon_k f_\sigma(q_\sigma \varepsilon_k)\frac{1}{2}\left[\left(\frac{\partial q_\sigma}{\partial P} - \frac{1}{e}\frac{\partial q_\sigma}{\partial e}\right)_{e=\sqrt{1-n+d^2},\quad p^2=\frac{n}{2}-d^2}\right]. \tag{4.32}$$

In the next section we show that the above system of equations may be solved exactly in the case when $T = 0$ and for the constant density of states.

4.2 Mean-field solution for the paramagnetic ground state

The following derivation is limited to the case when $T = 0$ and the bare density of states takes the featureless form:

$$\rho(\varepsilon) = \begin{cases} \frac{1}{W} & for \quad -\frac{W}{2} \leqslant \varepsilon \leqslant \frac{W}{2} \\ 0 & otherwise. \end{cases} \tag{4.33}$$

The center of gravity of the band is thus chosen as zero of energy scale.

Under the assumptions, the average number of particles with spin σ, (4.8) is

$$n_\sigma = \frac{1}{W} \int_{-\frac{W}{2}}^{\frac{W}{2}} d\varepsilon f_\sigma(q_\sigma \varepsilon_{\mathbf{k}}) = \frac{1}{2} + \frac{\mu_\sigma}{W q_\sigma}. \tag{4.34}$$

Eq. (4.34) combined with Eqs. (4.25) and (4.26) allows to evaluate the quantities $\mu^{(1)}$ and $\mu^{(2)}$ defined in (4.21), namely

$$\mu^{(1)} \equiv \mu - \lambda_0 = \frac{W}{4} \left[\left(q_\uparrow + q_\downarrow \right) (n-1) + \left(q_\uparrow - q_\downarrow \right) m \right], \tag{4.35}$$

and

$$\mu^{(2)} \equiv H_a - \beta_m = \frac{W}{4} \left[\left(q_\uparrow - q_\downarrow \right) (n-1) + \left(q_\uparrow + q_\downarrow \right) m \right], \tag{4.36}$$

which in turn allow to express μ_σ as a function of d^2, m and n. Thus, performing the summation in Eq. (4.24) one obtains the free energy functional in the form

$$\begin{aligned} \frac{F}{N} &= \sum_\sigma \frac{1}{W} \int_{-\frac{W}{2}}^{\mu_\sigma} d\varepsilon (q_\sigma \varepsilon) + U d^2 - H_a m \\ &= \frac{1}{8} W \sum_\sigma \left(q_\sigma \left((n - 1 + \sigma m)^2 - 1 \right) \right) + U d^2 - H_a m. \end{aligned} \tag{4.37}$$

Next, introducing dimensionless variables $u \equiv U/2W$, $h \equiv \mu_B H_a/W$, and the free energy per lattice site in units of the bandwidth W, $f \equiv F/NW$, one can rewrite the Eq. (4.37) as

$$f = 2ud^2 - hm - \frac{1}{2}\left(1 - n + 2d^2\right) - \sqrt{\left(d^2(1-n) + d^4\right)\left((n-2d^2)^2 - m^2\right)}. \quad (4.38)$$

Minimization of f with respect to magnetization, Eq. (4.27), yields

$$m = \frac{h\,(n-2d^2)}{\sqrt{h^2 + d^4 + d^2\,(1-n)}}. \quad (4.39)$$

Substituting this expression into Eq. (4.38) one obtains the free-energy functional dependent only on one unknown parameter $d^2 \equiv \eta$. Finally, the condition (4.28) leads to the third order algebraic equation on η variable, namely

$$\begin{aligned} 0 \;=\; & \eta^3(-64u) + \eta^2(-16u^2 - 80u + 96un) \\ & + \eta\,(16h^2 + 8n - 4n^2 - 16u - 64h^2u + 48nu - 32n^2u - 16u^2 + 16nu^2 - 4) \\ & + 16h^4 - 4h^2 + 8h^2n + n^2 - 8h^2n^2 - 2n^3 + n^4 - 16h^2u \\ & + 32h^2nu - 16h^2u^2. \end{aligned} \quad (4.40)$$

Since Eq. (4.40) has analytic solutions, all the quantities determined above can be also expressed as functions of parameters u, h and n. In general, the solutions are too complicated to be shown here. So, apart from the case $n = 1$ and $h = 0$, all other solutions for $n \neq 1$ and $h \neq 0$ will by displayed graphically.

4.3 Properties of almost localized Fermi liquid and the Mott-Hubbard localization

In the simplest case of $n = 1, h = 0$ Eq. (4.40) leads to

$$d^2 = \frac{1}{4}(1 - u)\,. \tag{4.41}$$

Since $u \equiv U/2W$, the value of $U = U_c \equiv 2W$ is the critical value of the repulsion potential U, i.e. it corresponds to the vanishing of the number of doubly occupied sites. Thus, it indicates that the system is undergoing a metal-insulator transition. The result was obtained by Brinkman and Rice [1] by using the variational wave function and the approximation scheme proposed by Gutzwiller [2], discussed in Chapter 1. Indeed, substituting the solution (4.41) (cf. Eq. (1.16)) into the free energy (4.38) and q_σ (4.17), Eqs. (1.17) and (1.18) are authomaticaly reproduced. Note that in the paramagnetic case, q_σ does not depends on spin: $q_\uparrow = q_\downarrow \equiv q$. In the case of $n \neq 1$, the electron localization does not appear and the average number of doubly occupied sites goes to zero only in the limit $u \to \infty$. This effect is displayed in Fig. 4.1. The situation $d^2 \to 0$ for $n = 1$ corresponds to the effective mass divergence, with $U \to U_c$. In all other cases i.e. for $n \neq 1$, effective mass enhancement m^*/m_B approaches to the finite value $(2 - n)/(2(1 - n))$ as $U \to \infty$. The effective mass enhancement with respect to the band mass m_B is displayed in Fig. 4.2. Similarly, the linear specific heat coefficient is divergent at $U = U_c$ only in the case $n = 1$. The singularity of the spin susceptibility (1.16) displayed in Fig. 4.3 shows that the metal-insulator transition is a continuous quantum phase transition.

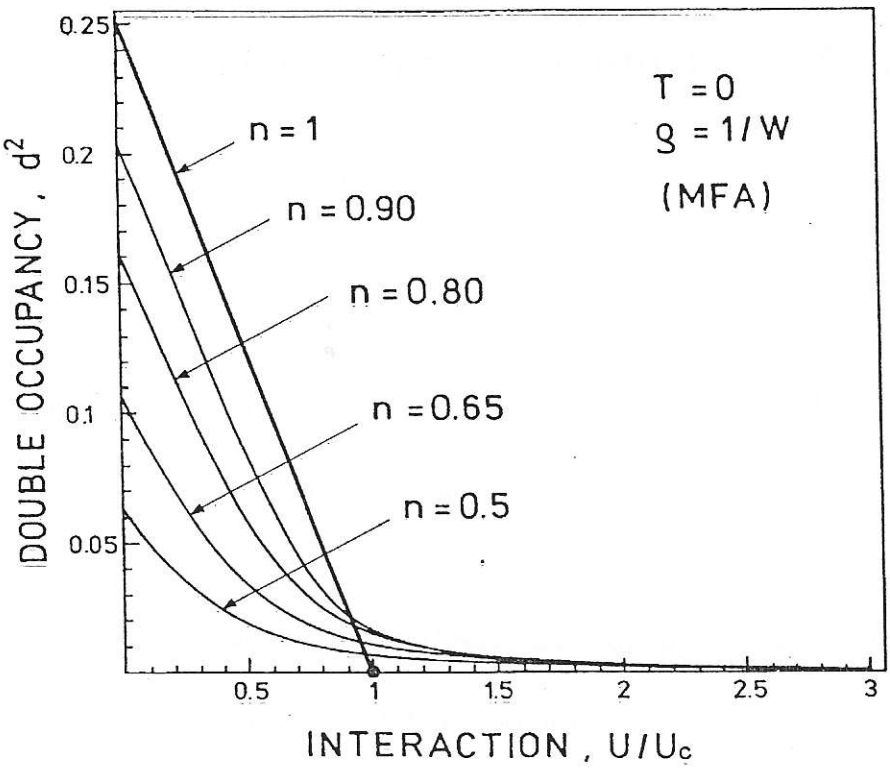

Figure 4.1: The double occupancy probability for the different band fillings as a function of the relative interaction strenght U/U_c.

Introducing the band narrowing factor q_σ, defined as in Eq. (3.24), Kotliar and Ruckenstein recovered the Brinkman-Rice transition but now at the level of the saddle point approximation. Such a theoretical description allows to investigate the dynamical aspect of the problem, which of course goes beyond the Gutzwiller variational scheme [3] . However, as it was mentioned by Lavagna , even at the mean field level the new information are contained within the saddle-point equations as compared with the Gutzwiller approximation. The manifestation of that fact is the presence of the Mott-Hubbard gap. To see how this gap can arise one may choose the density of

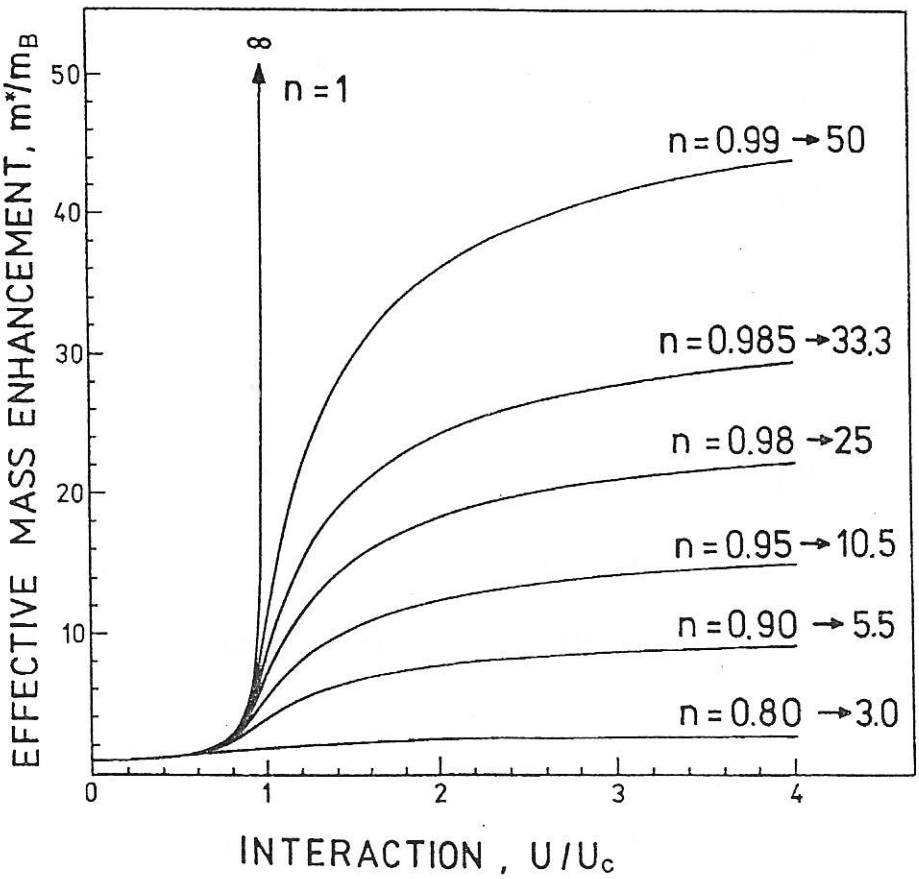

Figure 4.2: The interaction dependence of the effective mass. The m* diverges at n=1 and U/U_c=1. This is the Mott-Hubbard localization.

states function in the form of (4.33) and calculate the chemical potential μ. In this case μ is determined by the Eq.(4.35), where due to Eq.(4.31) λ_0 is given by

$$\begin{aligned}\lambda_0 &= \sum_\sigma \frac{1}{2Wq_\sigma^2}\left(\frac{\partial q_\sigma}{\partial P} - \frac{1}{e}\frac{\partial q_\sigma}{\partial e}\right) \int_{-\frac{W}{2}q_\sigma}^{+\frac{W}{2}q_\sigma} d\varepsilon\, \varepsilon f_\sigma(q_\sigma \varepsilon) \\ &= \sum_\sigma \frac{1}{2Wq_\sigma^2}\left(\frac{\partial q_\sigma}{\partial P} - \frac{1}{e}\frac{\partial q_\sigma}{\partial e}\right)\left(\mu_\sigma^2 - \frac{W^2}{4}q_\sigma^2\right). \qquad (4.42)\end{aligned}$$

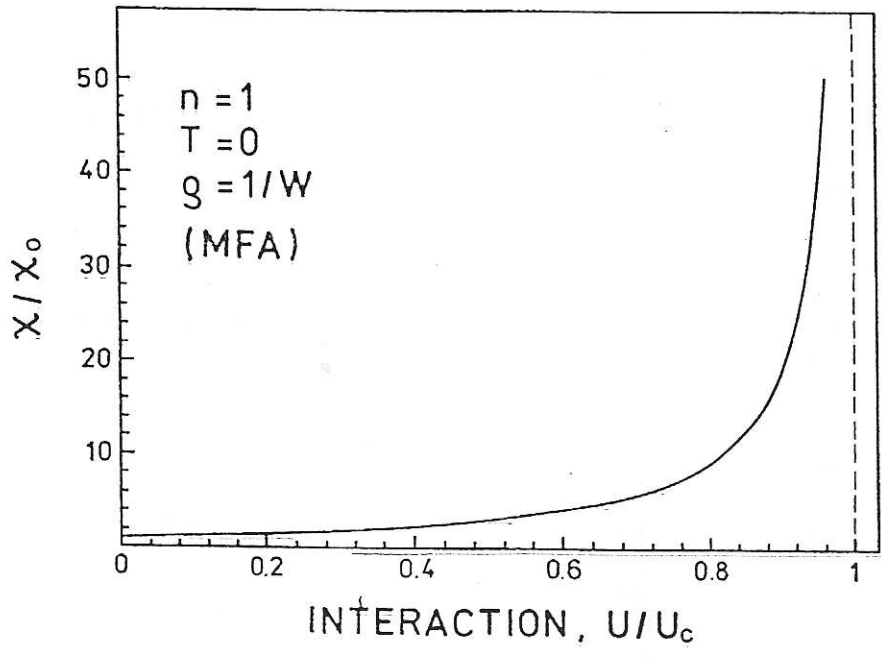

Figure 4.3: The spin susceptibility enchancement in the function of the interaction U/U_c. Its divergence at $U=U_c$ illustrates the fact that the Mott-Hubbard localization is a quantum phase transition.

Thus, the chemical potential in units of bandwidth takes the form

$$\frac{\mu}{W} = \frac{\mu^{(1)}}{W} - \sum_{\sigma} \left(\frac{1}{8} - \frac{\mu_\sigma^2}{2q_\sigma^2 W^2} \right) \alpha_\sigma, \tag{4.43}$$

where

$$\frac{\mu^{(1)}}{W} = \frac{1}{4} \left[\left(q_\uparrow + q_\downarrow \right) (n-1) + \left(q_\uparrow - q_\downarrow \right) m \right], \tag{4.44}$$

and

$$\alpha_\sigma = \left(\frac{\partial q_{\bar{\sigma}}}{\partial P} - \frac{1}{e} \frac{\partial q_\sigma}{\partial e} \right)_{e=\sqrt{1-n+d^2},\quad P=\frac{n}{2}-d^2}. \tag{4.45}$$

The apperance of Mott-Hubbard gap may be visualized as the splitting of the chemical potential when approaching the $n = 1$ limit either $n_+ = 1 + \epsilon$ or $n_- =$

$1-\epsilon$ sides ($\epsilon \to 0$). This splitting appears only when $U > U_c$, as displayed in Fig. 4.4, where the chemical potential (4.43) was calculated for the cases $n = 0.999$ and $n = 1.001$. Lavagna [4] showed that the width of the gap is $\Delta = U\sqrt{1 - U_c/U}$. This

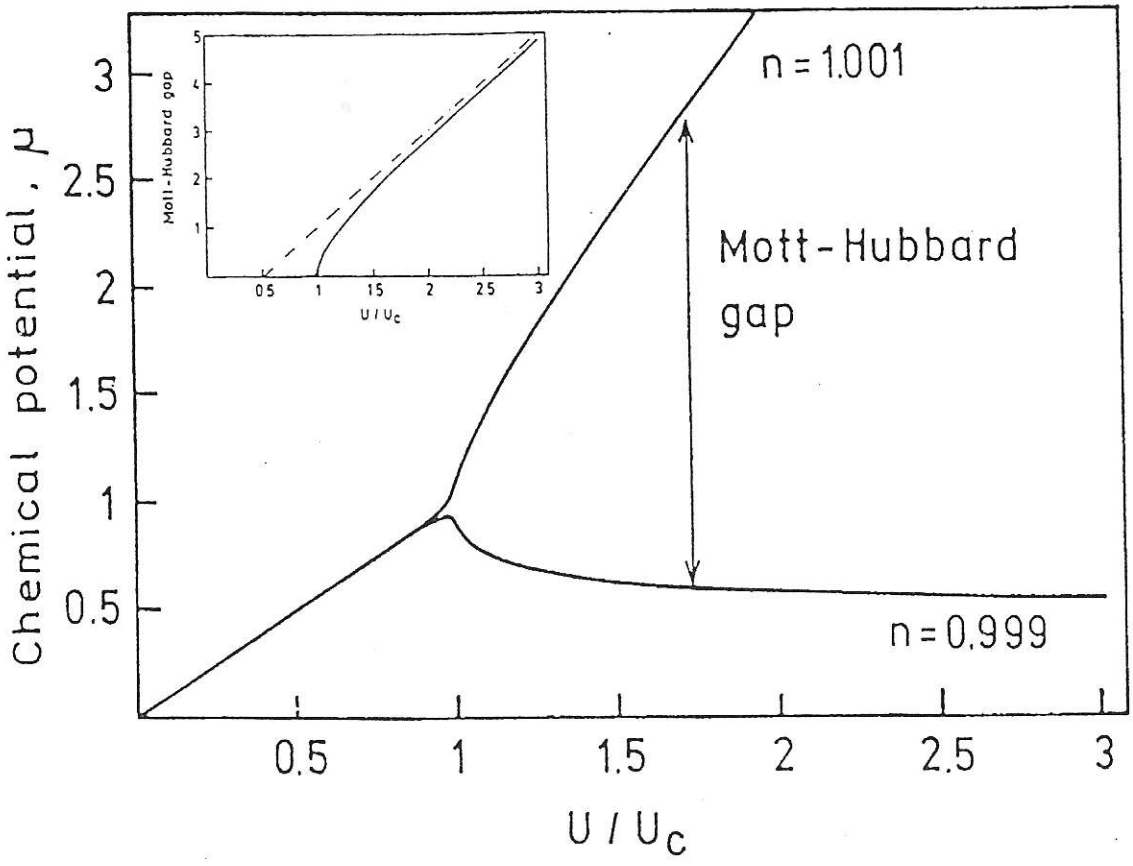

Figure 4.4: Opening of the Mott-Hubbard gap for U>U_c. The inset shows the U dependence of the gap.

result reproduces the split band picture obtained in Hubbard III solution discussed in Chapter 1. However, the slave boson approach provides one feature more: the infinite-mass enhancement in the lower band when $U \to U_c$ (from metallic side). In

summary, we have combined here the old results of Brinkman and Rice [1] with those of Lavagna [4] concerning the metal-insulator transition in the paramagnetic case.

REFERENCES

[1] W.F. Brinkman and T.M. Rice, Phys. Rev. **B2,** 4302 (1970).

[2] M.C. Gutzwiller, *Phys. Rev. Lett.* **10**, 159 (1963); *Phys. Rev.* **134**, A932; *Phys Rev.* **137**, A1726 (1965).

[3] M. Lavagna, *Helvetica Phys. Acta* **63**, 310 (1990); J. W. Rasul and T. C. Li, *J. Phys.* **C21**, 5119 (1988); T. C. Li and J.W. Rasul, *Phys. Rev.* **B39**, 4630 (1989).

[4] M. Lavagna *Phys. Rev.* **B41**, 142 (1990).

Chapter 5

Almost localized fermions in an applied magnetic field

In systems close to the Mott-Hubbard localization the band energy of quasiparticles is small (the effective mass $m^* \to \infty$) and almost compensated by the short-range repulsive interaction among the carriers [1]. In effect, the system is very susceptible to much weaker perturbations such as temperature or the applied magnetic field. In this chapter the novel features of almost localized fermions in the presence of an applied magnetic field are discussed, namely: (i) the spin dependence of the quasiparticle effective mass, which leads to quantum beats in the de Haas-van Alphen effect, and (ii) the appearance of a nonlinear molecular field and related metamagnetic behavior of the system.

5.1 Nonlinear molecular field and metamagnetism

The mean field solution of the Hubbard model for the case $T = 0$ and constant bare density of states is given by the Eq. (4.40). All the other quantities appearing in the problem can be expressed as the functions of $\eta \equiv d^2$, and thus regarded as functions of parameters u, n and h (cf. section 4.3). Physically, this approach depends on the number of doubly occupied sites d^2N, which plays the role of the order parameter distinguishing the Fermi liquid (metallic) state (when $d^2 \neq 0$) from the local-moment state (when $d^2 = 0$ and $m = n$). For $n = 1$ the latter state describes the Mott insulator in the mean-field approximation and without the exchange interactions.

We start our analysis of the behavior of the number of doubly occupied sites and strictly related with it magnetization through. In Fig. 5.1 we have displayed d^2 and m, both as a function of h, for $u = 0.95$. In Fig. 5.1(bottom) we see that for $n = 0.9$ and 0.95 the applied magnetic field reduces to zero the number of doubly occupied sites in a continuous way. For the case $n = 0.99$ the value of d^2 discontinuously drops to zero when the critical value of magnetic field, h_c, is reached. This corresponds to the metamagnetic transition displayed in Fig. 5.1 (top). The magnetization curve (which in contrary to the case of localized moments turns upward) reaches the magnetic saturation by the discontinuous way. For the cases $n = 0.95$ and $n = 0.9$ the magnetic field saturates the system continuously. In this case we say that system exhibits the metamagnetic behavior. The metamagnetic behavior is also displayed in Fig. 5.2. Only the inset displays the true metamagnetism for $n = 1$ (discussed in detail by Vollhardt [2]).

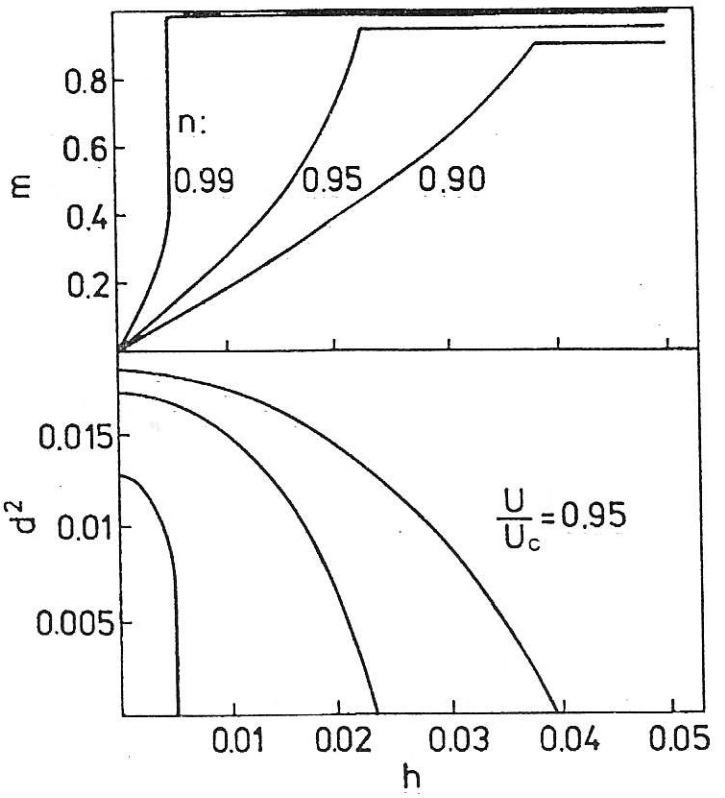

Figure 5.1: Field dependent magnetization (top) and double-occupancy (bottom), for $U/U_c = 0.95$ and three band fillings $n = 0.90$, 0.95, and 0.99.

The first-order metamagnetic transition disappears very rapidly when n deviates from unity. Nonetheless, the metamagnetic behavior persists over a substantial range of the filling. The metamagnetism is caused by a change in the nature of the ground state from the Fermi liquid state of heavy quasiparticle to a state of itinerant (for $n < 1$) or localized (for $n = 1$) spins. The discontinuity in $\chi \equiv dm/dh$ for $m \rightarrow 1$ is smeared out for $T > 0$, and the susceptibility then has a maximum when the system approaches magnetic saturation. The critical field for saturation is strongly reduced as $n \rightarrow 1$, making this phenomenon observable for the extremely narrow band systems

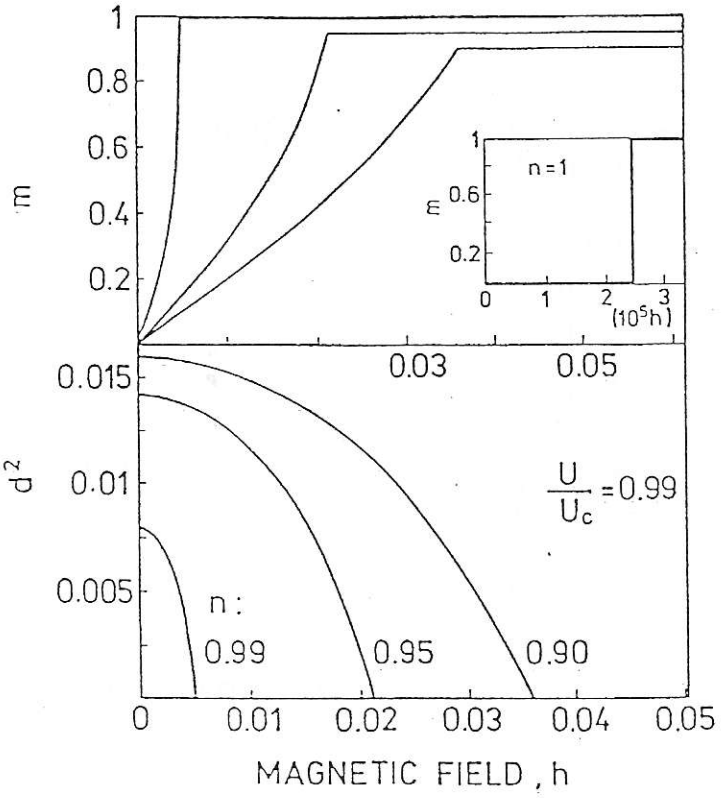

Figure 5.2: Field dependent magnetization (top) and double-occupancy (bottom), for $U/U_c = 0.99$ and three band fillings $n = 0.90$, 0.95, and 0.99. The inset displays the metamagnetism for the half-filled ($n = 1$) case.

such as heavy fermions or liquid ^{3}He. In ^{3}He a small number $\delta \sim 0.01$ of zero-point vacancies is sufficient to render the magnetization curve continuous.

In Fig. 5.3 we have summarized the type of magnetic behavior in the applied field assuming that the paramagnetic state is stable for $h = 0$ [3]. The upper panel characterizes the magnetic saturation field h_c if the magnetization process is continuous. This profile does not reflect the actual situation when a metamagnetic transition takes place, as specified by the dark area in the lower panel. True metamagnetism

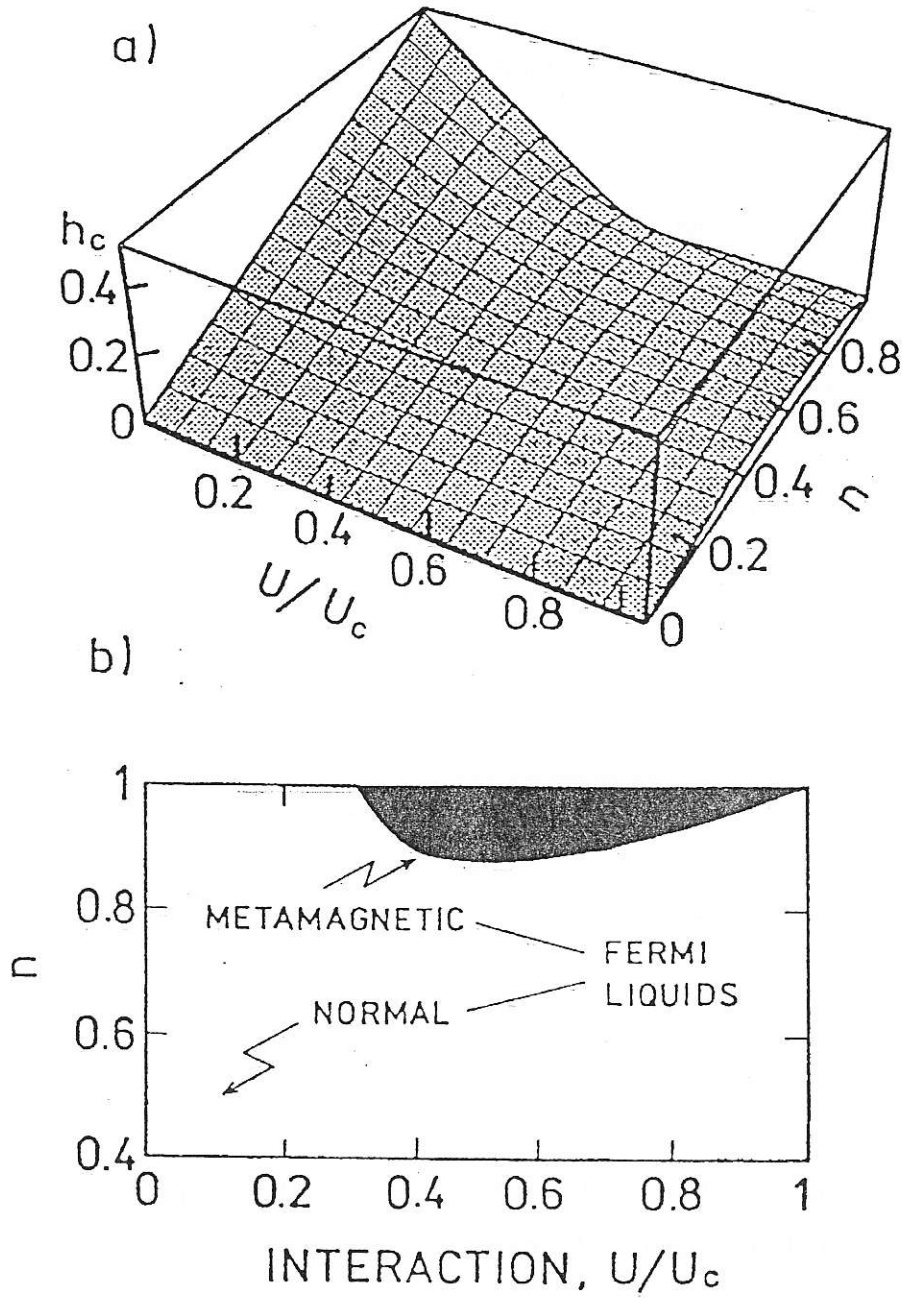

Figure 5.3: Critical field for magnetic saturation via a continuous magnetization (top), and the regime of metamagnetism (dark area in the bottom part). All points are drawn for $T = 0$.

occurs only for $n \geq 0.8$ and for $u \geq 0.28$. At low fillings and for small values of u one recovers the normal Fermi liquid behavior, since the interaction part varies roughly as $Un^2/4$.

The metamagnetic behavior is strictly related with the presence of nonlinear molecular field $\beta_m = \frac{1}{2}(\lambda_\uparrow - \lambda_\downarrow)$, Eq. (4.2). For the considered density of states (4.33) for bare electrons, Eqs. (4.25) and (4.26) allows to express β_m by the equation

$$\delta \equiv -\frac{\beta_m}{W} = \frac{1}{4}\left[(q_\uparrow - q_\downarrow)(n-1) + (q_\uparrow + q_\downarrow)\, m\right] - h. \tag{5.1}$$

To determine the character of the spin-splitting we have plotted in Fig.5.4 the magnetization (a) and field (b) dependences of the spin-splitting. This provides us

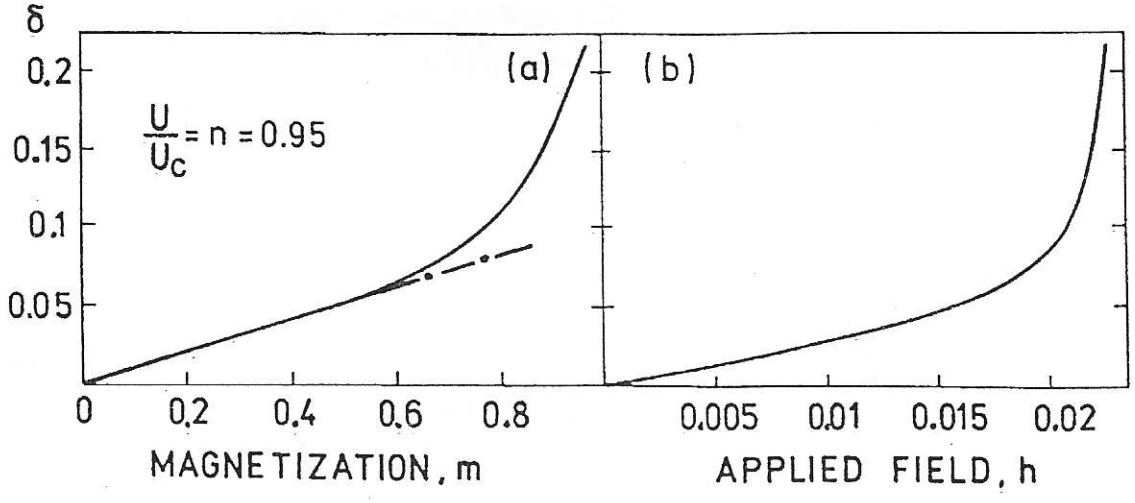

Figure 5.4: The effective field δ as a function of magnetization (a), and of applied field $h \equiv \mu_B H_a/W$ (b).

with information about the nonlinearity of the effective field. Clearly, the molecular

field β_m is a nonlinear function of m and grows rapidly with growing m. Such a behavior of molecular field, in combination with a similar nonlinear behavior of the effective mass, leads to either metamagnetism or to metamagnetic behavior. The effect of β_m on metamagnetic behavior is just a positive feedback effect; the mass increase leads to the band narrowing, which in turn makes easier the magnetization process, particularly very close to the Mott localization ($n \rightarrow 1$). Indeed, the quantity $-\beta_m$ is positive thus the effective field $H_a - \beta_m$ acting on the quasiparticle, Eq. (4.9), is stronger than the pure applied magnetic field H_a. The nonlinearity bears its origin in the field dependence of the effective mass. This dependence will be discussed next.

5.2 The spin-dependent effective mass and de Haas-van Alphen effect

Turning to the description of the quasiparticle characteristics we discuss now the concept of spin-dependent effective masses. The energy of the quasiparticle is given by Eq. (4.9). The factor q_σ leads in a natural manner to the spin-dependent mass via the relation $m_\sigma/m_0 = 1/q_\sigma$, cf. Eq.(1.26). The importance of this quantity derives from the fact that the spin-dependent effective masses m_σ are responsible for the quasiparticle properties, which in turn decide about the behavior of the system on the macroscopic level.

The field dependence of the few mass-enhancement factors $1/q_\sigma$ is displayed in Fig. 5.5. We display the spin-split masses as a function of h, for different band filings and

fixed $U/U_c = 0.95$, and at $T = 0$. One observes essentially three regimes: a) for n very

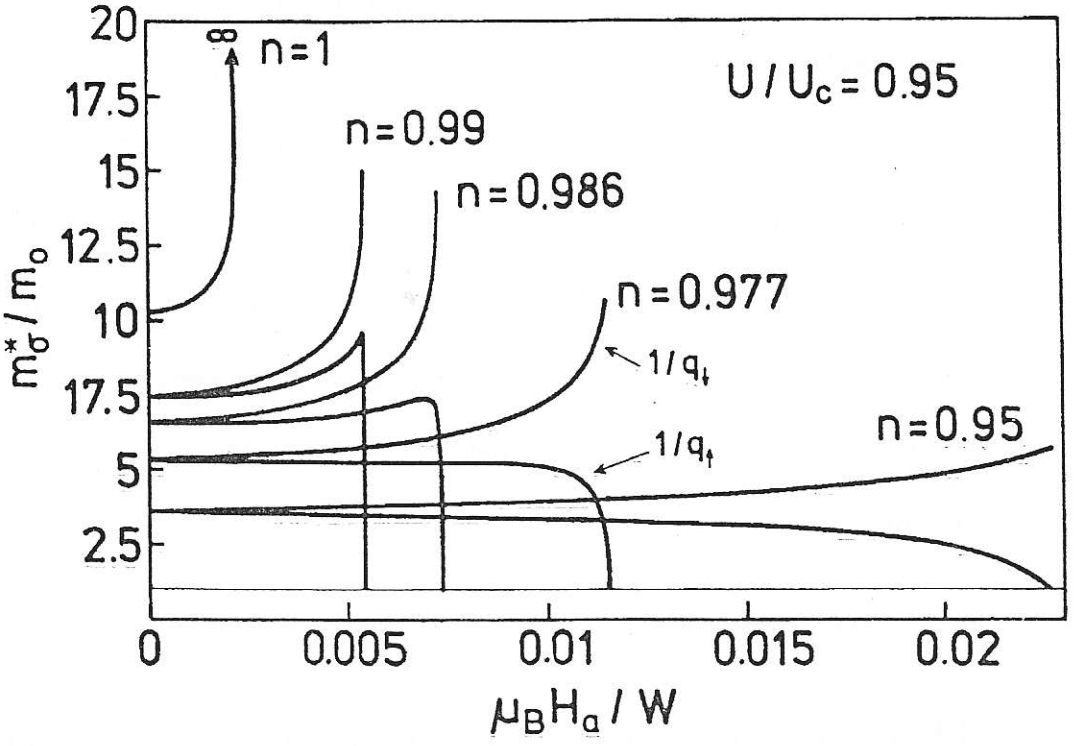

Figure 5.5: Applied field dependences of the effective mass enhancement factors $1/q_\uparrow$ and $1/q_\downarrow$, for different band fillings.

close unity both masses grow with the field (cf. $n = 0.99$), and at the metamagnetic transition point spin-minority carriers disappear, whereas the mass of spin-majority quasiparticles dives to the band-theory value m_0; b) for the 'intermediate' range of n (cf. $n = 0.986$) the situation is very similar to those in the case (a), however with the difference that close to the point of the metamagnetic transition the smaller mass turns continuously downward first, and then dives to the m_0 value. Finally, in the case c) for n still smaller (cf. $n = 0.977$, 0.95) the mass $m_\downarrow$ of carriers in the spin-minority

band increases, whereas $m_\uparrow$ decreases continuously. In fact, these cases correspond to the metamagnetic behavior of the system. Of course, if $n \equiv 1$, the masses are not spin dependent since q_σ does not depend on σ in that case, i.e. $q_\sigma \equiv q \equiv m_0/m^*$. One should note that intuitively one can expect that the mass $m_\downarrow$ should grow with h, as the minority carriers encounter a larger and larger number of scatterers with increasing m, while for the majority-spin carriers the opposite is true.

One can expose the difference $m_\downarrow \gg m_\uparrow$ as follows. For noninteracting electrons the probability of electron hopping is given by $n_\sigma(1-n_\sigma)$, whereas in the limit $U \to \infty$ it is $n_\sigma(1-n)$. Therefore, writing the band energy in the $U \to \infty$ limit as

$$E_B/N = zt\sum_\sigma n_\sigma(1-n) \equiv zt\sum_\sigma q_\sigma n_\sigma(1-n_\sigma), \tag{5.2}$$

we obtain that $q_\sigma = (1-n)/(1-n_\sigma)$. Noting that we had before that $m_\sigma^*/m_0 = 1/q_\sigma$, we immediately arrive at the conclusions that: (i) the mass enhancement is spin dependent, and that $m_\uparrow^*/m_0 \to 1$ as magnetic moment m approaches saturation ($n_\uparrow \to n$), while (ii) the minority mass increases with the magnetic moment reached the upper limit $m^*/m_0 = (1-n)^{-1}$ when the magnetic saturation is achieved. Also, the renormalization is particularly strong when $n \to 1$ and becomes infinite at the Mott-Hubbard boundary ($n = 1$). Obviously, this argument assumes that $d^2 = 0$, so it cannot reproduce the detailed behavior provided in Fig. 5.5, particularly when metamagnetic transition intervenes before the limit $d^2 \to 0$ is reached.

As mentioned before, close to the Mott localization both factors $1/q_\uparrow$ and $1/q_\downarrow$ grow with increasing h. In effect, the quantity $(1/q_\uparrow + 1/q_\downarrow)$ also increase sharply with increasing magnetic field until the saturation point is reached. At that point the

minority spin subband becomes empty and all the particles have the same spin; they acquire the bare band mass, since the Hubbard interaction $\sim U n_{i\uparrow} n_{i\downarrow}$ is then totally suppressed. This type of behavior manifests itself in the field dependence of the linear specific heat coefficient γ, which is proportional to the total density of states at the Fermi energy, *i.e.*, $\gamma = (2/3)\pi^2 \rho(\epsilon_F)(1/q_\uparrow + 1/q_\downarrow)$, where $\rho(\epsilon_F)$ is the density of bare states.

The effective masses are probably most directly measured with the help of de Haas - van Alphen effect. To calculate the spin resolved signal for the almost localized charged fermions with spin dependent masses one can adopt the Lifshitz-Kosevich approach [4]. The oscillating part of the magnetization can be expressed as follows

$$\widetilde{M_2} = -\frac{V}{4\pi^4\hbar^3}\left(\frac{e\hbar}{c}\right)^{3/2} H_a^{\frac{1}{2}} \sum_{m,\sigma} \frac{S_m^\sigma}{m_\sigma} \sum_{k=1}^{\infty} \frac{\psi(k\lambda^\sigma)}{k^{5/2}} A_\sigma \sin\left(k\frac{cS_m^\sigma}{e\hbar H_a} + \sigma k\pi \frac{m^\sigma}{m_0} \pm \frac{\pi}{4}\right) , \tag{5.3}$$

where the area of the m-th extremal orbit is $S_m^\sigma = \frac{e\hbar H_a}{c}(n_{m\sigma} + \gamma) = \pi(2m_\sigma \epsilon_\sigma - p_z^2)$, with $\epsilon_\sigma \equiv \mu + \sigma h$, $\psi(z) \equiv z/\sinh z$, $\lambda_\sigma = (2\pi^2 k_B T c m_\sigma / e\hbar H_a)$, and

$$A_\sigma = 1 - \sigma \frac{\pi}{m_0}\frac{e\hbar}{c}\frac{H_a^2}{S_m^\sigma}\frac{\partial m_\sigma}{\partial H_a} + \frac{H_a}{S_m^\sigma}\frac{\partial S_m^\sigma}{\partial H_a} . \tag{5.4}$$

Other symbols are standard . For each m_σ we have periodicity determined by the difference $\Delta(1/H_a)$ in the inverse applied field, $\Delta(1/H) = 2\pi e\hbar/cS_m^\sigma$. Thus, the spin-split masses will lead to two different cyclotron frequencies $\omega_\sigma = eH_a/(2m_\sigma c)$, for majority and minority spin subbands, respectively. In that situation the spin resolved components of the oscillating magnetization components $\widetilde{M}_{osc,\sigma}$ interfere with each other and produce the quantum beats. In Fig. 5.6 we display the inverse field ($1/h$, where $h \equiv \mu_B H_a/W$) dependence of the de Haas-van Alphen oscillations, as well as

show for comparison the observed oscillations by Takashita et al. [5] for $CeRu_2Si_2$. These spectacular quantum beats are caused by slightly different effective masses for majority (spin $\uparrow$) and minority heavy electrons. In fact, spin-split masses have not been detected directly as yet. Some indications are from the experiments on heavy-fermion system $CeRu_2Si_2$ [6], where the bands are extremely narrow, and therefore, the applied field effects are strong. For example, the metamagnetism is observed in that system in the field $H_c \simeq 7.8T$ [7], as well as $\gamma(h)$ exhibits [8] the same type of the behavior as that provided by the uppermost curve in Fig. 6.5 (see Chapter 6). However, a direct comparison of the present type of theory with the experimental results for $CeRu_2Si_2$ mentioned above would require generalization of the approach to the Anderson-lattice case (i.e. inclusion of the hybridization between f electrons and conduction electrons).

The spin-split masses will influence also other properties such as the electrical conductivity or the Hall effect. Let us take as an example an elementary view of the longitudinal resistivity ($j \| H_a$) in a magnetic field. (cf. Spałek et al., [9]) The Drude formula will now take the form

$$\frac{1}{\rho} = \frac{1}{\rho_\uparrow} + \frac{1}{\rho_\downarrow},$$

where $\frac{1}{\rho_\uparrow}$ and $\frac{1}{\rho_\downarrow}$ represent the contribution of the two *physically distinquishable* Fermi liquids (since their masses $m_\uparrow$ and $m_\downarrow$ *are different*). Therefore

$$\rho_\sigma \equiv \frac{m_\sigma}{n_{c\sigma} e^2} \frac{1}{\tau_\sigma}.$$

In the case $d \to 0$ one can take $m_\sigma^* \simeq m_0(1 - n_\sigma)/(1 - n)$, where as before, m_0

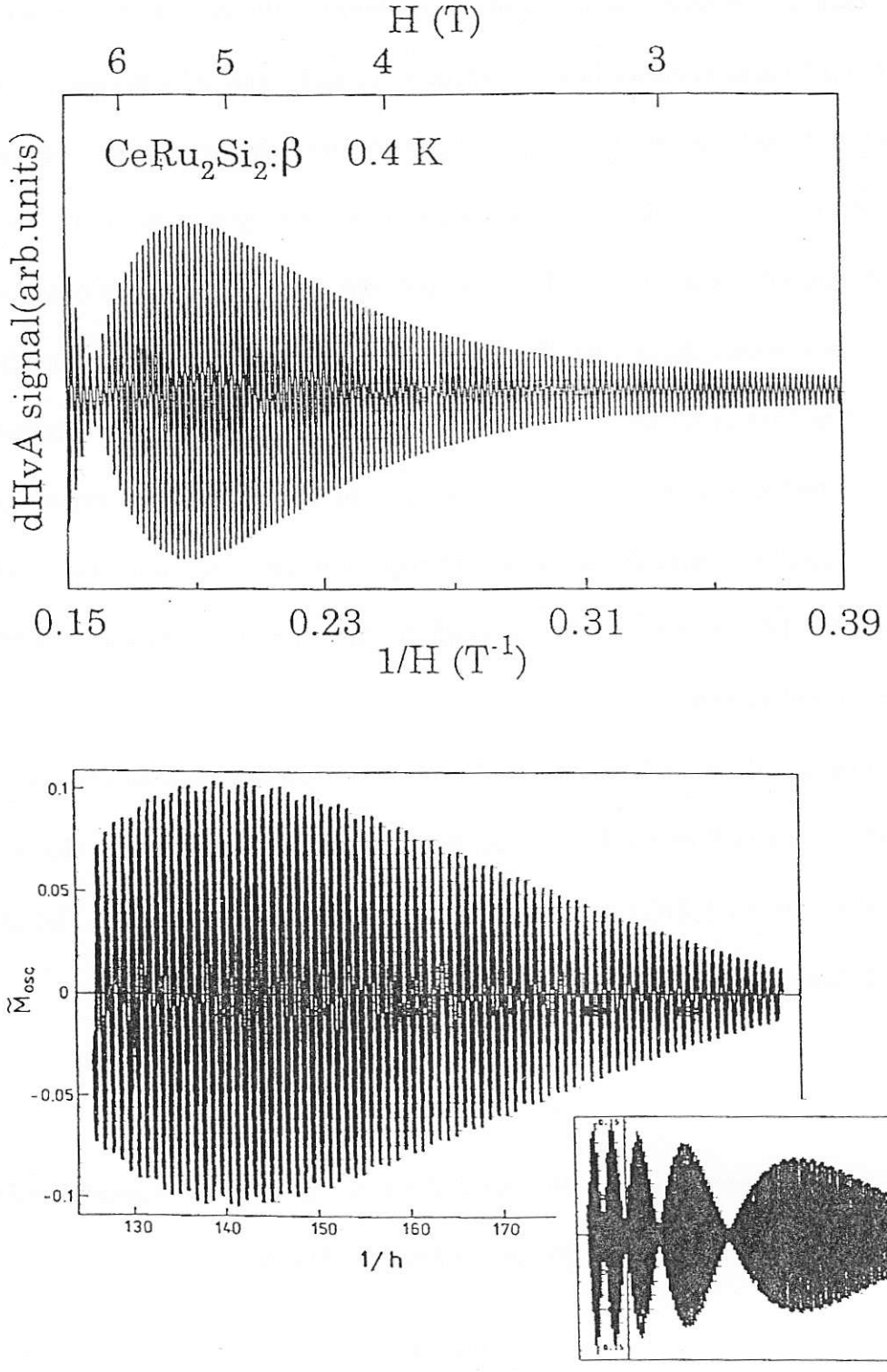

Figure 5.6: The observed de Haas-van Alphen oscillations for $CeRu_2Si_2$ (top [5]) and the predicted quantum beats for the spin-dependent masses (bottom).

represents the bare band mass. The relaxation time in low fields can be assumed in the usual form [10], here generalized to the spin-split situation

$$\frac{1}{\tau_\sigma} = const \frac{m_\sigma}{m_0} T^2,$$

so that at $H_a = 0 \quad \rho = AT^2$, with $A \sim \gamma^2$. In effect

$$\rho_\sigma \sim \frac{m_0}{n_{c\sigma} e^2} \left(\frac{m_\sigma}{m_0} \right)^2 T^2.$$

with $n_{c\sigma} = n_\sigma N/V$, where N is the number of lattice sites and V is the system volume.

This prediction could be tested by plotting ρ as a function of m and compare it with the formula provided here. Obviously, this point requires a careful study and is planned for the near future.

Summarizing this section, we would like to stress that the occurrence of spin-dependent effective masses, the metamagnetic behavior, and the presence of a nonlinear molecular field are the basic characteristics by which the almost localized Fermi liquid differs from the normal Landau Fermi liquid. In general, the Fermi liquid character of a metal close to the metal-insulator (Mott) boundary should not be taken for granted, since in those systems the Coulomb interaction energy is comparable to the band (and Fermi) energy of the relevant electrons [1]. In the next chapter we study explicitly the transition of the Fermi liquid to the non-Fermi liquid state induced by the applied magnetic field.

REFERENCES

[1] J. Spałek, A. Datta and J. M. Honig, Phys. Rev. Lett. **59**, 728 (1987); for review see: J. Spałek. J. Solid State Chem. **88**, 70 (1990).

[2] P. W. Anderson and W. F. Brinkman, in *The Physics of Liquid and Solid Helium*, Part II, edited by K. H. Bennemann and J. B. Ketterson (Wiley, New York, 1978); D. Vollhardt, Rev. Mod. Phys. **56**, 99 (1984).

[3] It is well known that close to the half filling an antiferromagnetic or spin-density-wave states are stable; this requires a separate analysis. We believe that the present results hold in the strong fields also for the weakly antiferromagnetic state; the metamagnetic behavior represents then the transition to the spin-flip phase (for discussion of antiferromagnetyzm for $H_a = 0$ see Chapter 7).

[4] We follow the exposition in: A. A. Abrikosov, *Fundamentals of the Theory of Metals* (North-Holland, Amsterdam, 1988) Ch. 10.

[5] M. Takashita, H. Aoki, T. Terashima, S. Uji, K. Maezawa, R. Setlai, and Y. Onuki, J. Phys. Soc. Japan **65**, 515 (1996).

[6] H. Aoki, private communication.

[7] P. Haen, J. Flouquet, F. Lappierre, P. Lejay, and G. Remenyi, J. Low Temp. Phys. bf 67, 391 (1987); for review see: J. Flouquet, S. Kambe, L.P. Regnault, P. Haen, J.P. Brisson, F. Lapierre, and P. Lejay, Physica B**215**, 77 (1995).

[8] H.P. van der Meulen, A. de Visser, J.J.M. Franse, T.T.J.M. Barendshot, J.A.A.J. Perenboom, H. van Kempen, A. Lacerda, P. Lejay, and J. Flouquet, Phys. Rev. B**44**, 814 (1991).

[9] J Spałek, W. Wójcik and P. Korbel, in *Proc. Int. School of Theoretical Phys.* Ustroń 1997, *Molecular Phys. Rep.* **17**, (1997).

[10] Cf. e.g. G. Baym and C.J. Pethick, *Landau Fermi-Liquid Theory. Concepts and Applications* (Wiley, New York, 1991).

Chapter 6

Fermi liquid instability and transition to statistical spin liquid

6.1 Introduction

The metallic state close to Mott-Hubbard localization is commonly regarded as a Fermi-liquid state of correlated fermions. As it was discussed, the quasiparticles in this liquid have spin-dependent effective masses (if the band filling $n \neq 1$), and experience a nonlinear molecular field in the spin polarized state [1]. The principal question is: what happens for $n \neq 1$ if we apply magnetic field and the number of double occupancy $d^2 \to 0$, i.e. magnetization $m \equiv n_\uparrow - n_\downarrow \to n$? Does it transform gradually into a gas of fermions with one spin direction or a non-Fermi liquid state comes into play before the system saturates magnetically? In this section we describe physical consequences coming from the presence of spin-dependent effective masses of carriers along with the magnetic-field induced transformation of the almost localized

Fermi liquid (ALFL) into a correlated fermionic liquid, hereafter referred to as the statistical spin liquid, SSL [2]. In other words, we predict the existence of anomalous low-temperature magnetic-field dependent phenomena for electrons close to the Mott-Hubbard localization, which should be observed experimentally if the mean-field slave boson approach is a correct starting point for those systems. The importance of our predictions is augmented by the assumed presence of a strong applied magnetic field, which suppresses quantum-spin-fluctuation contribution to the dynamic properties of almost localized fermions.

By statistical spin liquid we understand the state, for which the single-particle states are still characterized by the quasimomentum $\hbar\mathbf{k}$, but in which the doubly occupied quasiparticle configurations $|\mathbf{k}\uparrow\downarrow>$ with opposite spins are totally suppressed by the combined action of short-range Coulomb repulsive force (as characterized by the intraatomic repulsion U) and of the magnetic field. This restrictions leads to the corrections of system statistical properties [2],[8].

In the half-filled band case the (ALFL $\rightarrow$ SSL) transformation corresponds to the Mott-Hubbard (metal-insulator) transition. Here we concentrate on the partially filled band case (with filling $n < 1$), *i.e.*, we deal with **quantum liquids** on both sides of the transition and study the transformation (or crossover behavior) as a function of an applied magnetic field. In this manner, the present section extends the previous treatments [3]-[6] of almost localized fermions. We also indicate that our results reproduce qualitatively the properties of the heavy-fermion compound $CeRu_2Si_2$; these properties are summarized in Fig. 6.1 [9],[10],[11]. The principal claim of this section is that the field H_m in Fig. 6.1 specifies a novel (ALFL $\rightarrow$ SSL)

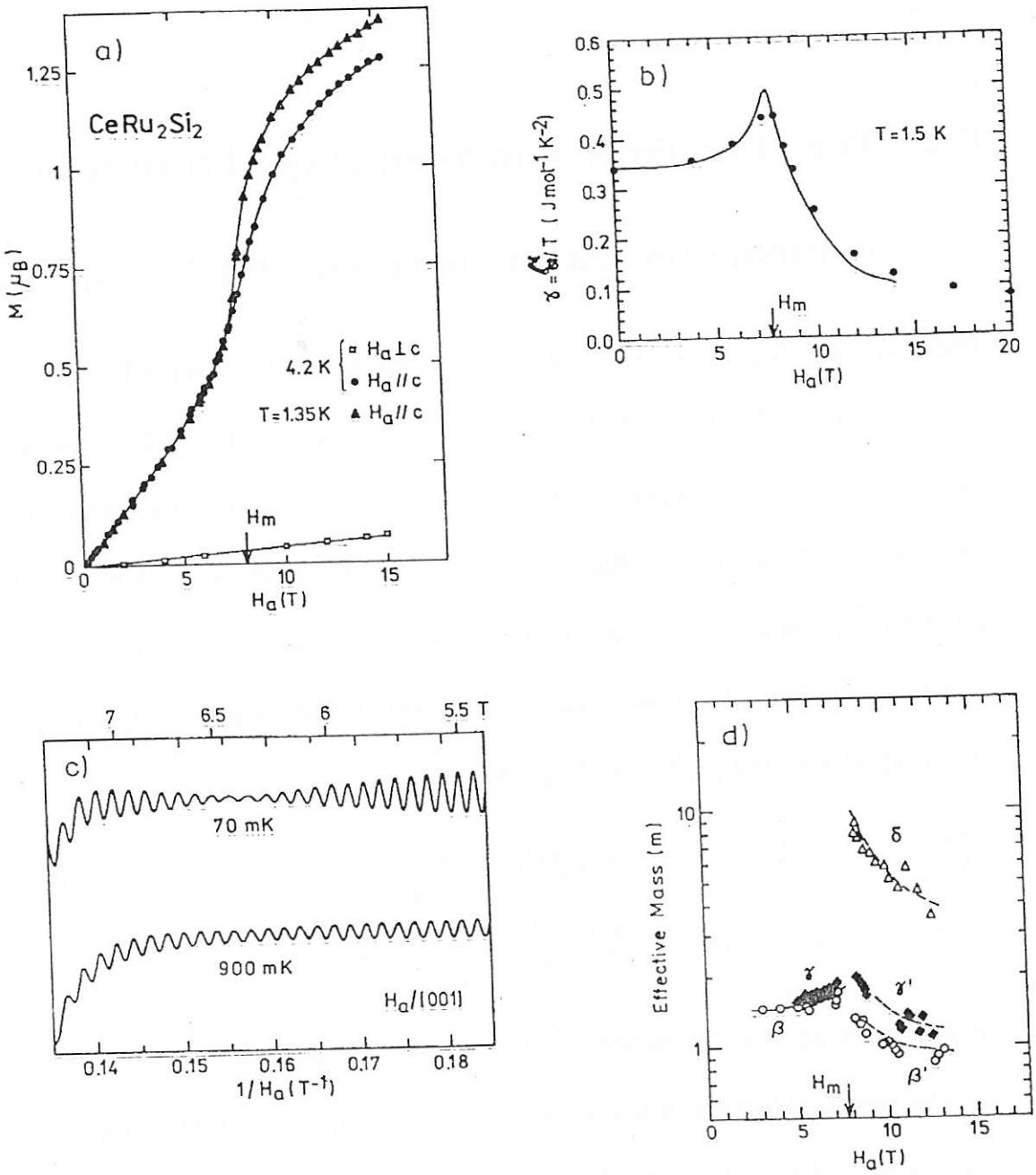

Figure 6.1: The magnetization curve (a), the linear specific heat coefficient γ (b), the de Haas-van Alphen oscilations (c) the effective masses (d) all as a functions of applied magnetic field for $CeRu_2Si_2$. Note the matamagnetic point at $H_m \sim 7.8T$.

change of state.

6.2 Fermi liquid to non-Fermi liquid transition and comparison with experiment for $CeRu_2Si_2$.

The quasiparticle picture involving the concepts of band narrowing factor q_σ and of the nonlinear molecular field β_m, introduced in Chapters 4 and 5 is used here to calculate the physical properties of ALFL. In effect, present approach reduces to the classic Gutzwiller-Brinkman-Rice analysis [6] in the simplest case with $n = 1$, $H_a = 0$, and for temperature $T = 0$, as well as to analysis of Spałek et al. [7] for $n = 1$ and $T > 0$. In the case of non-zero temperatures the low-temperature expansion for the Fermi liquid free energy, Eq.(4.24) yields

$$\begin{aligned}\frac{F_{FL}}{N} &= -W\left(\frac{n}{2}-d^2\right)\left(1-n+2d^2\right)-8W\sqrt{\left(d^2(1-n)+d^4\right)\left(\left(\frac{n}{2}-d^2\right)^2-\frac{m^2}{4}\right)} \\ &\quad +Ud^2-\mu_B H_a m-\frac{\pi^2}{3}\frac{(k_BT)^2}{W}\left(\frac{1}{q_\uparrow}+\frac{1}{q_\downarrow}\right), \qquad (6.1)\end{aligned}$$

were in deriving (6.1) the density of state function (4.33) was used.

The principal feature of this approach is the optimization of the balance between the renormalized band energy ($\sum_{\mathbf{k}\sigma} E_{\mathbf{k}\sigma} f(E_{\mathbf{k}\sigma})$, the entropy contribution ($-TS$, last term in (6.1)), and the Coulomb repulsive energy (Ud^2) by minimizing the total free energy with respect to the site double occupancy $d^2 \equiv \langle n_{i\uparrow} n_{i\downarrow}\rangle$ and magnetization m . In an applied magnetic field the probability d^2 vanishes at a critical field value $H_a \equiv H_c$, at which the system undergoes either a first-order metamagnetic transition or the magnetization curve changes its character from the metamagnetic to the localized-

moment type (*cf.* Fig. 6.1a).

It is important to note at the outset that the ALFL is unstable for $H_a \geqslant H_c$, even in the regime $U/U_c < 1$, where U_c is the critical value of interaction for the Mott-Hubbard localization for $n \equiv 1$ [6],[7]. This can be seen easily by computing d^2 for $n < 1$ and noting that $d^2(H_a > H_c) < 0$. Therefore, to describe consistently the metallic phase beyond the point $d^2 \equiv 0$ we invoke additionally the concept of statistical-spin-liquid [2],[8], for which double occupancies are excluded in reciprocal space. In other words, we assume that the double occupancy probability $\langle n_{\mathbf{k}_\uparrow} n_{\mathbf{k}_\downarrow} \rangle$ vanishes identically in the new phase. Physically, the SSL is the simplest type of state, which is represented by the itinerant spins rather than by Landau quasiparticles and encompasses the localized moment limit as a $n \rightarrow 1$. Therefore, it represents a natural choice for describing the doped Mott insulator, when the holes are itinerant and the exchange interactions are not crucial (*i.e.*, for $U < U_c$). The properties of this liquid have been studied before [2],[8]; we summarize next the features needed to analyze in detail the ALFL $\rightarrow$ SSL transformation.

First, this exclusion leads to a modified statistical distribution function:

$$\bar{n}_{\mathbf{k}} = \frac{1}{1 + ae^{\beta(\epsilon_{\mathbf{k}} - \mu)}}, \tag{6.2}$$

with $a = [2\cosh(\beta\mu_B H_a)]^{-1}$, where μ is the chemical potential, and $\beta = (k_B T)^{-1}$. Second, the magnetic moment per atom $m \equiv \langle n_{i_\uparrow} = n_{i_\downarrow} \rangle$ changes with field according to

$$m = \tanh(\beta\mu_B H_a), \tag{6.3}$$

i.e., it has the same shape as in the localized-moment case. Additionally, in the low-

temperature limit and for a constant density of states in the band with energies in the interval $[-W/2, W/2]$, the chemical potential is given by

$$\mu = \frac{W}{2} - k_B T \ln[\exp(\beta W(1-n)) - 1] - k_B T \ln[2\cosh(\beta \mu_B H_a)] \ . \qquad (6.4)$$

As $T \to 0$, we find that $\mu(T=0) = W(n-1/2) - \mu_B H_a$, *i.e.*, all moments are aligned and the band is filled for $n = 1$; the latter situation corresponds exactly to the localized-moment state. Finally, the Helmholtz free energy per site is determined from the expression

$$F_{SSL} = -k_B T \int_{-W/2}^{W/2} d\epsilon \ln[1 + \frac{1}{a}\exp(-\beta(\epsilon - \mu))] + \mu n \ , \qquad (6.5)$$

which for $n < 1$ reduces to

$$f_{SSL} \equiv \frac{F_{SSL}}{W} = -\frac{1}{2}n(1-n) - \frac{\pi^2}{6}t^2 - nt \ln[2\cosh(h/t)] \ , \qquad (6.6)$$

where $h \equiv \mu_\beta H_a / W$ and $t \equiv 1/(\beta W) = k_B T / W$. For $n = 1$ and $H_a = 0$ this expression should be replaced by the expression $(-t \ln 2)$ for free spins. Note that at $T = 0$, and for $h = h_c$, $f_{FL} = f_{SSL} = -\frac{1}{2}n(1-n) - hn$.

In Fig. 6.2, we display the free energies of the ALFL (as represented by $f_{FL} = F_{FL}/W$) and SSL states for $n = U/U_c = 0.95$ and $t = 5 \cdot 10^{-3}$. The two energies coincide exactly at the point H_c, at which $d^2 \equiv 0$. This means that the two states coexist at $H_a = H_c$, and that SSL is the stable phase for $H_a > H_c$. In other words, at H_c the Fermi liquid transforms into a gas of hopping spins with unrenormalized mass but with changed statistics. This statistics takes into account the total suppression of antiferromagnetic correlations by a sufficiently strong applied field. For the sake

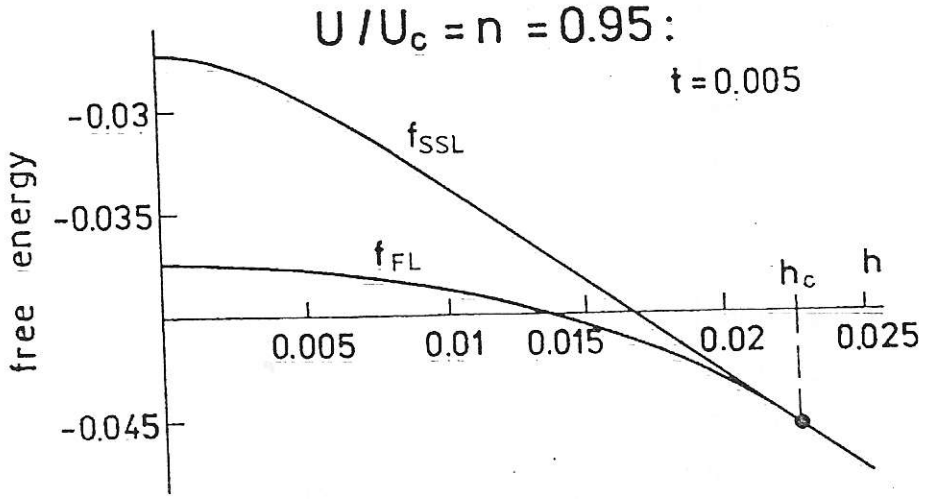

Figure 6.2: Field dependence of the free energies for an almost localized Fermi liquid f_{FL} and for the correlated liquid (f_{SSL}). The ALFL is unstable for $h > h_c$.

of completeness we have plotted in Fig. 6.3 the field dependence of d^2 in the ALFL state.

The resultant magnetization curve in the regime of the ALFL-SSL coexistence is shown in Fig. 6.4 for the parameters ($n = U/U_c = 0.95$), for which the *metamagnetism* occurs in ALFL state (the inset provides the temperature variation of the critical field). For $n > n_c \sim 0.973$ the magnetization will exhibit only an upward turn without a subsequent jump which indicates the metamagnetic behavior (discussed in Chapter 4).

To model the field dependence of the linear coefficient γ of the specific heat C we have calculated numerically $\gamma \equiv C/T$ as a function of h; it is shown in Fig. 6.5. The upper most curve for $U/U_c = 0.95$ and $n = 0.977$ has the same shape as the

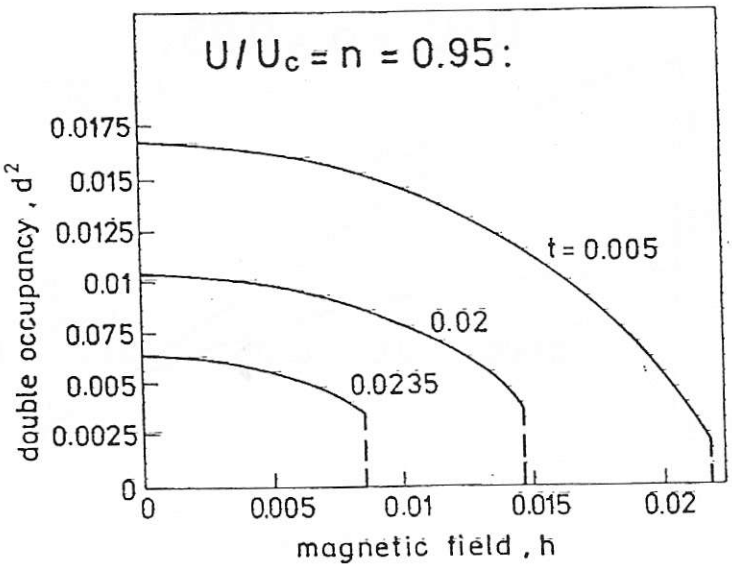

Figure 6.3: The variation of the double occupancy probability within magnetic field, for different temperatures.

data in Fig. 6.1b. Since $\gamma \sim m^*$, the $\gamma(h)$ curve models the field dependence of the total mass enhancement, which in the present situation contains two (spin-dependent) parts: $m^*/m_0 \sim 1/q_\uparrow + 1/q_\downarrow$. Note, that with comparison to the case $T = 0$, (cf. Fig. 5.5) the temperature influence rises up the effective masses enhancement (for the same H_a), or in other words, lowers the critical field h_c as shown in inset Fig. 6.4. Thus, the relation $m^*/m_0 = 1/2\,(1/q_\uparrow + 1/q_\downarrow)$ explains the character of the $m^*(h)$ data shown in Fig. 6.1d. Numerical results shows that the total effective mass m^* and thus γ can have a cusplike behavior as a function of applied field H_a. Note, that the left parts in Figs. 6.4 and 6.5 describe the properties of ALFL.

In Fig. 6.6 we exhibit the shape of the $T = 0$ de Haas-van Alphen oscillations for ALFL, near the ALFL $\rightarrow$ SSL transition. By contrast with the results displayed in

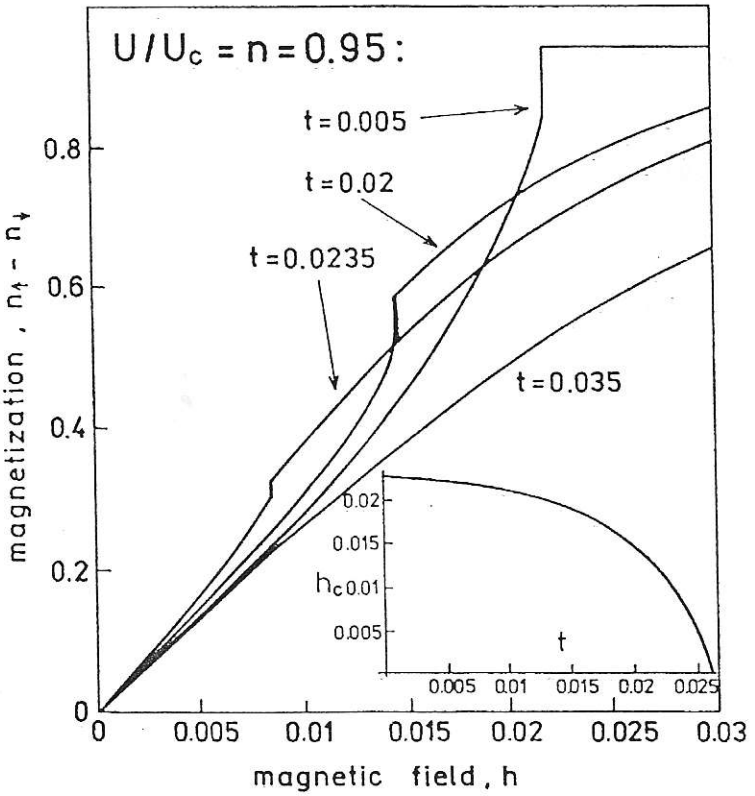

Figure 6.4: The theoretical magnetization curve; the inset shows the temperature dependence of the metamagnetic field h_c. Note a transition (or a crossover) from the metamagnetic to localized-moment character.

Fig. 5.6, close to the metamagnetic point, the spin resolved signals differ significantly and, hence, do not produce beats. Eventually, for $h > h_c$ (*cf.*, the upper inset in Fig. 6.6b) only the majority spin component is present (with the bare band mass!); the oscillations become very small and decrease with $1/h$ in the standard manner. However, the temperature dependence of the oscillations (with a corresponding crossover from a FL to a non-Fermi liquid) requires a separate analysis. Let us only mention

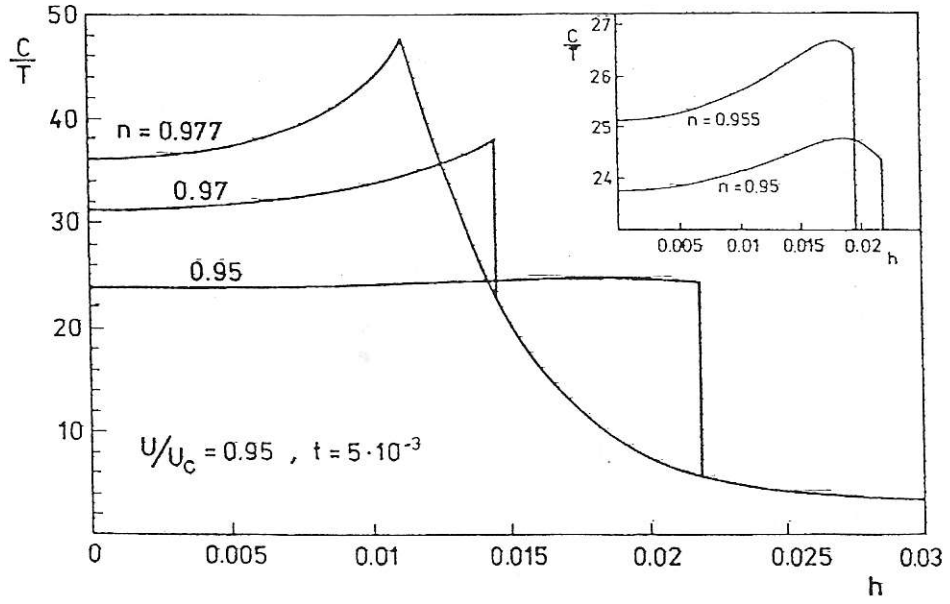

Figure 6.5: Field dependence of the linear specific heat coefficient for the specified parameters; note the cusp at $h = h_c$. The inset illustrates a rapid change of the $\gamma(h)$ curve with band filling n in the nearly half-filled situation.

that the transition is reached for $T > 0$ for a lower field than that required for $T = 0$. This feature is in agreement with the trend observed for the Mott localization [7] and is associated with the faster temperature change of the entropy for the localized and SSL states than that for ALFL.

The observed [11] magnetization oscillations (*cf.* Fig. 6.1c) represent the total signal $\widetilde{M}_{osc}$. To describe an individual oscillation mode by a single mass m^*, the effective cyclotron frequency must be introduced as $\omega_c^* = eH_a/(2m^*c)$, where m^* is the sum of $m_\uparrow$ and $m_\downarrow$. The field dependence of this frequency is shown in Fig. 6.7, where the lower inset provides the overall field dependence of ω_c^* in the range of the ALFL

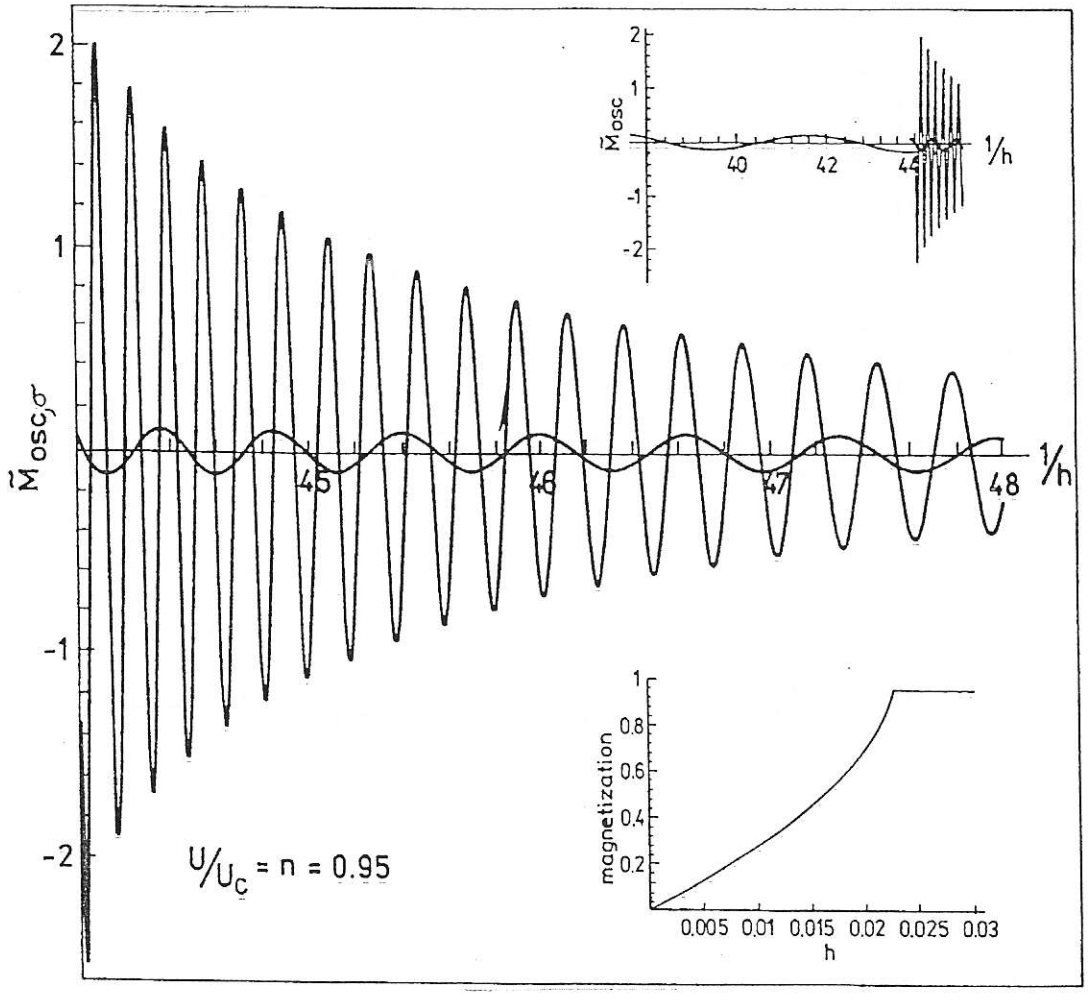

Figure 6.6: The shape of the oscillatory component of magnetization vs. $1/h$ in the Fermi-liquid regime (a), and near the ALFL $\rightarrow$ SSL transition (b). The upper inset illustrates the evolution of the de Haas-van Alphen oscillations across the metamagnetic transition whereas the lower specifies the shape of the magnetization curve in this case.

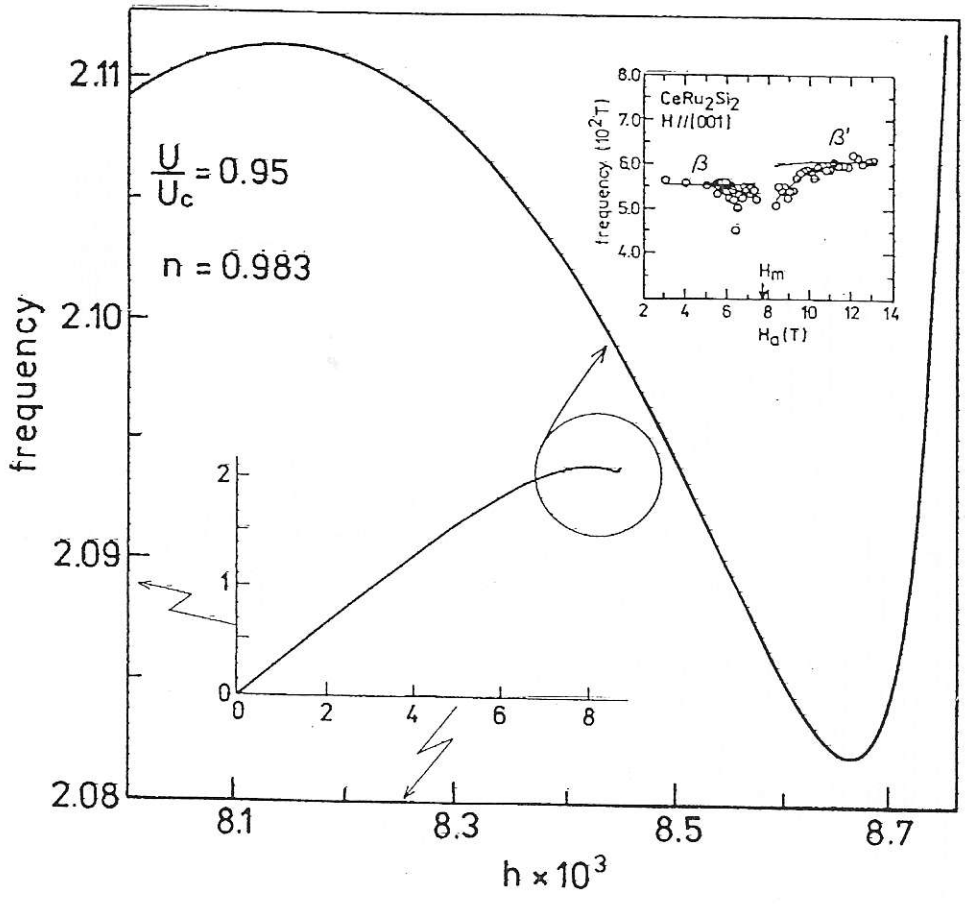

Figure 6.7: The cyclotron frequency as a function of applied field near the metamagnetic transition.

stability. The upper inset represents the experimental data for one of the $CeRu_2Si_2$ orbits [11]. The shallow dip in ω_c^* is intimately connected with the precursory metamagnetic behavior. Note that the steep part of the *rhs* of the theoretical curve levels off as the band masses (and the magnetic saturation) is reached. Therefore, the effective masses calculated from the band theory (in the version which does not include the present correlation effects) can be identified with m^* obtained experimentally only

for $H_a > H_c$.

In view of the above quantitative analysis we conclude that a crossover from the Fermi-liquid (albeit almost localized) to the non-Fermi liquid is signalled by a cusp-like behavior of γ and by a qualitative change of the de Haas-van Alphen oscillation with growing applied field. Both effects accompany the metamagnetic behavior of $m(h)$. Obviously, a direct confirmation of these predictions would involve the determination of the spin-split effective masses. Concerning this point, note that when $d^2 \to 0$ the effective masses in the ALFL phase are given by $m_\sigma/m_0 = (1 - n/2)/\delta - \sigma m/(2\delta)$, where $\delta = 1 - n$. Therefore, *the mass difference grows linearly with magnetization*, *i.e.*, $m_\downarrow - m_\uparrow \sim m/\delta$.

Finally, we interpret the present approach from a physical viewpoint. First, the almost localized nature of the Fermi liquid is essential, since only in that case is the band energy of quasiparticles sufficiently small to be almost compensated by the repulsive interaction among the carriers. In effect,the system is very susceptible to much weaker perturbations such as the temperature or the applied magnetic field. The heavy fermion materials are ideally suited for that purpose, since their kinetic energy is characterized in the FL regime by an energy of the order $T_K \sim 10 = 10^2 K$. Obviously, such a simplified single band approach is applicable for those systems only if $\mu_B H_a$ and $\hbar\omega_c^*$ are substantially smaller than the effective Kondo temperature $k_B T_K$, or equivalently, the hybridized quasiparticle band splitting.

Second, the physical reason behind the ALFL $\to$ SSL transformation is quite simple: the ALFL energy is always lower if only $d^2 > 0$, since the allowed double occupancies decrease it. At low temperature the zero-field entropy of the SSL state ($k_B \ln 2$

per carrier) is much higher than the entropy of the ALFL state ($(2\pi^2/3)k_B^2 T/W[1-(U/U_c)^2]^{-1}$). Thus, the entropy contribution ($-TS$) to the free energy favors the SSL state. Likewise, since the magnetization curve for the SSL is that for localized carriers, the SSL magnetizes much faster with increasing field than does the ALFL. In effect, the SSL becomes stable at higher fields and temperatures. From the coexistence condition $F_{FL} = F_{SSL}$ one can calculate the transition temperature.

REFERENCES

[1] Cf. J.Spałek, W.Wójcik and P. Korbel, in *Correlated Fermions Close to the Mott Localization: Deviation from the Landau Fermi-Liquid Picture*, Proc. of the Conf. "The European Conference **Physisc of Magnetism 96**", Poznań, June 24-28, 1996, *Acta Phys. Polonica* **A**, in press.

[2] J. Spałek, Phys. Rev. B **40**, 5180 (1989); Physica B **163**, 521 (1989); J. Spałek and W. Wójcik, Phys. Rev. B **37**, 1532 (1988); Y. Hatsugai and M. Kohmoto, J. Phys. Soc. Japan **61**, 2056 (1992).

[3] J. Spałek and W. Wójcik, in *Spectroscopy of the Mott Insulators and Correlated Metals*, Springer Series in Solid State Sciences, Vol. 119 (Springer-Verlag, Berlin, 1995) pp. 41–65; and unpublished.

[4] P. Korbel, J. Spałek, W. Wójcik, and M. Acquarone, Phys. Rev. B **52**, R2213 (1995); J. Spałek and P. Gopalan, Phys. Rev. Lett. **64**, 2823 (1990).

[5] R. Frésard and P. Wölfe, Int. J. Mod. Phys. B **6**, 237 (1992); **6**, 3087 (E) (1992).

[6] W. F. Brinkman and T. M. Rice, Phys. Rev. B**2**,4302 (1970).

[7] J. Spałek, A. Datta and J. M. Honig, Phys. Rev. Lett. **59**, 728 (1987); for review see *e.g.*, J. Spałek, J. Sol. St. Chem. **88**, 70 (1990). The principal results of this work have been recently rederived for the infinite dimensions, see: A. Georges, G. Kotliar, W. Krauth, and M. J. Rozenberg, Rev. Mod. Phys., in press.

[8] K. Byczuk and J. Spałek, Phys. Rev. B **51**, R7934 (1995).

[9] P. Haen *et al.*, J. Low Tem. Phys. **67**, 391 (1987)- magnetization curve (Fig. 1a).

[10] C.Paulsen *et al.*, J. Low Tem. Phys. **81**, 317 (1990)- linear specific heat (Fig. 1b).

[11] H. Aoki *et al.*, . Phys. Rev. Lett. **71**, 2110 (1993); Physica **B 201**, 231 (1994)- (Fig. 1c-d).

Chapter 7

Antiferromagnetic phase and transition to the Mott-Hubbard insulator

7.1 Introduction

Antiferromagnetism (AF) appears in the Hubbard model for an arbitrary interaction strength U provided we are close to the half-filled-band situation ($n \to 1$) [1].This is easy to understand qualitatively, since the intraatomic interaction $U \sum_i \langle n_{i\uparrow} n_{i\downarrow} \rangle$ is diminished by keeping apart the electrons with the opposite spins [2]. At the same time, the band energy is not increased because the concomitant nesting condition $\varepsilon_{\mathbf{k}+\mathbf{Q}} = -\varepsilon_{\mathbf{k}}$ (albeit achievable for bipartite lattices only) does not increase energy of the occupied states, even when going beyond the Hartree-Fock picture. In effect, the regime of the band filling n, for which the AF state is stable at given U has been

determined for variety of theoretical approaches [1,3]. The reliability of the results for the half-filled case is not in question, as they reduce to those in the Hartree-Fock and to the mean-field (Heisenberg) approximations in the weak- and strong-correlation limits, respectively. The theoretical results are in accord with the fact that *all* known Mott insulators with the half-filled configurations of the relevant group of atomic orbitals are also antiferromagnetic insulators. The basic question remaining is to what extent the existing [1] picture can be regarded as a proper mean-field theory of correlated fermions.

In this Chapter we concentrate our attention to two specific features of quasiparticle states not elaborated so far, namely, (i) to an evolution of the magnetic gap (renormalized by the electronic correlations) into the Mott-Hubbard gap, and (ii) to a rather weak renormalization of the effective mass for the half-filled-band case, which is in contrast with that calculated in the paramagnetic (PARA) case [3]. As in the preceding chapters these results are also obtained within the slave-boson approach in the mean-field approximation. We compare it briefly with the corresponding analysis in the infinite-dimension limit [1]. In particular, we introduce again the concept of a nonlinear staggered molecular field, which shows up as the effective (nonlinear-in-magnetization) magnetic gap, evolving at temperature $T = 0$ continuously with increasing U into the Mott-Hubbard gap. In connection with this evolution we single out the magnetic and Coulomb parts of the localization energy. This particular feature resolves explicitly the old question about the difference between the Slater and Mott-Hubbard insulators in the sense that only the Mott-Hubbard gap survives when antiferromagnetism disappears in the $U \rightarrow \infty$ limit. In the limit $U \rightarrow 0$ the magnetic

gap reduces to the original Slater (Hartree-Fock) gap.

In the following section we derive the free energy in the antiferromagnetic case, as well as calculate the principal physical quantities. In the last section we discuss the obtained analytic results.

7.2 Ground state energy

7.2.1 The Hamiltonian in the slave-boson representation

We start from the extended Hubbard model, which contains intersite exchange interactions. The model Hamiltonian decomposed into two sublattices A and B, each containing $N/2$ atomic sites, takes the form

$$\begin{aligned} H &= \sum_{<i_A j_B>\sigma} t_{i_A j_B} \left(c^{\dagger}_{i_A\sigma} c_{j_B\sigma} + c^{\dagger}_{i_B\sigma} c_{j_A\sigma} \right) + U \sum_{i_A} n_{i_{A\uparrow}} n_{i_{A\downarrow}} + U \sum_{i_B} n_{i_{B\uparrow}} n_{i_{B\downarrow}} \\ &\quad - \sum_{i_A} m_{i_A} H_a - \sum_{i_B} m_{i_B} H_a + 4J \sum_{<i_A j_B>} \mathbf{S}_{i_A} \cdot \mathbf{S}_{j_B} - \mu N_e. \end{aligned} \tag{7.1}$$

The first term represents single-particle hopping of electrons between the sublattices (nearest neighbors), the second and the third express the intraatomic interaction of the same magnitude on *all* sites, the fourth includes the Heisenberg exchange between the sublattices and $(-\mu N_e)$ is the reference energy with μ being the chemical potential, and $N_e (\leq N)$ the total number of fermions. In the mean-field approximation for the slave bosons, the rotationally invariant approach of Li et al [4] and the Kotliar-Ruckenstein [1] formulations can be brought to an equivalent form [5]. The effective AF-Hamiltonian written in the slave-boson representation takes the form

$$H_{AF} = \widetilde{H}^{(1)}_{AF} + \widetilde{H}^{(2)}_{AF} - \mu N_e, \tag{7.2}$$

where the dynamic part is

$$\begin{aligned}\widetilde{H}^{(1)}_{AF} - \mu N \equiv & \sum_{<i_A j_B>\sigma} t_{i_A j_B}\left(z^{\dagger}_{i_A\sigma} z_{j_B\sigma} f^{\dagger}_{i_A\sigma} f_{j_B\sigma} + z^{\dagger}_{i_B\sigma} z_{j_A\sigma} f^{\dagger}_{i_B\sigma} f_{j_A\sigma}\right) + \\ & + \sum_{i_A\sigma} f^{\dagger}_{i_A\sigma} f_{j_A\sigma}(-\mu - \sigma H_a - \sigma J z m_B) + \sum_{i_A} U d^{\dagger}_{i_A} d_{i_A} \\ & + \sum_{i_B\sigma} f^{\dagger}_{i_B\sigma} f_{j_B\sigma}(-\mu - \sigma H_a + \sigma J z m_A) + \sum_{i_B} U d^{\dagger}_{i_B} d_{i_B} \\ & + \frac{NJz}{2} m_A m_B, \end{aligned} \tag{7.3}$$

and the part containing constraints is

$$\begin{aligned}\widetilde{H}^{(2)}_{AF} = & \sum_{i_A} \lambda^{(1)}_{i_A}\left(e^{\dagger}_{i_A} e_{i_A} + p^{\dagger}_{i_A\uparrow} p_{i_A\uparrow} + p^{\dagger}_{i_A\downarrow} p_{i_A\downarrow} + d^{\dagger}_{i_A} d_{i_A} - 1\right) \\ & + \sum_{i_B} \lambda^{(1)}_{i_B}\left(e^{\dagger}_{i_B} e_{i_B} + p^{\dagger}_{i_B\uparrow} p_{i_B\uparrow} + p^{\dagger}_{i_B\downarrow} p_{i_B\downarrow} + d^{\dagger}_{i_B} d_{i_B} - 1\right) \\ & + \sum_{i_A\sigma} \lambda^{(2)}_{i_A\sigma}\left(f^{\dagger}_{i_A\sigma} f_{i_B\sigma} - p^{\dagger}_{i_A\sigma} p_{i_A\sigma} - d^{\dagger}_{i_A} d_{i_A}\right) \\ & + \sum_{i_B\sigma} \lambda^{(2)}_{i_B\sigma}\left(f^{\dagger}_{i_B\sigma} f_{i_B\sigma} - p^{\dagger}_{i_B\sigma} p_{i_B\sigma} - d^{\dagger}_{i_B} d_{i_B}\right). \end{aligned} \tag{7.4}$$

Here in order to decouple the intersite part the Hartree-Fock approximation was used

$$\mathbf{S}_{i_A}\mathbf{S}_{j_B} \approx S^z_{i_A}\frac{1}{2}\langle m_{j_B}\rangle + \frac{1}{2}\langle m_{i_A}\rangle S^z_{j_B} - \frac{1}{4}\langle m_{i_A}\rangle\langle m_{j_B}\rangle, \tag{7.5}$$

where $m_i \equiv n_{i_\uparrow} - n_{i_\downarrow}$ and thus, for a two-sublattices antiferromagnetic state: $\langle m_{i_A}\rangle \equiv m_A$ and $\langle m_{j_B}\rangle \equiv -m_B$.

In order to perform the integration over the fermion degrees of freedom one needs to express H_{AF} in the bilinear form for fermions. Then (7.2) reduces to

$$H_{AF} = H^{(1)}_{AF} + H^{(2)}_{AF}, \tag{7.6}$$

where

$$H^{(1)}_{AF} = \sum_{<i_A j_B>\sigma} t_{i_A j_B}\left(z^{\dagger}_{i_A\sigma} z_{j_B\sigma} f^{\dagger}_{i_A\sigma} f_{j_B\sigma} + z^{\dagger}_{i_B\sigma} z_{j_A\sigma} f^{\dagger}_{i_B\sigma} f_{j_A\sigma}\right)$$

$$+\sum_{i_A\sigma} f^{\dagger}_{i_A\sigma} f_{j_A\sigma} \left(\lambda^{(2A)}_{i_A\sigma} - \mu - \sigma\left(Jzm_B + H_a\right)\right)$$
$$+\sum_{i_B\sigma} f^{\dagger}_{i_B\sigma} f_{j_B\sigma} \left(\lambda^{(2B)}_{i_B\sigma} - \mu + \sigma\left(Jzm_A - H_a\right)\right)$$
$$+\frac{NJz}{2} m_A m_B, \tag{7.7}$$

and

$$\begin{aligned} H^{(2)}_{AF} &= \sum_{i_A} \left(U d^{\dagger}_{i_A} d_{i_A} + \lambda^{(1)}_{i_A}\left(e^{\dagger}_{i_A} e_{i_A} + p^{\dagger}_{i_A\uparrow} p_{i_A\uparrow} + p^{\dagger}_{i_A\downarrow} p_{i_A\downarrow} + d^{\dagger}_{i_A} d_{i_A} - 1\right)\right) \\ &+ \sum_{i_A\sigma} \lambda^{(2)}_{i_A\sigma}\left(p^{\dagger}_{i_A\sigma} p_{i_A\sigma} - d^{\dagger}_{i_A} d_{i_A}\right) \\ &+ \sum_{i_B} \left(U d^{\dagger}_{i_B} d_{i_B} + \lambda^{(1)}_{i_B}\left(e^{\dagger}_{i_B} e_{i_B} + p^{\dagger}_{i_B\uparrow} p_{i_B\uparrow} + p^{\dagger}_{i_B\downarrow} p_{i_B\downarrow} + d^{\dagger}_{i_B} d_{i_B} - 1\right)\right) \\ &+ \sum_{i_B\sigma} \lambda^{(2)}_{i_B\sigma}\left(p^{\dagger}_{i_B\sigma} p_{i_B\sigma} - d^{\dagger}_{i_B} d_{i_B}\right). \end{aligned} \tag{7.8}$$

In the saddle point approximation all bosonic fields are assumed again constant in space and time, e.g. $e_{i_A} \rightarrow < e_{i_A} > = < e^{\dagger}_{i_A} > \equiv e_A$. Additionally, the fields that does not depends on spin must have the same values on both sublattices, namely, $e_A = e_B \equiv e$ and $d_A = d_B = d$. The Hamiltonian (7.6) takes the form

$$H_{AF} = H_F + H_B, \tag{7.9}$$

where

$$\begin{aligned} H_F &= \sum_{<i_A, j_B>\sigma} q_\sigma t_{i_A j_B}\left(f^{\dagger}_{i_A\sigma} f_{j_B\sigma} + f^{\dagger}_{i_B\sigma} f_{j_A\sigma}\right) \\ &+ \sum_{i_A\sigma} f^{\dagger}_{i_A\sigma} f_{j_A\sigma}\left(\lambda^{(2A)}_{\sigma} - \mu - \sigma\left(Jzm_B + H_a\right)\right) \\ &+ \sum_{i_B\sigma} f^{\dagger}_{i_B\sigma} f_{j_B\sigma}\left(\lambda^{(2B)}_{\sigma} - \mu + \sigma\left(Jzm_A - H_a\right)\right), \end{aligned} \tag{7.10}$$

and

$$H_B \equiv \frac{N}{2} Jzm_A m_B + NUd^2 + \tag{7.11}$$

$$+\frac{N}{2}\left(\lambda_A^{(1)}\left(e^2+d^2+\sum_\sigma p_{A\sigma}^2-1\right)-\sum_\sigma \lambda_{A\sigma}^{(2)}\left(p_{A\sigma}^2+d^2\right)\right)$$
$$+\frac{N}{2}\left(\lambda_B^{(1)}\left(e^2+d^2+\sum_\sigma p_{B\sigma}^2-1\right)-\sum_\sigma \lambda_{B\sigma}^{(2)}\left(p_{B\sigma}^2+d^2\right)\right).$$

In (7.10) $q_\sigma = < z_{i_A\sigma}^\dagger z_{j_B\sigma} >$ i.e. due to Eq. (4.1), here it takes the form

$$q_\sigma = \frac{ep_{A\sigma}+dp_{A\bar{\sigma}}}{\sqrt{\left(1-d^2-p_{A\sigma}^2\right)\left(1-e^2-p_{A\bar{\sigma}}^2\right)}}\frac{ep_{B\sigma}+dp_{B\bar{\sigma}}}{\sqrt{\left(1-d^2-p_{B\sigma}^2\right)\left(1-e^2-p_{B\bar{\sigma}}^2\right)}}. \tag{7.12}$$

Transformation to the momentum space is carried out by the sublattices, i.e.

$$f_{i_A\sigma}^\dagger = \frac{1}{\sqrt{N/2}}\sum_k e^{ikR_{i_A}}a_{Ak\sigma}^\dagger, \quad and \quad f_{j_B\sigma} = \frac{1}{\sqrt{N/2}}\sum_k e^{-ikR_{j_B}}a_{Bk\sigma}. \tag{7.13}$$

Note that the sublattices comprise $(N/2)$ atoms. In effect, the reduced Brillouin zone contains $(N/2)$ states (is halved with respect to that for paramagnetic state). This transformation allows to write the Hamiltonian (7.10) in the form

$$\begin{aligned} H_F &= \sum_{k\sigma} q_\sigma \varepsilon_k \left(a_{Ak\sigma}^\dagger a_{Bk\sigma} + a_{Bk\sigma}^\dagger a_{Ak\sigma}\right) \\ &+ \sum_{k\sigma} a_{Ak\sigma}^\dagger a_{Ak\sigma}\left(\lambda_\sigma^{(2A)} - \mu - \sigma\left(Jzm_B + H_a\right)\right) \\ &+ \sum_{k\bar{\sigma}} a_{Bk\sigma}^\dagger a_{\bar{B}k\sigma}\left(\lambda_\sigma^{(2B)} - \mu + \sigma\left(Jzm_A - H_a\right)\right), \end{aligned} \tag{7.14}$$

with

$$\varepsilon_k = \sum_{<i_A,j_B>} t_{i_Aj_B}e^{ik(R_{i_A}-R_{j_B})}. \tag{7.15}$$

The Bose part (7.11) acquires a classical value, whereas the Fermi part (7.14) is of single-particle nature and therefore, can be diagonalized by the Bogolyubov transformation we discuss next.

7.2.2 The Bogolyubov transformation

The Bogolyubov transformation corresponds to the following change of the basis

$$\begin{pmatrix} a^{\dagger}_{A k\sigma} \\ a^{\dagger}_{B k\sigma} \end{pmatrix} = \begin{pmatrix} \cos\theta_{k\sigma} & \sin\theta_{k\sigma} \\ -\sin\theta_{k\sigma} & \cos\theta_{k\sigma} \end{pmatrix} \begin{pmatrix} \alpha^{\dagger}_{k\sigma} \\ \beta^{\dagger}_{k\sigma} \end{pmatrix}, \tag{7.16}$$

where the quasimomentum (k-vector) runs over the values in the reduced Brillouin zone. This transformation allows to write H_F in the form

$$H_F = H_F^{(0)} + H_F^{(mix)}, \tag{7.17}$$

where

$$\begin{aligned} H_F^{(0)} &= \sum_{k\sigma} \beta^{\dagger}_{k\sigma}\beta_{k\sigma} \left[q_\sigma \varepsilon_k \sin 2\theta_{k\sigma} + \sin^2\theta_{k\sigma} \left(\lambda_\sigma^{(2A)} - \mu - \sigma \left(Jzm_B + H_a \right) \right) \right. \\ &\left. + \cos^2\theta_{k\sigma} \left(\lambda_\sigma^{(2B)} - \mu + \sigma \left(Jzm_A - H_a \right) \right) \right] + \\ &\sum_{k\sigma} \alpha^{\dagger}_{k\sigma}\alpha_{k\sigma} \left[-q_\sigma \varepsilon_k \sin 2\theta_{k\sigma} + \cos^2\theta_{k\sigma} \left(\lambda_\sigma^{(2A)} - \mu - \sigma \left(Jzm_B + H_a \right) \right) \right. \\ &\left. + \sin^2\theta_{k\sigma} \left(\lambda_\sigma^{(2B)} - \mu + \sigma \left(Jzm_A - H_a \right) \right) \right], \end{aligned} \tag{7.18}$$

and

$$\begin{aligned} H_F^{(mix)} &= \sum_{k\sigma} \left(\alpha^{\dagger}_{k\sigma}\beta_{k\sigma} + \beta^{\dagger}_{k\sigma}\alpha_{k\sigma} \right) \\ &\times \left[q_\sigma \varepsilon_k \cos 2\theta_{k\sigma} - \frac{1}{2} \sin 2\theta_{k\sigma} \left(\left(\lambda_\sigma^{(2A)} - \lambda_\sigma^{(2B)} \right) + \sigma J z m_A m_B \right) \right]. \end{aligned} \tag{7.19}$$

Since the angle $\theta_{k\sigma}$ is not fixed as yet one may choose it such in such way that the Hamiltonian $H_F^{(mix)} = 0$. This is guaranteed by the condition

$$\tan 2\theta_{k\sigma} = \sigma \frac{2q_\sigma \varepsilon_k}{Jz(m_A + m_B) + \sigma \left(\lambda_\sigma^{(2A)} - \lambda_\sigma^{(2B)} \right)}. \tag{7.20}$$

So, due to Eq. (7.20) the Hamiltonian $H_{AF} = H_F^{(0)} + H_B$. The corresponding free energy functional is evaluated the same way like in the paramagnetic case. Namely, after performing the integration over the fermionic variables as well as introducing the new variables (cf. Eqs. (4.3))

$$\begin{aligned} 2p_L^2 &= p_{L\uparrow}^2 + p_{L\downarrow}^2 \quad , \qquad & M_L &= p_{L\uparrow}^2 - p_{L\downarrow}^2, \\ 2\lambda_{0_L} &= \lambda_{L\uparrow}^{(2)} + \lambda_{L\downarrow}^{(2)} \, , \qquad & 2\beta_{m_L} &= \lambda_{L\uparrow}^{(2)} - \lambda_{L\downarrow}^{(2)}, \end{aligned} \tag{7.21}$$

which provides the relations

$$\begin{aligned} p_{i_{L\sigma}}^2 &= p_{i_L}^2 + \tfrac{1}{2}\sigma M_{i_L}, \\ \lambda_{i_{L\sigma}}^{(2)} &= \lambda_{i_L} - \sigma\beta_{mi_L}, \end{aligned} \tag{7.22}$$

for $L = \{A, B\}$, one obtains the free energy functional per lattice site is in the form

$$\begin{aligned} \frac{F_{AF}}{N} \;=\; & -\frac{k_B T}{N} \sum_{k\sigma} \ln\left[1 + e^{-\beta\left(E_{k\sigma}^{(\alpha)} + \Lambda_{k\sigma}^{(\alpha)} - \sigma H_a - \mu\right)}\right] \\ & -\frac{k_B T}{N} \sum_{k\bar{\sigma}} \ln\left[1 + e^{-\beta\left(E_{k\sigma}^{(\beta)} + \Lambda_{k\sigma}^{(\beta)} - \sigma H_a - \mu\right)}\right] \\ & + \frac{1}{2} J z m_A m_B + U d^2 + \mu n \\ & + \frac{1}{2}\left[\lambda_{0A}\left(e^2 + d^2 + 2p_A^2 - 1\right) - 2\lambda_{0A}\left(p_A^2 + d^2\right) - \beta_{mA} M_A\right] \\ & + \frac{1}{2}\left[\lambda_{0B}\left(e^2 + d^2 + 2p_B^2 - 1\right) - 2\lambda_{0B}\left(p_B^2 + d^2\right) - \beta_{mB} M_B\right], \end{aligned} \tag{7.23}$$

where

$$\begin{aligned} E_{k\sigma}^{(\alpha)} &= -\left[q_\sigma \varepsilon_k \sin 2\theta_{k\sigma} + \sigma J z (m_A \cos^2\theta_{k\sigma} - m_B \sin^2\theta_{k\sigma})\right], \\ E_{k\sigma}^{(\beta)} &= +\left[q_\sigma \varepsilon_k \sin 2\theta_{k\sigma} + \sigma J z (m_A \cos^2\theta_{k\sigma} - m_B \sin^2\theta_{k\sigma})\right], \end{aligned} \tag{7.24}$$

and

$$\begin{aligned} \Lambda_{k\sigma}^{(\alpha)} &= (\lambda_{0A} + \sigma\beta_{mA})\cos^2\theta_{k\sigma} + (\lambda_{0B} + \sigma\beta_{mB})\sin^2\theta_{k\sigma}, \\ \Lambda_{k\sigma}^{(\beta)} &= (\lambda_{0A} + \sigma\beta_{mA})\sin^2\theta_{k\sigma} + (\lambda_{0B} + \sigma\beta_{mB})\cos^2\theta_{k\sigma}. \end{aligned} \tag{7.25}$$

The value of the $\theta_{k\sigma}$ is given by the Eq. (7.20).

7.2.3 Saddle-point conditions

The free energy functional (7.23) depends on 12 bosonic fields: e, d, $p_{(A,B)}$, $\lambda_{0(A,B)}$, $\lambda^{(1)}_{(A,B)}$, $\beta_{m(A,B)}$, $M_{(A,B)}$ and the chemical potential μ. First, the minimization with respect to fields $\lambda^{(1)}_{(A)}$, $\lambda^{(1)}_{(A)}$ provides

$$\frac{\partial F_{AF}}{\partial \lambda^{(1)}_{(A,B)}} = e^2 + d^2 + 2p^2_{(A,B)} - 1 = 0, \tag{7.26}$$

which yields

$$p^2_A = p^2_B = \frac{1}{2}\left(1 - e^2 - d^2\right) \equiv p^2. \tag{7.27}$$

The minimization with respect to the chemical potential $\frac{\partial F_{AF}}{\partial \mu} = 0$ gives

$$\frac{1}{2}\frac{1}{N/2}\sum_{k\sigma}\left(f\left(\overline{E}^{(\alpha)}_{k\sigma}\right) + f\left(\overline{E}^{(\beta)}_{k\sigma}\right)\right) = n, \tag{7.28}$$

where $f\left(\overline{E}\right)$ is the Fermi-Dirac distribution function with the quasiparticle energy

$$\overline{E}^{(\alpha,\beta)}_{k\sigma} \equiv E^{(\alpha,\beta)}_{k\sigma} + \Lambda^{(\alpha,\beta)}_{k\sigma} - \sigma H_a, \tag{7.29}$$

and n is an average electron number per lattice site.

The conditions $\frac{\partial F_{AF}}{\partial \lambda_{0A}} = 0$ and $\frac{\partial F_{AF}}{\partial \lambda_{0B}} = 0$ yields respectively

$$\frac{1}{2}\frac{1}{N/2}\sum_{k\sigma}\left(f\left(\overline{E}^{(\alpha)}_{k\sigma}\right)\cos^2\theta_{k\sigma} + f\left(\overline{E}^{(\beta)}_{k\sigma}\right)\sin^2\theta_{k\sigma}\right) = p^2 + d^2, \tag{7.30}$$

and

$$\frac{1}{2}\frac{1}{N/2}\sum_{k\sigma}\left(f\left(\overline{E}^{(\alpha)}_{k\sigma}\right)\sin^2\theta_{k\sigma} + f\left(\overline{E}^{(\beta)}_{k\sigma}\right)\cos^2\theta_{k\sigma}\right) = p^2 + d^2. \tag{7.31}$$

Note that due to the Bogolyubov transformation

$$\begin{aligned} n_{Ak\sigma} &= n^{(\alpha)}_{k\sigma}\cos^2\theta_{k\sigma} + n^{(\beta)}_{k\sigma}\sin^2\theta_{k\sigma} + \tfrac{1}{2}\left(\alpha^\dagger_{k\sigma}\beta_{k\sigma} + \beta^\dagger_{k\sigma}\alpha_{k\sigma}\right)\sin 2\theta_{k\sigma}, \\ n_{Bk\sigma} &= n^{(\alpha)}_{k\sigma}\sin^2\theta_{k\sigma} + n^{(\beta)}_{k\sigma}\cos^2\theta_{k\sigma} - \tfrac{1}{2}\left(\alpha^\dagger_{k\sigma}\beta_{k\sigma} + \beta^\dagger_{k\sigma}\alpha_{k\sigma}\right)\sin 2\theta_{k\sigma}, \end{aligned} \tag{7.32}$$

with $n_{(A,B)k\bar{\sigma}} = a^{\dagger}_{(A,B)k\sigma} a_{(A,B)k\bar{\sigma}}$, $n^{(\alpha)}_{k\sigma} = \alpha^{\dagger}_{k\sigma}\alpha_{k\bar{\sigma}}$, and $n^{(\beta)}_{k\sigma} = \beta^{\dagger}_{k\sigma}\beta_{k\sigma}$. The particle number conservation requires

$$\sum_{i_A, j_B} \left\langle f^{\dagger}_{i_A\sigma} f_{i_A\sigma} + f^{\dagger}_{j_B\sigma} f_{j_B\sigma} \right\rangle = \sum_{k\sigma} \left\langle n_{Ak\sigma} + n_{Bk\sigma} \right\rangle = \sum_{k\sigma} \left\langle n^{(\alpha)}_{k\bar{\sigma}} + n^{(\beta)}_{k\bar{\sigma}} \right\rangle, \tag{7.33}$$

which is authomaticaly obeyed in the sense of average values. Similarly, due to the Eqs. (7.32) and (7.30),(7.31) one obtains

$$\begin{aligned} \frac{1}{2} n_A &\equiv \frac{1}{2}\frac{1}{N/2} \sum_{k\sigma} < \widehat{n}_{Ak\bar{\sigma}} > \\ &= \frac{1}{2}\frac{1}{N/2} \sum_{k\sigma} \left(f\left(\overline{E}^{(\alpha)}_{k\sigma}\right) \cos^2\theta_{k\sigma} + f\left(\overline{E}^{(\beta)}_{k\sigma}\right) \sin^2\theta_{k\sigma} \right) = p^2 + d^2, \end{aligned} \tag{7.34}$$

and

$$\begin{aligned} \frac{1}{2} n_B &\equiv \frac{1}{2}\frac{1}{N/2} \sum_{k\sigma} < \widehat{n}_{Bk\sigma} > \\ &\equiv \frac{1}{2}\frac{1}{N/2} \sum_{k\sigma} \left(f\left(\overline{E}^{(\alpha)}_{k\sigma}\right) \sin^2\theta_{k\sigma} + f\left(\overline{E}^{(\beta)}_{k\sigma}\right) \cos^2\theta_{k\sigma} \right) \equiv p^2 + d^2, \end{aligned} \tag{7.35}$$

where n_A and n_B simply means the average number electrons per lattice site in the sublattices A and B and due to the Eq. (7.33) is related with the overall average particles number n according to

$$n = \frac{n_A + n_B}{2} = 2\left(p^2 + d^2\right). \tag{7.36}$$

Eq. (7.36) strictly corresponds to relation (4.12) derived in the paramagnetic case.

Finally, the conditions $\frac{\partial F_{AF}}{\partial \beta_{mA}} = 0$ and $\frac{\partial F_{AF}}{\partial \beta_{mB}} = 0$ provides

$$\frac{1}{N/2} \sum_{k\sigma} \sigma \left(f\left(\overline{E}^{(\alpha)}_{k\sigma}\right) \cos^2\theta_{k\sigma} + f\left(\overline{E}^{(\beta)}_{k\sigma}\right) \sin^2\theta_{k\sigma} \right) = \frac{1}{2} M_A, \tag{7.37}$$

and

$$\frac{1}{N/2} \sum_{k\sigma} \sigma \left(f\left(\overline{E}^{(\alpha)}_{k\bar{\sigma}}\right) \sin^2\theta_{k\sigma} + f\left(\overline{E}^{(\beta)}_{k\bar{\sigma}}\right) \cos^2\theta_{k\sigma} \right) = \frac{1}{2} M_B. \tag{7.38}$$

Note that due to the transformation Eqs. (7.32) and the definition of the sublattice magnetization (cf. Eq. (7.5)), $m_A \equiv M_A$ and $m_B \equiv M_B$. Thus, the free energy (7.23) takes the form

$$\begin{aligned}\frac{F_{AF}}{N} &= -\frac{1}{2}\frac{k_B T}{N/2}\sum_{k\sigma}\ln\left[1+e^{-\beta\left(E^{(\alpha)}_{k\sigma}+\Lambda^{(\alpha)}_{k\sigma}-\sigma H_a-\mu\right)}\right] \\ &-\frac{1}{2}\frac{k_B T}{N/2}\sum_{k\sigma}\ln\left[1+e^{-\beta\left(E^{(\beta)}_{k\sigma}+\Lambda^{(\beta)}_{k\sigma}-\sigma H_a-\mu\right)}\right] \\ &+\frac{1}{2}Jzm_Am_B+Ud^2+n\left(\mu-\lambda_{0A}-\lambda_{0B}\right) \\ &-\frac{1}{2}\beta_{3A}m_A-\frac{1}{2}\beta_{3B}m_B.\end{aligned} \tag{7.39}$$

7.2.4 The free energy and magnetization at H_a=0

At $H_a = 0$, the sublattices magnetization must be equal,

$$m_A = m_B \equiv m, \tag{7.40}$$

as well as the symmetry conditions imply that $\lambda^{(2)}_{A\uparrow} = \lambda^{(2)}_{B\downarrow}$, and $\lambda^{(2)}_{A\downarrow} = \lambda^{(2)}_{B\uparrow}$. Thus, due to Eqs. (7.21) one obtains

$$\lambda_{0A} \equiv \lambda_{0B} \equiv \lambda, \tag{7.41}$$

and

$$\beta_{mA} = -\beta_{mB} \equiv -\beta_m. \tag{7.42}$$

Consequently, the band energy renormaliztion factor q_σ Eq.(7.12) does not depends on σ and takes the form

$$q = \frac{(1-n+2d^2)\sqrt{\left(\frac{n}{2}-d^2\right)^2-\left(\frac{m}{2}\right)^2}+2d\left(\frac{n}{2}-d^2\right)\sqrt{1-n+d^2}}{\sqrt{\left(1-\frac{n}{2}\right)^2-\left(\frac{m}{2}\right)^2}\sqrt{\left(\frac{n}{2}\right)^2-\left(\frac{m}{2}\right)^2}}. \tag{7.43}$$

Note that in the case of vanishing magnetization q_{AB} reduces to one in the paramagnetic case (cf. Eq.(4.17)). The Eq.(7.20) becomes now

$$\tan 2\theta_{k\sigma} = \sigma \frac{\varepsilon_k q}{\Delta}, \tag{7.44}$$

with half of the Slater gap

$$\Delta = Jzm + \beta_m, \tag{7.45}$$

which yields

$$\sin 2\theta_{k\sigma} = \pm\sigma \frac{\varepsilon_k q/\Delta}{\sqrt{1+(\varepsilon_k q/\Delta)^2}}, \quad \cos 2\theta_{k\sigma} = \pm \frac{1}{\sqrt{1+(\varepsilon_k q/\Delta)^2}}. \tag{7.46}$$

The formulas (7.44)-(7.46) allow us to write Eqs. (7.24),(7.25) in the form

$$E_{k\sigma}^{(\alpha,\beta)} + \Lambda_{k\sigma}^{(\alpha,\beta)} - \mu = \widetilde{E}_k^{(\alpha,\beta)} - \mu_{eff}, \tag{7.47}$$

where

$$\widetilde{E}_k^{(\alpha,\beta)} = \mp\sqrt{(q\varepsilon_k)^2 + \Delta^2}, \tag{7.48}$$

is the effective quasiparticle energy, and

$$\mu_{eff} = \mu - \lambda, \tag{7.49}$$

is the effective chemical potential.

Performing calculations analogues to those in the paramagnetic case (cf. Chapter 4), one finds that in the low temperature regime the free energy of the antiferromagnetic phase is

$$\frac{F_{AF}}{N} = \frac{E}{N} - TS. \tag{7.50}$$

where the band energy per lattice site is

$$\frac{E}{N} = \frac{1}{N/2}\sum_{k}\left[\widetilde{E}_k^{(\alpha)} f\left(\widetilde{E}_k^{(\alpha)}\right) + \widetilde{E}_k^{(\beta)} f\left(\widetilde{E}_k^{(\beta)}\right)\right] + \frac{1}{2}Jzm^2 + Ud^2 + m\beta_m, \tag{7.51}$$

and the entropy

$$\frac{S}{k_B N} = \frac{1}{N/2}\sum_{k}\sum_{\nu=\alpha}^{\beta} f\left(\widetilde{E}_k^{(\nu)}\right)\ln f\left(\widetilde{E}_k^{(\nu)}\right) + \frac{1}{N/2}\sum_{k}\sum_{\nu=\alpha}^{\beta}\left(1-f\left(\widetilde{E}_k^{(\nu)}\right)\right)\ln\left(1-f\left(\widetilde{E}_k^{(\nu)}\right)\right). \tag{7.52}$$

Here, the Fermi-Dirac distribution function $f(E)$, is defined with the effective chemical potential as follows

$$f(E) = \frac{1}{e^{\beta\left(E-\mu_{eff}\right)}+1}. \tag{7.53}$$

Note, that the quantity β_m plays a role of the molecular field, since it adds to the effective Heisenberg field $Jzm/2$, and in the case $J = 0$ (taken in the numerical analysis) constitutes the entire gap (cf. Eq.(7.45)). On the whole, the first two terms in (7.51) provide the contribution to the thermodynamics coming from the single particle excitations in the Slater subbands having energies $\pm E_{\mathbf{k}}$. These quasiparticle energies comprise the effective mass renormalization $m^*/m_0 = 1/q$, and the molecular field β_m, both to be determined in a self-consistent manner detailed below. The field β_m arises from the local constraints (3.9) and (3.10), (here additionally decomposed due to the sublattice structures) imposed by the correlations induced by the intraatomic interactions.

Finally, the sublattice magnetization Eqs.(7.37) or (7.38) takes now the form

$$\frac{1}{2}m = \frac{1}{N/2}\sum_{k\sigma}\sigma\left(f\left(\widetilde{E}_k^{(\alpha)}\right)\cos^2\theta_{k\sigma} + f\left(\widetilde{E}_k^{(\beta)}\right)\sin^2\theta_{k\sigma}\right), \tag{7.54}$$

and due to the Eqs. (7.46) transforms into

$$\frac{1}{2}m = \frac{1}{N/2}\sum_k \left[f\left(\widetilde{E}_k^{(\alpha)}\right)\frac{\Delta}{\left|\widetilde{E}_k^{(\alpha)}\right|} - f\left(\widetilde{E}_k^{(\beta)}\right)\frac{\Delta}{\left|\widetilde{E}_k^{(\beta)}\right|}\right]. \tag{7.55}$$

7.2.5 The special case H_a=0, T=0

In order to evaluate the expression for the free energy, one needs first to express the chemical potential μ_{eff} as a function of the band filling n. At zero temperature this can be done exactly.

Due to Eq.(7.28) one finds

$$n = \frac{1}{N/2}\sum_k \left[f\left(\widetilde{E}_k^{(\alpha)}\right) + f\left(\widetilde{E}_k^{(\beta)}\right)\right]. \tag{7.56}$$

Assuming that the range of energy for bare particles includes in the of band of width W, i.e., $-\frac{W}{2} \leqslant \varepsilon_k \leqslant \frac{W}{2}$, Eq.(7.56) transforms into

$$\begin{aligned} n \;=\; & \int_{-\frac{W}{2}}^{\frac{W}{2}} d\varepsilon \rho(\varepsilon) \times \\ & \left[\Theta\left(\mu_{eff} + \sqrt{(q\varepsilon)^2 + \Delta^2}\right) + \Theta\left(\mu_{eff} - \sqrt{(q\varepsilon)^2 + \Delta^2}\right)\right], \end{aligned} \tag{7.57}$$

where density of state function for the bare particles

$$\rho(\varepsilon) = \frac{1}{N/2}\sum_k \delta(\varepsilon - \varepsilon_k), \tag{7.58}$$

and the step function is

$$\Theta(x) = \begin{cases} 1 & if \;\; x \geqslant 0, \\ 0 & otherwise. \end{cases} \tag{7.59}$$

Let as assume next that $\mu_{eff} \leqslant 0$ (for the symmetric distribution of $\rho(\varepsilon)$, with gravity center at zero this corresponds to the case with $n \leqslant 1$). Therefore, the second term

in (7.57) vanishes authomaticaly. Assuming that $\rho(\varepsilon) = \frac{1}{W}$ (cf. Eq. (4.33)), the remaining part of the integral can be written as

$$n = \int_{-\frac{W}{2}}^{\frac{W}{2}} d\varepsilon \frac{1}{W} \Theta\left(\sqrt{(q\varepsilon)^2 + \Delta^2} - |\mu_{eff}|\right), \tag{7.60}$$

which shows clearly that there are two integration regimes for which $\Theta \neq 0$, namely

$$n = \int_{-\frac{W}{2}}^{-\varepsilon_0} \frac{d\varepsilon}{W} + \int_{\varepsilon_0}^{\frac{W}{2}} \frac{d\varepsilon}{W} = \frac{1}{W/2} \int_{-\frac{W}{2}}^{-\varepsilon_0} d\varepsilon, \tag{7.61}$$

where

$$\varepsilon_0 = \frac{1}{q}\sqrt{\mu_{eff}^2 - \Delta^2} \quad . \tag{7.62}$$

Thus, one finds that the relation between the effective chemical potential and the band filling is

$$\frac{1}{Wq}\sqrt{\mu_{eff}^2 - \Delta^2} = \frac{1}{2}(1-n). \tag{7.63}$$

The consideration of the case $n > 1$ is straightforward because of the electron-hole symmetry.

It is useful to transform the obtained formulas for the free energy and the magnetization into the dimensionless form. Namely, starting from Eq. (7.50), at $T = 0$ and replacing the summation over $\mathbf{k}$ by the integration over energies ε one obtains the formula

$$\frac{F_{AF}}{N} = -\frac{1}{W/2} \int_{-\frac{W}{2}}^{-\frac{W}{2}(1-n)} d\varepsilon \sqrt{(q\varepsilon)^2 + \Delta^2} + \frac{1}{2}Jzm^2 + Ud^2 + m\beta_m. \tag{7.64}$$

Similarly, Eq.(7.55) for the sublattice magnetization has the form

$$m = \frac{1}{W/2} \int_{-\frac{W}{2}}^{-\frac{W}{2}(1-n)} d\varepsilon \; \frac{\Delta}{\sqrt{(q\varepsilon)^2 + \Delta^2}} \,. \tag{7.65}$$

The above integrals can be evaluated by using standard integrals tables. Note that integral appearing in (7.64) can be expressed through the integral (7.65), i.e. through the magnetization. Thus, finally we obtain the following expression for the ground state energy per site in the units of W, ($f_{AF} \equiv F_{AF}/NW$) is

$$\begin{aligned} f_{AF} \;=\; & -\frac{1}{2}\sqrt{\left(\frac{q}{2}\right)^2 + \left(\frac{\Delta}{W}\right)^2} \\ & + \frac{1-n}{2}\sqrt{\left(\frac{q\,(1-n)}{2}\right)^2 + \left(\frac{\Delta}{W}\right)^2} + 2ud^2 + \frac{1}{2}m\left(\frac{\Delta}{W} - jm\right), \end{aligned} \tag{7.66}$$

where $u \equiv U/2W$, and $j \equiv Jz/W$.

The evaluation of the integral (7.65) provides the following magnetization formula

$$m = x \ln \left| \frac{\sqrt{x^2 + (1-n)^2} - (1-n)}{\sqrt{x^2+1} - 1} \right| \quad with \quad x \equiv \frac{2\Delta}{Wq}. \tag{7.67}$$

The next step is to minimize the functional (7.66) with respect to the variables d and m. However, contrary to the paramagnetic case the free energy functional cannot be brought to the form explicit in magnetization m. This problem can be solved by minimizing first the ground state energy with respect to x and then, due to the relation (7.67), expressing m *via* x. So, the expression for the ground state energy takes the final form

$$f_{AF} = -\frac{1}{4}q\sqrt{1+x^2} + \left(\frac{1-n}{4}\right) q\sqrt{(1-n)^2 + x^2} + 2ud^2 + \frac{1}{2}m\left(\frac{1}{2}xq - jm\right), \tag{7.68}$$

with the parameters m and q determined respectively by the Eqs.(af30) and (7.43). The numerical minimization of the expression (7.68) allows us to calculate d^2 and m.

7.2.6 Chemical potential

Combining relations (7.49) and (7.63) one finds the chemical potential in the form

$$\mu = \lambda + \mu_{eff} = \lambda \pm \sqrt{\Delta^2 + \left(\frac{Wq}{2}\right)^2 (1-n)^2}. \tag{7.69}$$

Since the numerical minimization of (7.68) allows us to determine the quantities $d^2$and x for settled parameters: u, j and n, the only unknown variable in Eq.(7.69) remains λ. In order to find λ one needs to make use of the two remaining minimum conditions, namely $\frac{\partial F_{AF}}{\partial p^2} = 0$ and $\frac{\partial F_{AF}}{\partial e} = 0$. First of them yields

$$\begin{aligned} 0 \;=\; & 2\lambda^{(1)} + 2\lambda + \left[q \left(\frac{\partial q_{AB}}{\partial p^2} \right)_{e=\sqrt{1-n+d^2},\quad p^2=\frac{n}{2}-d^2} \right] \times \\ & \frac{1}{N/2} \sum_k \left[\left(f\left(\widetilde{E}_k^{(\beta)}\right) - f\left(\widetilde{E}_k^{(\alpha)}\right) \right) \frac{\varepsilon_k^2}{\sqrt{(q\varepsilon_k)^2 + \Delta^2}} \right], \end{aligned} \tag{7.70}$$

and similarly the condition $\frac{\partial F_{AF}}{\partial e} = 0$, leads to

$$\begin{aligned} 0 \;=\; & 2\lambda^{(1)} e + \left[q \left(\frac{\partial q}{\partial e} \right)_{e=\sqrt{1-n+d^2},\quad p^2=\frac{n}{2}-d^2} \right] \times \\ & \frac{1}{N/2} \sum_k \left[\left(f\left(\widetilde{E}_k^{(\beta)}\right) - f\left(\widetilde{E}_k^{(\alpha)}\right) \right) \frac{\varepsilon_k^2}{\sqrt{(q\varepsilon_k)^2 + \Delta^2}} \right]. \end{aligned} \tag{7.71}$$

Combining these two above equations, one obtains

$$\lambda = Q\Omega, \tag{7.72}$$

where

$$Q = q \left[\left(\frac{\partial q}{\partial p^2} \right) + \frac{1}{e} \left(\frac{\partial q}{\partial e} \right) \right]_{e=\sqrt{1-n+d^2},\quad p^2=\frac{n}{2}-d^2},$$

and

$$\Omega = \frac{1}{N/2} \sum_k \left[\left(f\left(\widetilde{E}_k^{(\beta)}\right) - f\left(\widetilde{E}_k^{(\alpha)}\right) \right) \frac{\varepsilon_k^2}{\sqrt{(q\varepsilon_k)^2 + \Delta^2}} \right]. \tag{7.73}$$

Next, replacing the summation in (7.73) by integration, and assuming that $n \leqslant 1$, one finds

$$\lambda = -\frac{Q}{W} \int_{-\frac{W}{2}}^{-\frac{1}{2}W(1-n)} d\varepsilon \frac{\varepsilon^2}{\sqrt{(q\varepsilon)^2 + \Delta^2}}. \tag{7.74}$$

Note, that in the case $n = 1$, chemical potential $\mu = \lambda$, while for the cases when n differs infinitesimally from unity

$$\mu = \begin{cases} \lambda - \Delta, & for \quad n \to 1^- \\ \lambda + \Delta, & for \quad n \to 1^+, \end{cases} \tag{7.75}$$

i.e. the discontinuity in the Fermi energy appears when n approaches half filling from below or from above.. The conditions (7.75) allows to display the effective Slater gap and compare it with the previously obtained Mott-Hubbard gap.

7.3 From Slater to Mott picture

The discussed results are based on the numerical minimization of the free energy (7.68) with respect to the variables d and x. The variable x, displayed on Fig. 7.1, has a physical meaning of the ratio of the Slater gap to the renormalized band energy. The growing ratio $\Delta/(Wq)$ drives the system towards localization induced by a formation of magnetic moments arranged in the sublattices, whereas the growing ratio U/W drives the system towards localization independent of magnetic ordering. In result, the present formulation allows us to single out the contributions coming from the two factors. The magnetic energy is thus measured with respect to the effective band energy ($\sim Wq$), renormalized by the Coulomb interaction.

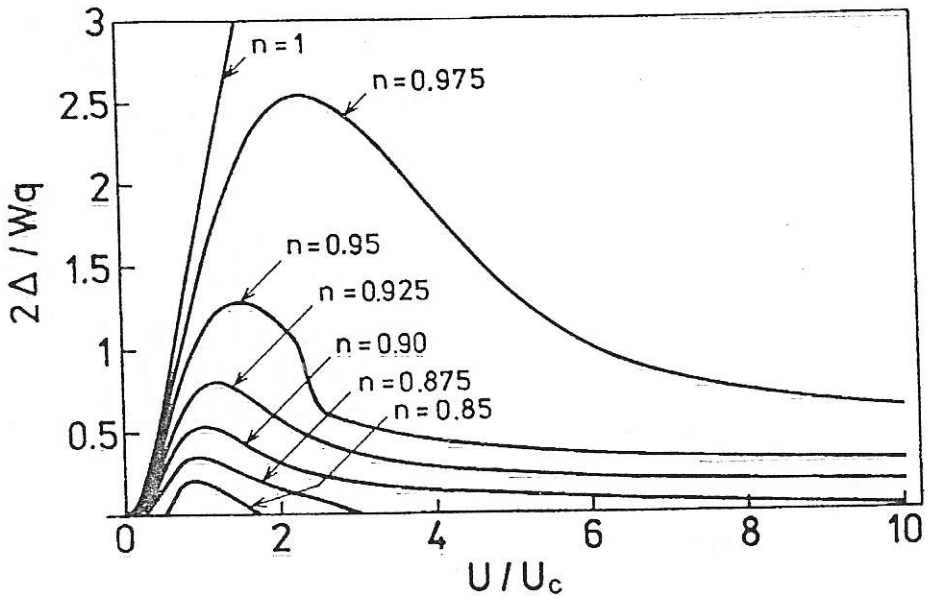

Figure 7.1: The dependense of the variable $x \equiv 2\Delta/Wq$ from the interaction U/U_c.

In Fig. 7.2 we have exhibited both the effective Slater gap 2Δ and the Mott-Hubbard gap for $n = 1$. Those characteristics are plotted for the ground state. The chemical potential is then $\mu(T = 0) = \lambda$. The Mott- Hubbard gap is expressed through the difference in the chemical potential in the paramagnetic case ($\Delta = 0$) for $n = 1.001$ (the upper part) and for $n = 0.999$ (the lower part), and was discussed also earlier [6]. For $n = 1$ the antiferromagnetic Slater split-band picture appears for arbitrary small U, and Δ increases with increasing U/U_c. In the limit $U/U_c \sim 1$ the gap is composed of the Slater and the Mott-Hubbard parts, and when $U \to \infty$ the former merges gradually with the latter. This can be seen explicitly in Fig.7.3, where we have shown the ground state energy $E/(WN)$ versus U/U_c. In the strong-correlation limit the energy is determined by the kinetic-exchange contribution $\sim 1/U$

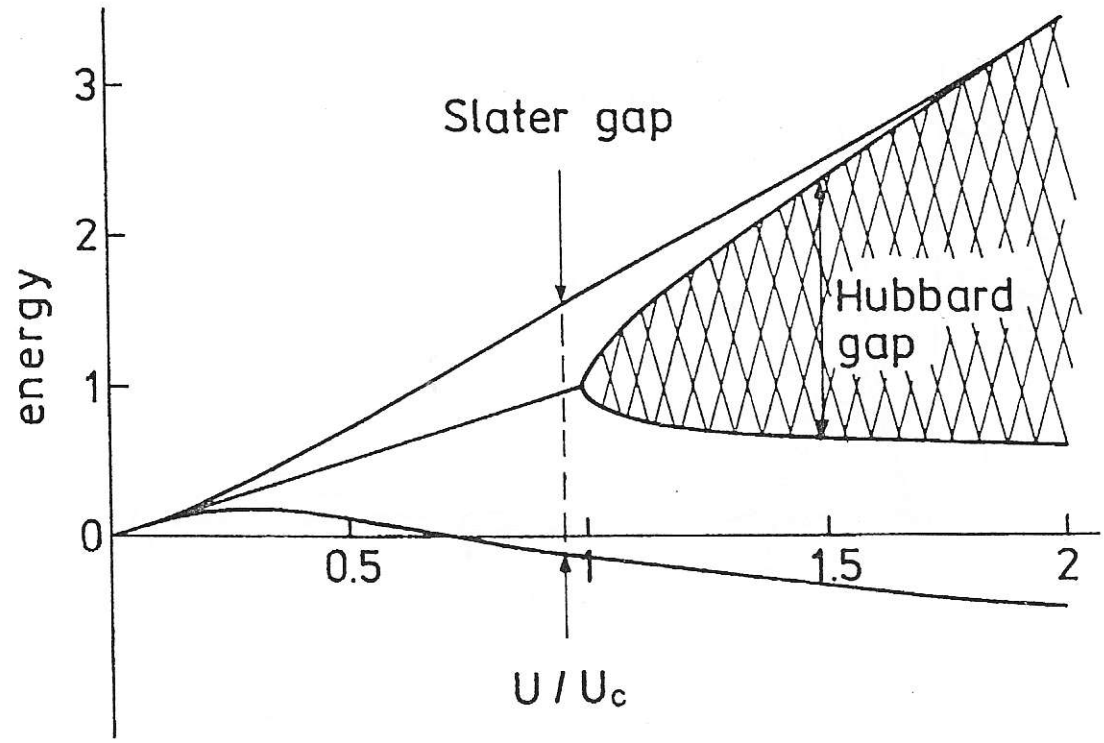

Figure 7.2: $2\Delta/W$ and the Hubbard gap as the functions of interaction strength. The Slater gap merges with the Mott-Hubbard gap as $U/U_c \to \infty$.

[2]. Therefore, the energies of para- and antiferro-magnetic states are the same in the $U \to \infty$ limit. The inset illustrates another interesting characteristic of the solution namely, the magnetic gap is *not* proportional to the magnetization, as one would expect from the Hartree-Fock solution. In other words, the molecular field β_m is a nonlinear function of m, since from the condition $\partial f/\partial\Delta = 0$ we obtain the relation $2\Delta/W = mq/\sqrt{1-m^2}$. Also, AF solution disappears altogether for $n \simeq 0.83$. In the strong correlation limit the kinetic exchange contribution determines the free energy behavior also if $n < 1$, as shown on Fig. 7.4. Of course, in that case system is always in the metallic phase.

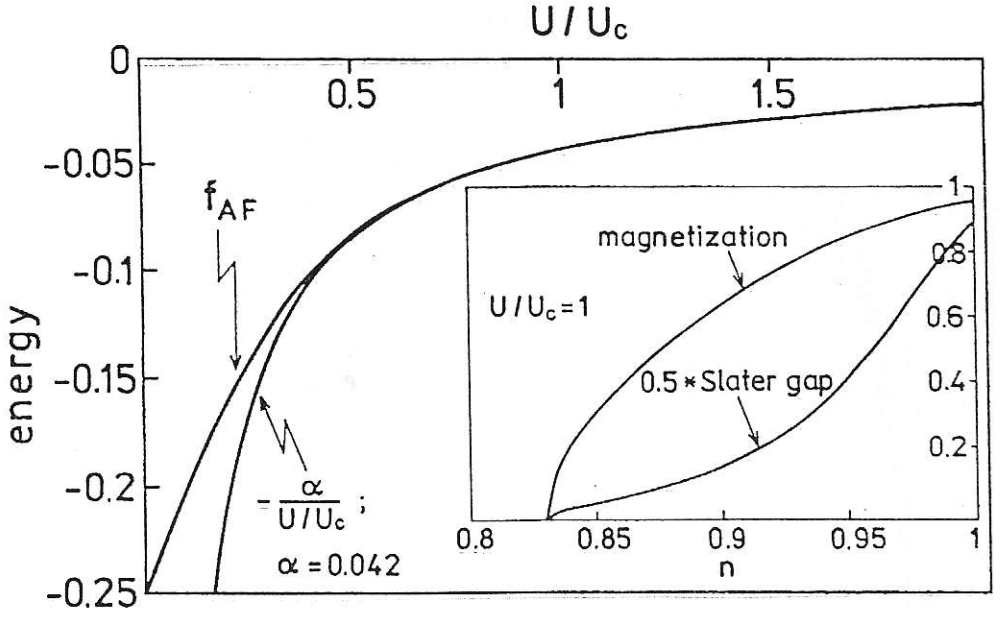

Figure 7.3: Ground state energy for (AF) state at $n = 1$ vs. U/U_c. The lower curve is the fit to the expression $(-0.042 \times U_c/U)$. The inset displays the difference in behavior of magnetic moment m and half of the Slater gap (Δ/W), both plotted as a function of the band filling.

To visualize the difference between the magnetic gap and the magnetization we have plotted in Fig. 7.5 both quantities as a function of the interaction strength $U/U_c \equiv U/2W$, for different band filling n. While for $n = 1$ the magnetic moment saturates gradually with growing U/U_c, it displays a maximum for $n < 1$. This means that the holes in the lower Slater subband have a stronger detrimental influence on AF phase in strong-correlation limit; their dynamics is incorporated coherently in the low-U magnetism when $d^2 \gtrsim (1 - n)$. The Slater gap for $n = 1$ obviously grows $\sim U$ and this indicates again that it merges with the Hubbard gap, which can be

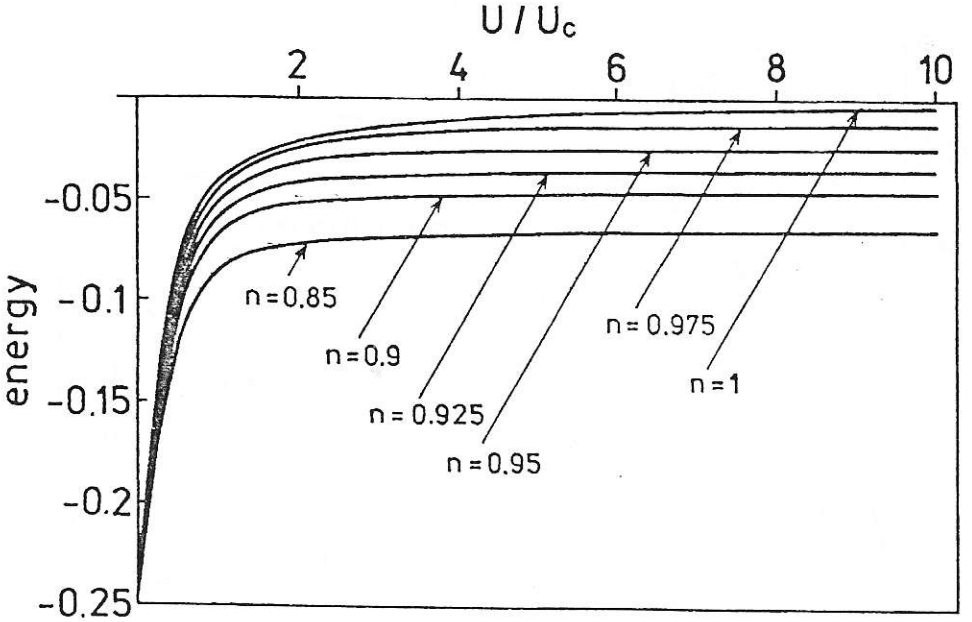

Figure 7.4: Ground state energy for AF state versus U/U_c, for different band fillings.

estimated analytically and is $\approx U - W + 4UW^2/(z(U^2 + W^2)) \approx U - W$.

The double occupancy $d^2 = \langle n_{i\uparrow} n_{i\downarrow} \rangle$ is shown in Fig. 7.6 for different band fillings. It decreases continuously with growing U/U_c, i.e. the charge fluctuations are gradually suppressed, while the magnetic moment behaves differently (cf. Fig. 7.5). The difference in the behavior of d^2 and m is caused by the circumstance that the d^2 is of intraatomic nature, whereas m is determined from the competition between the magnetic energy $\sim \beta_m^2$ (also of intraatomic nature) and the renormalized band energy $\sim Wq$ (i.e. the processes frustrating the spins on sublattices). The inset to Fig. 7.6 exemplifies the difference between the diminution of d^2 with growing U/U_c for $n = 1$ in two situations. For paramagnetic (PARA) case $d^2 \equiv 0$ for $U \geq U_c$; this feature is concurrent with the effective mass divergence at the Mott-Hubbard local-

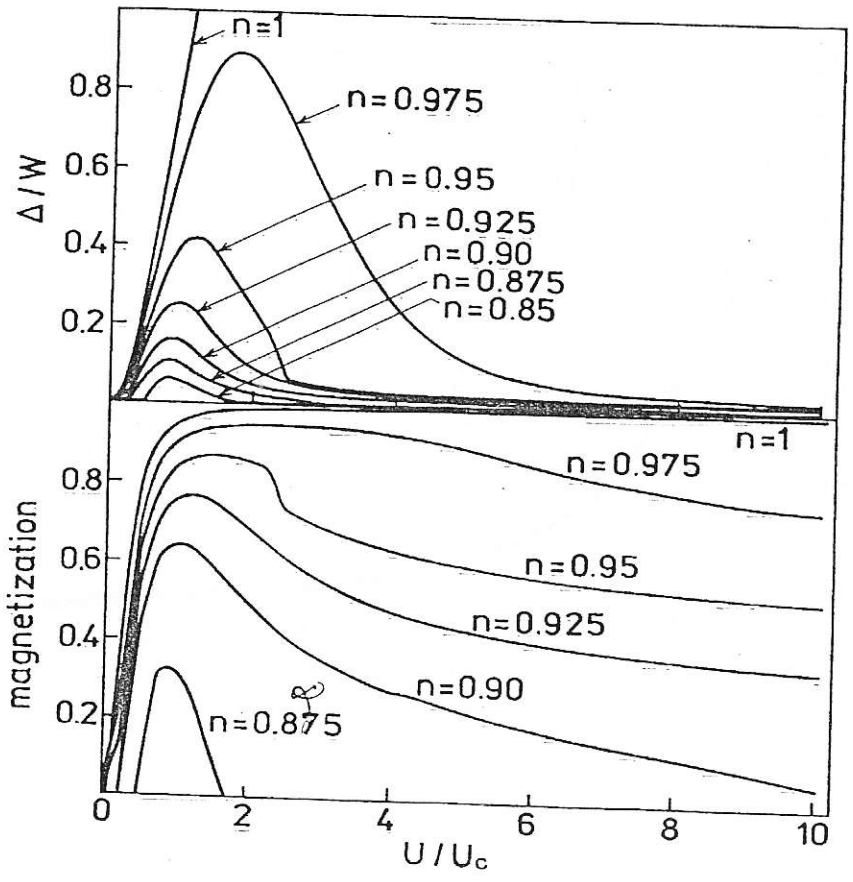

Figure 7.5: Δ/W (top panel) and the magnetic moment $m = \langle n_{i\uparrow} - n_{i\downarrow} \rangle$ (bottom) versus U/U_c and for different values of n.

ization boundary [7]. This divergence does not emerge in the antiferromagnetic state, as d^2 approaches zero gradually in the same manner, as m approaches saturation ($m \rightarrow 1$). Therefore, we have displayed in Fig. 7.7 the effective mass renormalization $m^*/m_0 = 1/q$ as a function of U/U_c for different n values. Again, the inset illustrates the difference with the $n = 1$ case. One should note that the enhancement factor in AF state is very small compared to that in PARA state, which is equal to

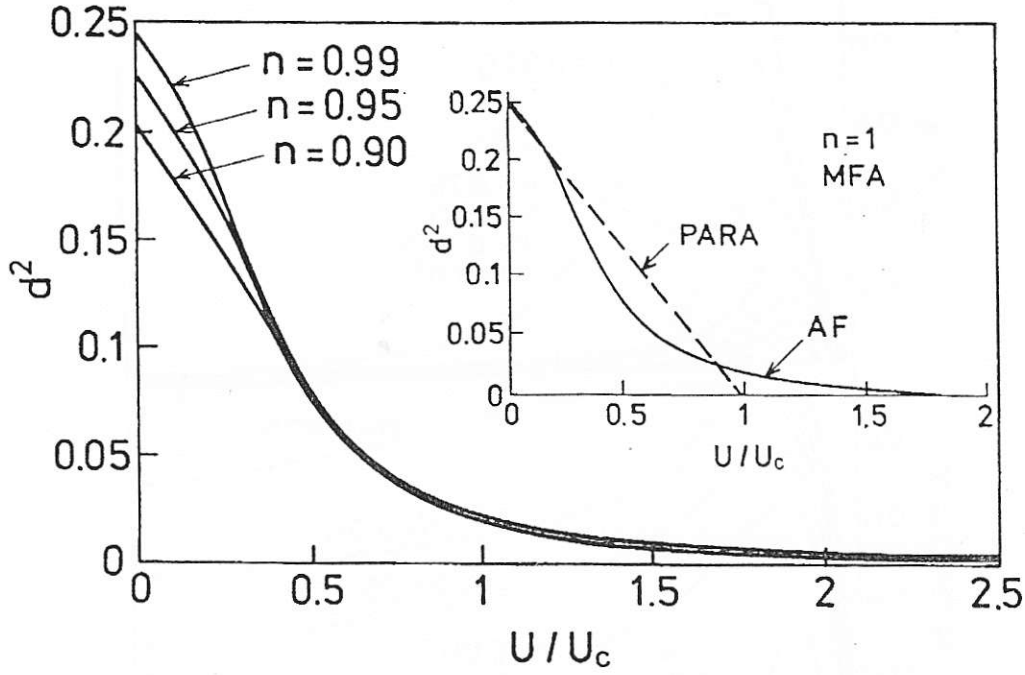

Figure 7.6: $d^2 = \langle n_{i\uparrow} n_{i\downarrow} \rangle$ vs U/U_c, and for the different n values. The inset display the difference in behavior for para- and antiferro-magnetic cases for $n = 1$.

$1/q = \left[1 - (U/U_c)^2\right]^{-1}$. The difference between AF and PARA states diminishes with decreasing n, as in that situation the magnetic moment is reduced rapidly. So, the weak mass enhancement in the $n = 1$ can be associated with the appearance of the gap. Also, the physical parameters $d^2, 1-m$, and $1-n$ are all of the same magnitude. This is easy to envisage when estimating e.g. the band narrowing q, which is in the AF state roughly $\sim 2d^2/(1-m^2)$ and is of the order of unity.

In order to visualize the relative contribution to the ground state energy coming from the Coulomb interaction Ud^2 and the magnetic term $\beta_m \cdot m$, in Fig. 7.8 we have plotted the difference of these two terms. As one would expect, along with decreasing

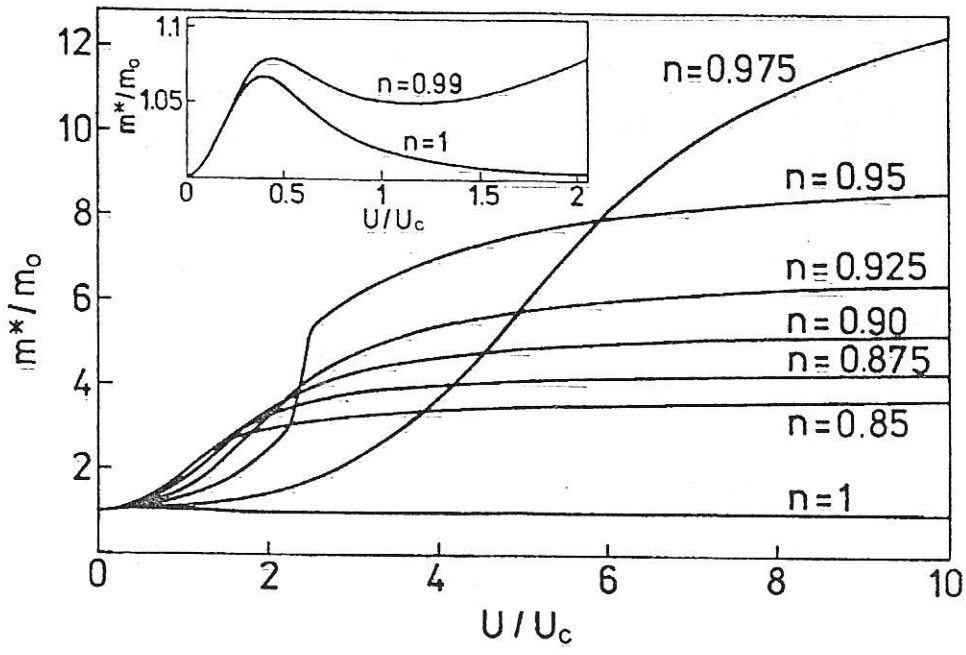

Figure 7.7: m^*/m_0 (with respect to the band value m_0) vs U/U_c and for the n values shown. The inset shows a rather weak enhancement close to the Mott-Hubbard limit.

n the magnetic contribution disappears and the system turns to the behavior of the paramagnetic metal. On the other hand, the closer is the system to the half filling, the stronger is the magnetic contribution. Note, that in case $n = 1$ the system approaches the Mott-Hubbard insulating state, as $U \Rightarrow \infty$.

Finally, in Fig. 7.9 we have displayed the stability regime $n - U/U_c$ of AF phase. The inset has been obtained [8] in the limit of infinite dimension with the help of quantum Monte Carlo simulation. One should note the regime of the filling n of the stable AF phase is the broadest for $U/U_c \sim 1$, i.e. when the molecular field is the strongest (cf. Fig. 7.5).

The Mott-localization is achieved gradually at $T = 0$ in AF state. In other words,

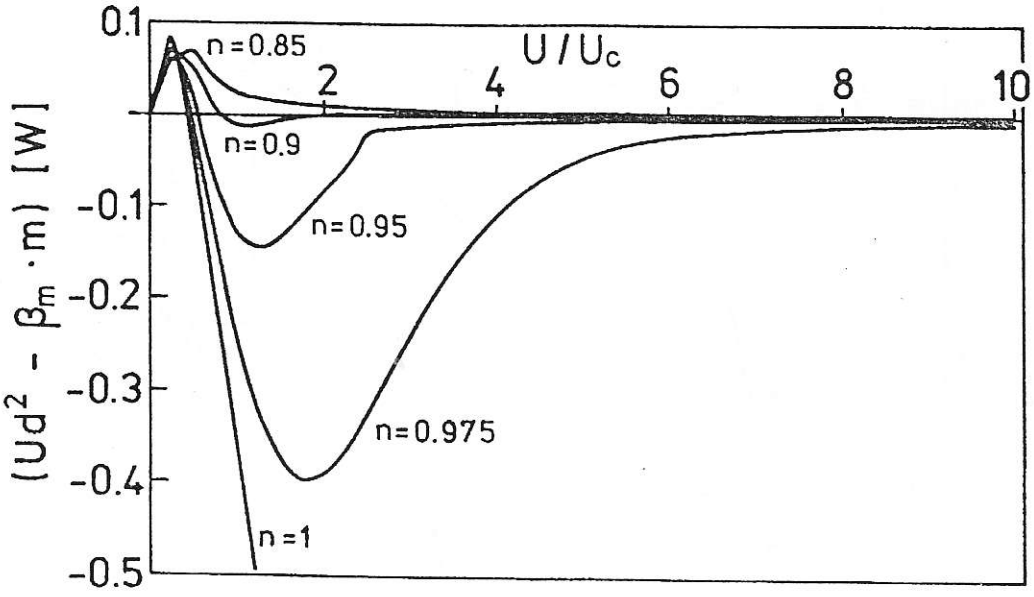

Figure 7.8: Comparation between the magnetic and the Coulom term contributions to the free energy.

the present approach provides a continuous evolution from Slater to Mott insulator, as shown e.g. in the bottom of Fig. 7.3. The same holds true even when we include the intersite exchange ($J > 0$). The continuous evolution with growing U/W does not preclude the first order transition at nonzero temperature, as has been demonstrated some time ego [9], and subsequently reconfirmed in the limit $d \rightarrow \infty$ [10].

In summary, in this Chapter we have addressed the question of crossover from Slater to Mott-Hubbard picture in the half-filled band case, as well as have discussed detailed the behavior of quasiparticle properties in AF state in the nonhalf-filled band case. Although our analysis is based on the saddle-point solution of the slave-boson functional-integral approach, the results can serve as a proper mean-field analysis,

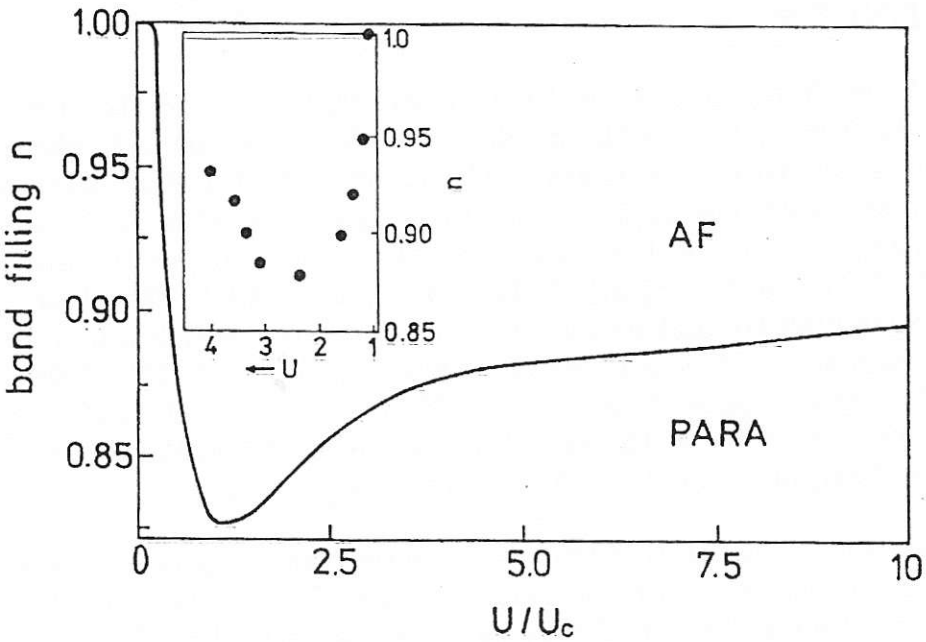

Figure 7.9: The stability regime of AF solution; the inset: results of Monte-Carlo calculations in the $d \rightarrow \infty$ limit [10].

since they interpolate between those in the Hartree-Fock approximation in the limit $U \rightarrow 0$ and those in mean-field approximation for the Heisenberg model (for $n = 1$) in the $U \rightarrow \infty$ limit. Thus they represent the basis for inclusion of Gaussian fluctuations [11] in a magnetically ordered (AF) state close to the Mott-Hubbard localization. Also, the full analysis of the Mott-Hubbard boundary should include the disordered local-moment phase [12], not analyzed in the present thesis.

REFERENCES

[1] See: J. des Cloizeaux, J. Phys. Radium. **20**, 606 (1959), and D.R. Penn, Phys. Rev.**142**, 350 (1966), - for the stability of antiferromagnetic (AF) phases in the Hartree-Fock (HF) approximation. The stability of AF in the present context (i.e. in the Gutzwiller approximation) has been obtained in: K.Kubo and M. Uchinami, Prog. Theor. Phys. **54**, 1289 (1975). For a comparative analysis see: e.g. A.M. Oles and J. Spałek Z. Phys.B **44**, 177 (1981). The phase diagram recovering both HF and strong correlation limits correctly has been discussed in G. Kotliar and A.E. Ruckenstein, Phys. Rev. Lett. **57**, 1362 (1986)-within the slave-boson approach; and in: W. Metzner and D. Vollhardt, Phys. Rev. Lett. **62**, 324 (1989); P. Fazekas, B. Menge and E. Müler-Hartmann, Z. Phys. **78**, 69 (1990)-in the limit of infinite dimension ($d \to \infty$).

[2] In that respect the AF stability should be considered against the onset of the ferromagnetism, for which the Pauli principle plays similar role. However, in the large-U limit, the virtual hopping processes, particularly for $n = 1$ lead to a stable AF state; see e.g. P.B. Vischer, Phys. Rev. B**10**, 943 (1974); J.Spałek et al., phys. stat. solidi (b) **108**, 329 (1981). Cf. also: K. A.Chao et al., J. Phys. C**10**, L271 (1977).

[3] J. Spałek and P. Gopalan, Phys. Rev. Lett. **64**, 2823 (1990); P. Korbel et al., Phys. Rev. B**52**, R2213 (1995).

[4] T. Li et al., Phys. Rev. B**40**, 6817 (1989); R. Frésard and P. Wölfle, Int. J. Mod. Phys. B**6**, 237 (1992); **6**, 3087(E) (1992).

[5] J. Spałek and W. Wójcik, in *Spectroscopy of the Mott Insulators and Correlated Metals*, Springer Series in Solid State Sciences, vol **119**, pp.41-65 (1995).

[6] M. Lavagna, Phys. Rev. B**41**, 142 (1990).

[7] W.F. Brinkman and T.M. Rice, Phys. Rev. B**2**, 4302 (1970).

[8] M. Jarrell, Phys. Rev. Lett. **69**, 168 (1992); M. Jarrell and T. Pruschke, Z.Phys. B**90**, 187 (1993). For the comparison the men-field slave-boson and the quantum Monte-Carlo approaches see: L. Lilly et al., Phys. Rev. Lett. **65**, 1379 (1990).

[9] J. Spałek et. al., Phys. Rev. Lett. **48**, 729 (1987); for review see: J. Spałek, J. Solid State Chem. **88**, 70 (1990).

[10] For review see: A. Georges et. al., Rev. Mod. Phys. **68**, 13 (1996).

[11] The Gaussian fluctuations in PARA state are treated in Ref. 6, and in: P. Wölfle and T. Li, Z. Phys. **78**, 45 (1990); R. Raimondi and C. Castellani, Phys. Rev. B**48**, 11453 (1993).

[12] R.M. Ribeiro-Teixeira and M. Avignon, in *New Trends in Magnetism, Magnetic Materials, and Their* Applications, edited by J. L. Moran-López and J.M. Sanchez (Plenum Press, New York, 1994) p. 373

Chapter 8

Summary and conclusions

In this thesis we have discussed properties of the Fermi liquid close to the Mott - Hubbard localization, as well as have determined its transition to either correlated liquid or to the antiferromagnetic phase. These results were derived within the mean -field picture of correlated narrow-band electrons. Among the new effects determined and discussed in the thesis are:

(i) The importance of the spin-split masses and the appearance of a nonlinear molecular field, as well as their role in the physical properties of systems with almost localized fermions;

(ii) The instability of the Fermi liquid of almost localized quasiparticles against the non-Fermi-liquid state in an applied magnetic field;

(iii) The determination of the regime, in which the system exhibits metamagnetism and differentiation of the form a metamagnetic behavior; and

(iv) A detailed discussion of the antiferromagnetic state for an arbitrary band filling, and in particular, of a crossover behavior from the Slater antiferromagnetic

insulator to the Mott-Hubbard insulator with the growing magnitude of Coulomb interaction.

Apart from that, in the first three chapters we have summarized the slave boson approach and with this tool we have reproduced the older results of Gutzwiller, Hubbard and Brinkman and Rice. Thus, the slave boson approach represents an unification of the older concepts already on the mean-field level, as well as allows for an interpolation between the Hartree-Fock and the strong-correlation limits (see e.g. Fig. 7.3).

A number of topics, which would make the present thesis more complete, have *not* been included. Among them probably the most important is the effect of quantum Gaussian fluctuations on the antiferromagnetic state. Also, it seems interesting to compare the corrections to the mean-field free energy (coming from the Gaussian fluctuations) in the antiferromagnetic and paramagnetic cases, the more so, since in the mean-field approach we observe the separation between spin and charge fluctuations in the paramagnetic phase, whereas in the antiferromagnetic case we do not. In general, a closer look into the dynamical properties of almost localized Fermi liquid has to be carried out to determine the stability conditions for the saddle-point solutions. The existing analysis of the Gaussian in the paramagnetic state [1] confirms the stability of this state. Work along this line for the antiferromagnetic phase is planed foe the near future. Apart from that, the existing comparison between the mean-field slave-boson solution and the Mote-Carlo simulations [2] speaks also in favor of our picture. However, it must be said that even though the present approach reduces

correctly to the Hartree-Fock approximation as far as the equilibrium properties are concerned, it does not provide correctly the sum rule for the dynamical spectral function [3] in the Hartree-Fock limit. Thus, putting into agreement the static and the dynamic properties in the weak correlation limit poses still a problem.

REFERENCES

[1] J. W. Rasul and T. C. Li, *J. Phys.* **C21**, 5119 (1988); T. C. Li and J.W. Rasul, *Phys. Rev.* **B39**, 4630 (1989); P. Wölfle and T. Li, *Z Phys.* **B78**, 45 (1990); M. Lavagna, *Helvetica Phys. Acta* **63**, 310 (1990); M. Lavagna *Phys. Rev.* **B41**, 142 (1990).

[2] L. Lilly et al., Phys. Rev. Lett. **65**, 1379 (1990).

[3] R. Raimondi and C. Castellani, Phys. Rev. B**48**, 11453 (1993).